Hyperfinecourse A: the nucleus

February 5, 2020

Abstract

This document is meant for optional background reading when studying www.hyperfinecourse.org. It deals with one of the chapters of this course. The formal course content is defined by the website and videos. The present document does not belong to the formal course content. It covers the same topics, but usually with more mathematical background, more physical background and more examples. Feel free to use it, as long as it helps you mastering the course content in the videos. If you prefer studying from the videos only, this is perfectly fine.

The present text has been prepared by Jeffrey De Rycke (student in this course in the year 2018-2019). He started from a partial syllabus written by Stefaan Cottenier for an earlier version of this course, and cleaned, edited and elaborated upon that material. That syllabus was itself inspired by a course taught by Michel Rots at KU Leuven (roughly 1990-1995).

1 Nuclear Properties

This course will focus on the hyperfine splitting of the energy levels of the atoms, alone or incorperated in molecules or solids. A thorough understanding of different properties of the atom, and in particular about the nucleus, is therefore needed. This part will cover a list of certain nuclear properties. The values of different properties can be found at https://www-nds.iaea.org/nuclearmoments/.

1.1 Z, N, and A

These three numbers were probably the first properties you learned about the nucleus. They are the atomic number, the neutron number, and the mass number. They represent the amount of protons (Z), the amount of neutrons (N), and the total amount of nucleons (A) inside the atom. It follows naturally that Z + N = A. The atomic number uniquely identifies a chemical element. Whilst the neutron number will have an effect on the mass(number), the shape, the stability,... of the nucleus. Nuclei with the same atomic number but with a different amount of neutrons are called isotopes. Nuclei with the same neutron number but with a different amount of protons are called isotones. This word was formed by replacing the **p** (for proton) in isotopes with the letter **n** (for neutron). Nuclei with the same mass number are called isobars. A more exotic term is isodiaphers, which are nuclei with equal neutron excess. The neutron excess is defined as the amount of neutrons minus the amount of protons. Lastly, there are isomers. Which are nuclei with same Z and N, but in a different energy state. Not to be confused with the different energy states of the electron cloud. When representing nuclei, one uses the short notation such as "C" for carbon or "Fe" for iron. In the top left, the mass number is depicted. If one were to plot all known nuclei on a N/Z plot, it would look like the figure on the next page. As the amount of Z grows the amount of N also needs to grow to keep the nuclei stable. This is needed to overcome the electromagnetic force between the protons, using the strong force between the nucleons. There are also nuclei which are more stable than one would expect from a first look. These states can be explained via the nuclear shell model. Much like the atomic shell model, it uses the Pauli exclusion principle to order the nucleons and describe the nucleus. When adding nucleons, there are states with clear jumps and falls in the binding energy. These number of protons and neutrons are called magic numbers. It shouldn't come as a surprise that these numbers are 2, 8, 20... Which are the same amount of electrons giving full shells. If both the amount protons and neutrons are magic numbers, one speaks of "double magic numbers". As the total amount of nucleons grows, it becomes harder and harder to find "stable" nuclei. It becomes harder to overcome the electromagnetic repulsion. The most stable nucleus (highest binding energy per nucleon) is Nickel-62. Not to be confused with Iron-56, which has the lowest mass per nucleon. Therefore, fission of elements heavier than Nickel-62 will release energy, whilst one needs fusion of elements lighter than Nickel-62 to release energy. In nature, only elements up to Uranium are found. The lightest elements were created during the Big Bang

and the following Big Bang nucleosynthesis. Heavier elements (up to Nickel) can be created via fusion during the latest stages of stars, when the pressure (due to gravity) is high enough to let said fusion take place. Heavier elements are created during events such as supernovae.

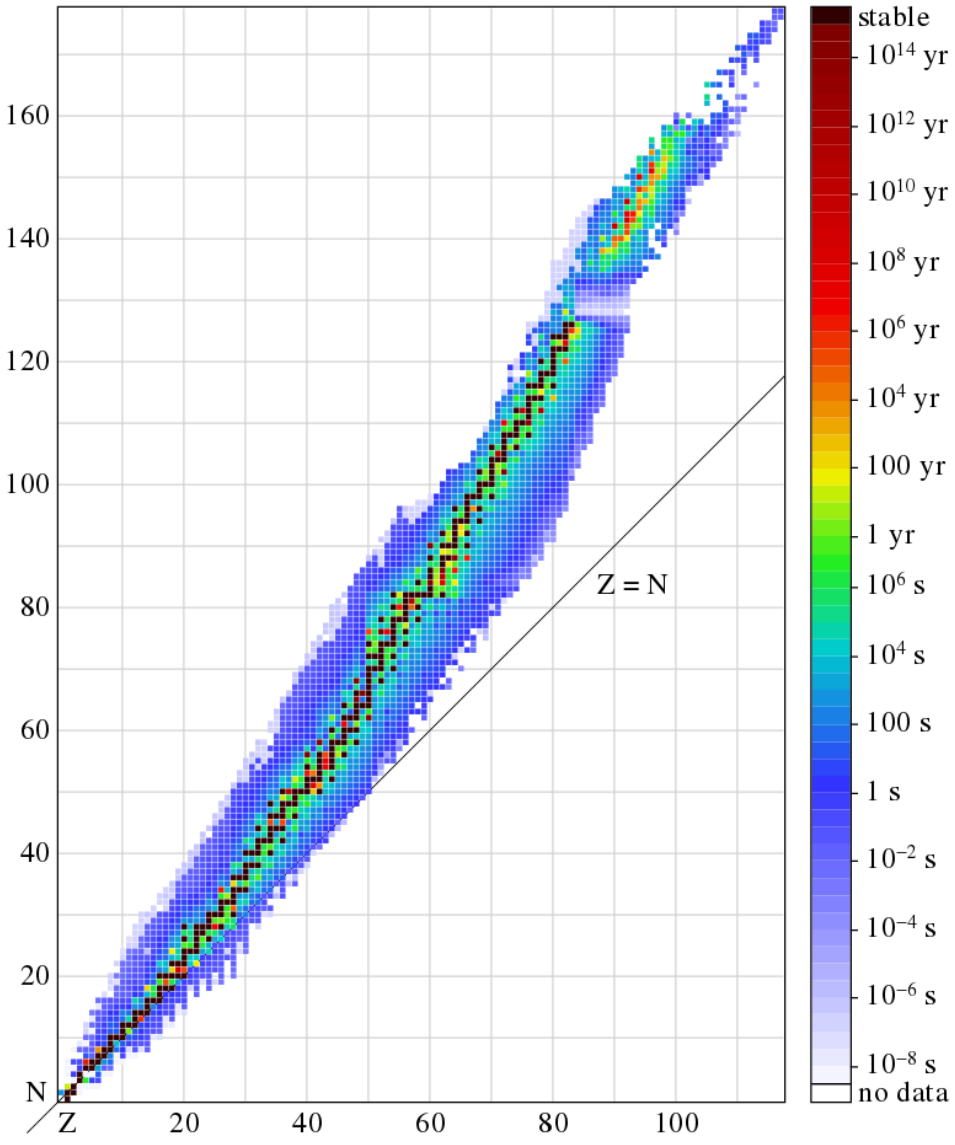

Figure 1: Plot of all known nuclei. N i.f.o. Z.

1.2 Mass

The mass of a proton, as wall as a neutron, is about 1 GeV[1]. The mass of a nucleus is not simply the sum of all nucleon masses. When nucleons come together to form a nucleus, some mass is lost as "binding energy". As discussed before, this binding energy can serve as a measure for how tight the nucleons hold together. To correct for the amount of nucleons, the binding energy is often expressed as binding energy per nucleon. The mass of a nucleus is also often expressed in a.m.u.'s, which is the same as 1 gram per mole. Which is, by definition, 1/12th of the mass of a Carbon-12 atom[2], or $1.66 \cdot 10^{-27} kg$.

1.3 Lifetime

Not all nuclei are stable. Some can decay to other nuclei (or pairs of nuclei). The lifetime can range from yoctoseconds to infinity. But more typical values are femtoseconds to 10^{10} seconds. The experimentally verified lifetime of the proton (Hydrogen nucleus) is, as for now, longer than the age of the universe. It is therefore accepted to be a stable particle. This is needed to conserve baryon number. Some new physics theorems propose proton decay and therefore violation of baryon number. This violation is needed to explain e.g. the matter anti-matter discrepancy in the universe. Observing the decay of a proton would therefore have interesting consequences in our understanding of the universe.

There are different kinds of decay. For example: a neutron can decay to a proton and an electron (and an anti-electronneutrino). Therefore shifting to Z+1 and N-1. This is called beta decay. A proton can decay to a neutron, a positron (and an electronneutrino). This process is called inverse beta decay. This can not be confused with "pure" proton decay. An isolated proton can not decay (as far as we have observed). But when inside a nucleus, the daughter nucleus can have a greater binding energy, therefore allowing said decay. A proton can also absorb an electron, creating a neutron (and an electronneutrino). Therefore shifting to Z-1 and N+1. When this happens, we talk about electron capture. A nucleus can emit an entire Helium nucleus, this is called alpha-decay (and the Helium nucleus an alpha particle). A nucleus can also break apart in other pairs of nuclei, this is certainly true for really heavy elements. Lastly, the internal distribution of protons and neutrons can change, resulting in a configuration with exactly the same particles, yet with a lower overall energy (i.e. a lower energy level). With this process, photons (gamma-rays) are emitted.

[1] In nuclear physics, as well as particle physics, mass is oftentimes expressed in terms of energy. Which can be found via Einstein's energy-mass relation.

[2] Therefore, the masses of the electrons are included.

1.4 Size

The size of a nucleus is in the order of femtometre. Where the proton has a diameter of 1.6 fm, while more heavier atoms such as uranium can have a diameter of 15 fm. The radius (and therefore the diameter) is often defined as the rms (root-mean-square) of the radius.

1.5 Spin and Parity

Two other properties are the spin and parity of a nucleus. The parity is either even or odd. It is a rather quantum mechanical property. When the wave function of the nucleus changes sign upon spatial coordinates reflection, one has odd parity. When the sign stays the same, one has even parity. When representing parity, "+" is used for even parity and "-" for odd parity. A nucleus (in its ground state or excited) always has a well defined parity. This is also true for the parity of the entire wave function of an atom. A well defined parity of a quantum system is not something one usually has. More information regarding the parity of nuclei and atoms can be found at section 5 of https://en.wikipedia.org/wiki/Parity_(physics).

The spin of a nucleus is the resulting effect of the alignment of the spins of the nucleons, and how they orbit around each other. A single proton or neutron has spin 1/2. When combining nucleons into a nuclei, these nucleons will pair together following the shell model. A ground level nucleus with 2 protons and 2 neutrons and no orbital momentum will have spin 0. As the two protons and the two neutrons will be paired up, thus each pair having zero spin. When we only have one proton and one neutron, they will not pair together (we fill the shells separate for protons and neutrons). Thus resulting in a spin 1 particle if the orbital momentum is zero. For ground level nuclei and no orbital momentum, the spins can only be 0, 1/2, or 1. Corresponding to all paired nucleons, 1 unpaired nucleon, or both protons and neutrons being unpaired. When exciting the nucleons, much as in the atomic shell model, more unaligned spins are possible. Therefore resulting in higher nuclear spins. Gaining orbital momentum between the nucleons will also result in a higher nuclear spin. The spin can easily go up to spin 10.

1.6 Deformation Parameter and Magnetic Moment

These are the two new properties which will get much attention in this course. As they are directly related to the hyperfine splitting. The magnetic moment arises from the spin of the nuclei and is often expressed in nuclear magneton units $= \frac{e\hbar}{2m_p} = 5.05 \cdot 10^{-27} J/T$. The value in this unit can range from 0 to about 10. The deformation parameter is used to describe the deviation from spherical symmetry. It is often denoted as β_2 and is directly linked to the electric quadrupole moment. It has unit of Coulomb times square meter, and is

often denoted in units $e \cdot 10^{-24} cm^2$. This last surface value is called a "barn", therefore the quadrupole moment is often written as "eb" for electron-barn, sometimes even shortened to simply "b". The value in this unit can range from 0 to about 5, but has been measured as high as 8 (for Lutetium-176). A broader description and use of these parameters will follow in the course of this course.

2 Multipole Moments

2.1 mathematical description

When describing the orbit of a satellite around the Earth, we concentrate all the mass of the sphere inside the centre of the Earth. This gives quite decent solutions within a certain precision, due to the Earth being sort off equal to a sphere[3]. Treating the Earth as a point like particle is the same as treating it as a "gravitational monopole". If one would take said assumed perfectly round Earth and stretch it along one axis, one would need more information to accurately describe the mass distribution. One could introduce a dipole term to accomplish that. The more we deform said distribution of mass, the more terms one would need to describe the mass distribution up to a (self) desired precision. This is precisely how a multipole expansion works. You take a random general distribution of mass or charge, and calculated the multipole terms needed for your calculations, as illustrated in the image below.

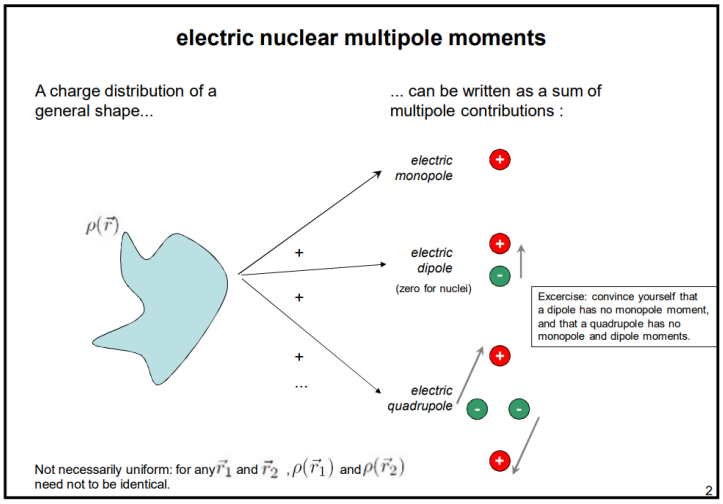

Figure 2: Visual representation of a multipole expansion of a random charge distribution.

[3]For a perfect spheroidal Earth, concentrating all the mass within a point would no longer be an approximation, but would give an exact solution.

If the distribution is really far away or rather spherical symmetric, you might only need the monopole term. If you want more precision on the forces and energy effects, you need a more precise description of the distribution, thus needing more multipole terms.

We all know an electric monopole. The electron, for example, is an electric monopole. A dipole is two monopoles with opposite charge, separated by a certain distance. A quadrupole is two dipoles seperated by a certain distance, and so forth. It is clear that the higher order terms consist of more and more charges, thus closer mimicking the original charge distribution. We will list the first 3 multipole moments: what they are, and how to calculate them.

- The monopole term. This is just one charge. It will translate itself mathematically to the total charge of the distribution, therefore a scalar[4]. It is the same as treating a planet as a point mass. With the change that we can also have negative charges (and no negative masses). Translating this to a formula gives us for a continuous distribution:

$$Q = \int \rho(\mathbf{r}')d\mathbf{r}'$$

  And for a discrete distribution:

$$Q = \sum_{i=1}^{i=N} q_i$$

- The dipole term. This is no longer a scalar, but a vector[5]. It has three components k = x, y, z. One for each spatial coordinate. We will need to multiply each charge with the spatial coordinate of said charge. Translating this to a formula gives us for a continuous distribution for one of the three components:

$$Q_k = \int r'_k \rho(\mathbf{r}')d\mathbf{r}'$$

  And for a discrete distribution:

$$Q_k = \sum_{i=1}^{i=N} q_i d_{ik}$$

- The quadrupole term. This component has 9 terms, corresponding to all possible matches between x, y, z and x, y, z. This term can not be represented by a vector but needs a 3x3 traceless symmetric matrix. Or, in other words, a tensor of rank two. Again, we let k range from x to y to z. The same goes for l. These formulas may seem rather ad hoc, but

[4] This is the same as a rank-0 tensor.
[5] This is the same as a rank-1 tensor.

they are rather difficult to derive purely from searching for a mathematical analogue to the physical representation. It is best to accept them at face value and try to understand them. The symbol δ_{kl} is called a "Kronecker delta". It is zero when $k \neq l$ and 1 when $k = l$. Due to the fact that it is a traceless symmetric matrix, one can check your answers, making sure $Q_{xx} + Q_{yy} + Q_{zz} = 0$ and $Q_{kl} = Q_{lk}$ for all k's and l's. Translating this to a formula gives us for a continuous distribution for one of the nine components:

$$Q_{kl} = \int (3r'_k r'_l - r'^2 \delta_{kl}) \rho(\mathbf{r}') d\mathbf{r}'$$

And for a discrete distribution:

$$Q_{kl} = \sum_{i=1}^{i=N} (3d_{ik} d_{il} - ||\mathbf{d}_i||^2 \delta_{kl}) q_i$$

Higher order formulas will not be given but can be found via the general expression in spherical coordinates:

$$f(\theta, \phi) = \sum_{0}^{\infty} \sum_{m=-l}^{m=l} C_l^m Y_l^m(\theta, \phi)$$

Where the $Y_l^m(\theta, \phi)$'s are the standard spherical harmonics, and the C_l^m's are coefficients which depend on the function.

2.2 The Nucleus

Let us now apply this knowledge to the nucleus. The electric monopole term of the nucleus will simply be the charge of the nucleus. Representing the nucleus as a point charge. This is the representation that we are used to. When dealing with hyperfine interactions, we no longer represent the nucleus as a point charge, but as an object with a shape and size. Higher order multipole terms are therefore needed. As seen in the course video "Why are odd electric moments zero?", the electric dipole moment does not exist. The electric quadrupole term represents, as discussed before, the deviation from spherical symmetry. You will find the electric quadrupole term as a single number β_2[6]. However, in the future we will see that there will be no contradiction between using this one number, or the 5 components in the rank-2 tensor. Higher terms such as the hexadecapole will be labeled as β_4. It is important to note that the multipole expansion only gives info about the shape of the distribution, not the size of the distribution. For the size, we have the rms of the radius.

The electric quadrupole moment is large when the nucleus is heavy, and when the nucleus is strongly deformed. Explained by needing higher order multipole terms to accurately describe said type of nuclei. The rms of r increases as well with increasing mass.

Until now, we used the multipole expansion to describe a static charge distribution, the same can be done for a static current distribution. The words "static" and "current" might seem as an oxymoron, but just imagine an electron revolving around the same point in space indefinitely. The electron is moving, but the current (the electronloop) stays in the same position. Regarding magnetic multipole terms, the opposite for electric multipole terms is true. The odd terms survive while the even terms vanish. This represents itself e.g. into a magnet splitting into two other magnets when breaking in two. Instead of splitting into a monopole magnetic southpole and a monopole magnetic northpole[7]. The first non-zero term therefore is the magnetic dipole moment. The second non-zero term is the magnetic octopole moment. Which is often more than we need for our hyperfine interactions, but can be used to further accurately describe the energy levels. As said before, the magnetic dipole moment is represented by one number, often in terms of nuclear magnetons. This number is the magnitude of the dipole vector.

[6] It is now clear what this two represents, it is the "second" multipole term. Zero being the monopole term.

[7] Magnetic monopoles are predicted in new advanced theories within particle physics, there is ongoing search for them. So far, none have been found.

2.3 Multipole Radiation

This section will be rather short, as a more in-depth description of the video would soon derail too much.

Classical multipole radiation is created when an oscillating charge distribution is present. To be clear, it is the position of the charges that oscillate, not the charges itself. This would break charge conservation, and one would rather not like breaking physics. The gravitational equivalence of multipole (EM) radiation, are gravitational waves. Just as in gravitational waves, energy is lost from the system when multipole radiation is created. One needs to fed the system energy to let it oscillate and create multipole radiation. An oscillating multipole can therefore not be used to represent a decaying nucleus emitting radiation, as a nucleus is not powered. A nucleus is not an oscillating multipole moment, yet it can still emit multipole radiation. How does this work? Each exited state of the same nucleus can be represented via a multipole expansion, unique to each state. When the nucleus decays, it changes from one multipole to another multipole. This transition between multipoles will be the multipole radiation, and can be unshockingly expressed as a multipole expansion. It is important to note that the nucleus is not allowed to have e.g. an electric dipole moment, but the transition expansion can perfectly have said moment.

Hyperfinecourse A: framework

February 5, 2020

Abstract

This document is meant for optional background reading when studying www.hyperfinecourse.org. It deals with one of the chapters of this course. The formal course content is defined by the website and videos. The present document does not belong to the formal course content. It covers the same topics, but usually with more mathematical background, more physical background and more examples. Feel free to use it, as long as it helps you mastering the course content in the videos. If you prefer studying from the videos only, this is perfectly fine.

The present text has been prepared by Jeffrey De Rycke (student in this course in the year 2018-2019). He started from a partial syllabus written by Stefaan Cottenier for an earlier version of this course, and cleaned, edited and elaborated upon that material. That syllabus was itself inspired by a course taught by Michel Rots at KU Leuven (roughly 1990-1995).

1 VIP-1

This section will deal with the logical build up of VIP-1. It will cover the same "ladder" model the video has, but each step will be explained more in details. We will start from how we used to describe basic atoms. Then work our way down from high energy level splitting (excited nuclei), to the energy levels of the excited electrons, to the L-S coupling (fine splitting), all the way to hyperfine splitting.

1.1 Approximations of Basic Nuclei

To describe the H (or even the He atom) we made some basic approximations to make the calculations feasible, these approximations were will be described in short.

1.1.1 Non-relativistic

The non-relativistic quantum mechanical equation for the hydrogen atom (and for any other quantum system) is the Schrödinger equation. Its relativistic analogue is the Dirac equation. To first order in v^2/c^2, the Dirac equation can be approximated by the Schrödinger equation plus three extra terms. Those terms represent the most important relativistic effects. They are:

- *The mass-velocity effect.* The dependence of the electron mass on the electron velocity causes altered orbits for high-speed electrons (= the ones closest to the nucleus).
- *The Darwin effect.* In relativistic quantum physics, the electron can be shown to execute extremely fast random movements over a short length scale, known as the *zitterbewegung* [1]. Therefore, the electron experiences the Coulomb potential by the nucleus as somewhat smeared out, which slightly changes the energy levels of the hydrogen and other atoms.
- *Spin-orbit coupling.* The orbit of an electron (and hence the energy of both the electron and the atom) does not depend only on the electromagnetic interaction of its charge with the charge of the nucleus, but also on its spin: the electron's orbital motion generates a magnetic field, that interacts with its spin magnetic moment. This interaction between spin and orbit is called spin-orbit coupling. Because spin-orbit coupling – and therefore spin – naturally shows up in the Dirac theory, spin can be understood as being a relativistic effect.

[1] This should not be confused with one of the Heisenberg uncertainty principles, which is present already in non-relativistic quantum physics.

1.1.2 Effective Electron-Electron Interactions

When having multiple electrons, solving the electron-electron interactions is exceedingly difficult. Solving the Hamiltonian directly (by expanding the many-electron wave function into a linear combination of Slater determinants) becomes unfeasible as one needs many Slater determinants when the amount of electrons grows and one wants a reasonable accurate solution.

A solution to this is identifying a subspace of the full Hilbert space in which the e-e interactions plays a decisive role. The e-e interaction is then treated explicitly within this limited subspace, while the influence of the rest of the Hilbert space is treated via a mean-field approximation. This greatly reduces the interaction terms as we let the prominent interactions happen in small spaces.

This process of describing the e-e interactions as prominent in certain subspaces (and the rest of the space via a mean-field) is what effective electron-electron interactions are comprised off.

1.1.3 Infinitely Heavy Nucleus

When the nucleus is not infinitely massive any more, electron and nucleus will move about their common centre of mass which lies close to the nucleus[2]. The orbit of the electron (therefore also its energy)will slightly change. Energies corrected for this effect are obtained by multiplying the results from the infinitely massive proton by a factor $\frac{1}{1+\frac{m_e}{M}}$ (M is the mass of the nucleus) . This increases the ground state energy of H by 0.008 eV. For Deuterium ('heavy Hydrogen', with a nucleus of 1 proton and 1 neutron) this formula tells its ground state is 0.004 eV lower than the H ground state. For really heavy nuclei where M is high, the effect of this approximation becomes progressively small.

In contrast to this classical mass effect, a second correction due to finite mass is of a purely quantumphysical origin: the zero-point motion of light objects. A quantummechanical object can never be at rest, even not at 0 K and in its absolute ground state. Always there will be a random vibration about its rest position, a phenomenon that is called zero-point motion and can be understood as a consequence of the uncertainty principle. The lighter the object, the more important the zero-point motion. Nuclei are usually sufficiently heavy to make this zero-point motion negligibly small, but for the lightest nuclei it can become significant.

[2]The proton-to-electron mass ratio is about 1836.

1.1.4 Point Nucleus

The fourth approximation we will discuss is the assumption that the nucleus has no structure. What do we mean by this? In the first place that all protons and neutrons in the nucleus coincide with the same mathematical point. If this is not the case - imagine a spherical, cigar-shaped or even more complex nucleus - the Coulomb potential due to the nucleus will not be spherically symmetric any more. This will result in other solutions and therefore energy levels of our Hamiltonian.

The same happens if the nucleus has structure in a magnetic sense: it can have a magnetic dipole moment (or even a higher order multipole moment). Because of the dipole moment the nucleus will generate a magnetic field, and this breaks the spherical symmetry and hence leads to preferred orientations of the electrons.

And now we have finally arrived at the subject of this course: the role of the structure of the nucleus, in its spatial and magnetic sense. As we will calculate later, the new influence of the nucleus we take now into account will introduce new shifts and splittings of the order of μeV. Because the energy scale which is needed to describe these new splittings is orders of magnitude smaller than the energy scale for the fine structure, the new details in the atomic spectrum are called the *hyperfine structure* of the atom.

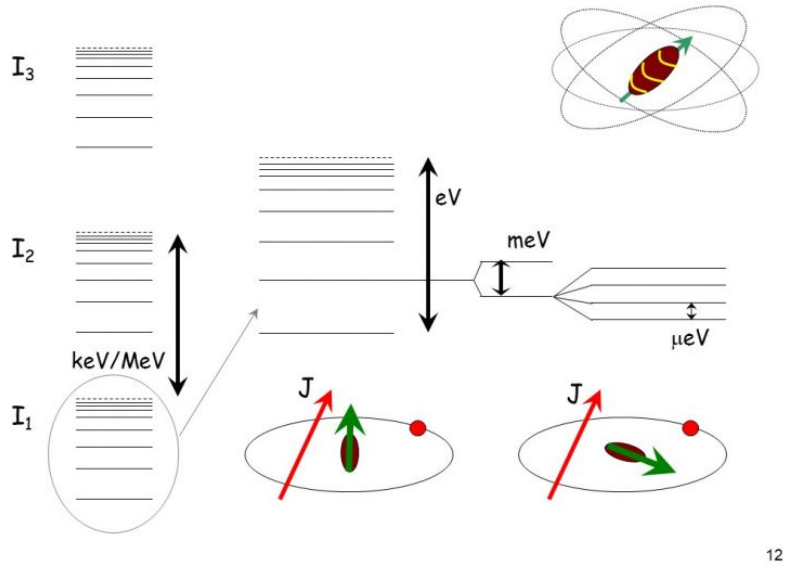

Figure 1: VIP number one. It shows the different energy levels and splittings of an atom.

1.2 The Energy Levels

While reading this section, keep an eye on Fig. 1 p.4. We will constantly be referencing the energy levels on this picture while describing every part of said image. The energy levels on the left are all possible energy levels of the "nucleus + electrons" system. The sections below describe the different attributions to said energy levels. Unfortunately it is not possible to "see" all different energy levels on said energy scale. That's why we zoom in where needed in the centre and on the right side of the image.

1.2.1 Nucleus Excitations

As described in the previous chapter, a nucleus can get excited when the internal distribution of protons and neutrons change. This results in a configuration with exactly the same particles, yet with a higher overall energy (i.e. a higher energy level). These configurations are the most left energy levels I_1, I_2,... This can be done via absorbing a photon in the keV/MeV energy range. Or when a nucleus decays to another nucleus, which can be not yet in its ground state after decaying. As seen via the energy of the photons, the difference in energies are of order keV/MeV.

1.2.2 Electron Excitations

In the Rutherford-Bohr model, electrons orbit the nucleus in well defined orbits. These well defined orbits have well defined energy levels, which are quantized, as seen on the second energy splitting (counting from the left). The difference in energy values are of order eV. It therefore also takes photons in the order of eV to excite electrons to higher orbits.

1.2.3 Spin-Orbit Coupling (fine splitting)

This is where the energy splitting starts to get more complicated. The spin-orbit coupling is a weak magnetic interaction (coupling) between the electron spin and its orbital motion. The intrinsic spin of the electron creates a spin magnetic dipole moment. While, from the restframe of the electron, the rotating nucleus creates a magnetic field. This is why it is called a relativistic effect, it arises from putting ourselves at the position of a stationary electron and moving nucleus. For light atoms, the individual spins $\mathbf{s}_i$ will interact with each other to form a total spin angular momentum $\mathbf{S}$. Likewise, the individual orbital angular momentum $\mathbf{l}_i$ form a total orbital angular momentum $\mathbf{L}$. These quantum numbers $\mathbf{S}$ and $\mathbf{L}$ interact with each other via what is called Russell-Saunders coupling (or simply LS coupling). The $\mathbf{S}$ and $\mathbf{L}$ couple together and form a total angular momentum $\mathbf{J} = \mathbf{L} + \mathbf{S}$. This value depends on the relative orientation between $\mathbf{L}$ and $\mathbf{S}$. Just as how the energy of a system is different between different orientations of a bar magnet in a magnetic field, the energy correction is different for different values of $\mathbf{J}$ as illustrated in the figure on the next page.

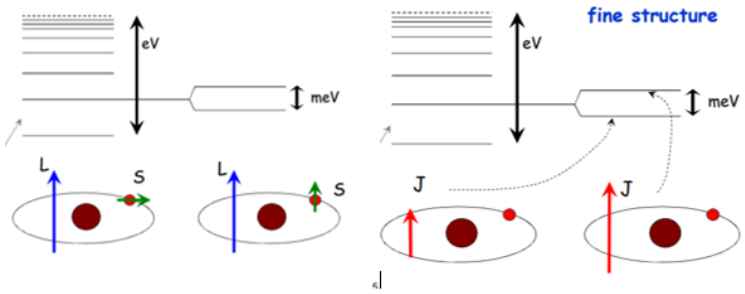

Figure 2: Coupling of different **L** and **S** into different **J**, and its effect on the energy splitting.

On the left, two different relative orientations are shown, each resulting in a different **J**. These different values result in different energy splitting of order of meV.

There is a way of characterizing different states, this is done via the term symbols. A term symbol is defined via ${}^{2S+1}L_J$. For same values of S and L, different orientations (and therefore different values of J) are possible. J ranges from L+S to |L-S| in steps of -1. When filling in L, we use the symbols S, P, D, F, G, H,... instead of 0, 1, 2,...

As stated before, different orientations will result in different energy levels. To know the relative orientation of the energy levels, we can use Hund's rules. They say the following:

- The highest multiplicity (defined as 2S+1) has the lowest energy.
- For the same multiplicity, the largest L has the lowest energy.
- For the same L and half filled or less filled shells, the lowest J has the lowest energy. For the same L and more than half filled shells, the highest J as the lowest energy.

When talking about shells, we of course mean the outer most shell. As electrons of filled shells balance each other in $\mathbf{s}_i$ and $\mathbf{l}_i$, therefore creating S = L = 0 and by extend J = 0.

Take, for example, Sodium. It has a filled s and p shell, and one electron in the 2s shell. This gives us the term ${}^2S_{1/2}$. When exciting this electron to the 2p shell, we have two possible terms. ${}^2P_{1/2}$ and ${}^2P_{3/2}$ (via S = 1/2, the same as before, and L now = 1). Where Hund's rules dictate that $\mathrm{E}({}^2P_{3/2}) > \mathrm{E}({}^2P_{1/2})$. This fine splitting of energy levels is something one can see when looking at the spectrum of a Sodium lamp. An orange doublet can be seen at wavelengths of 589.6 nm and 589.0 nm.

1.2.4 Hyperfine Splitting

Two different hyperfine splittings can be identified. The electric hyperfine splitting and the magnetic hyperfine splitting. The following two sections will be rather short, as they both get their own chapter where they will be broadly discussed.

The electric hyperfine splitting has to do with the interaction of the nuclear quadrupole moment and the electric-field gradient (of the electron cloud). The electric-field gradient measures the change of the electric field at the nucleus generated by the electronic charge distribution. We will see later that this can be described as a coupling between the two parameters (here tensors of rank 2) and this will give an energy splitting (in the order of μeV).

The magnetic hyperfine splitting has to do with the interaction of the nucleur dipole moment and the magnetic hyperfine field. We have seen such a magnetic field before, it is the magnetic field associated with the total angular momentum J. The coupling betwheen these two parameters (both vectors) will give our energy splitting (again in the order of μeV).

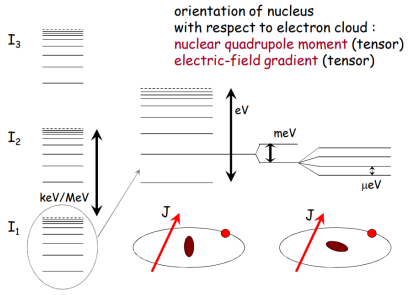

Figure 3: Illustration of the different terms in the electric hyperfine splitting.

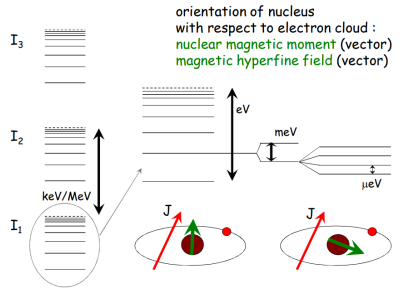

Figure 4: Illustration of the different terms in the magnetic hyperfine splitting.

2 Gravitational Analogue

This section extensively discusses a problem from classical mechanics. We will highly benefit from this when discussing the quantum multipole expansion and the quadrupole term where very similar reasonings appear. The full mathematics will be developed only once here, where we can profit from the absence of quantum mechanics, which could possibly distract us. In the later parts about the multipole expansion and the quadrupole term we will just have to copy the results, and concentrate on the interpretation. Sometimes notation becomes weird in this chapter. We prefer however to give the mathematical objects very explicit names, to point out the often subtle differences between them and hence avoid misconceptions.

2.1 Two Mass Distributions: Multipole Expansion

Take a look at the image bellow. How can we find the potential energy E_{pot} of said static system of two bodies M_1 and M_2 in situation 1? Where both masses are in each others gravitational fields, with their center of mass separated by a vector $\vec{r_0}$.

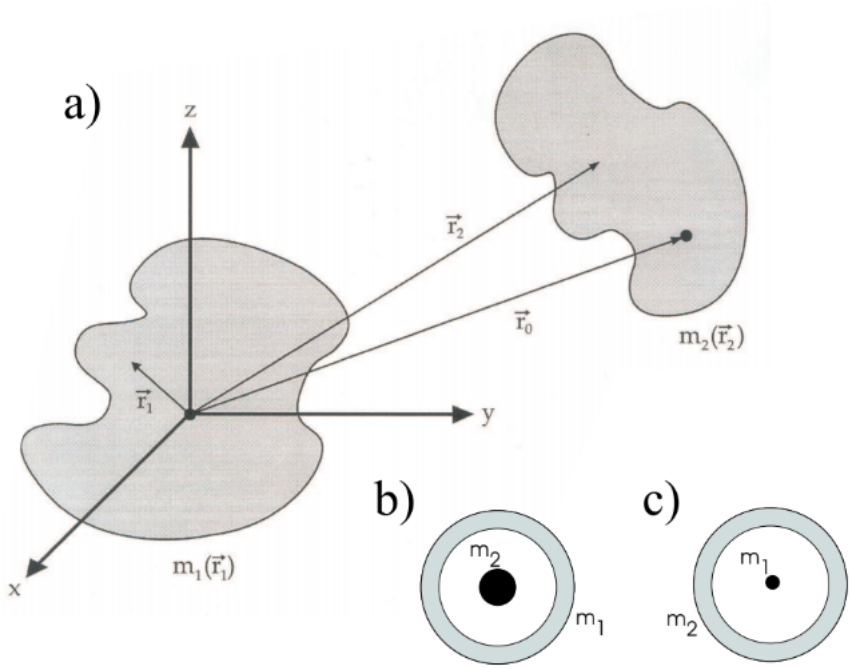

Figure 5: Three situations of two mass distributions interacting via gravitation.

We use the following notation: M_i is the name of the body, m_i its total mass, and $\rho_i(\vec{r_i})$ is its mass density distribution function. Our reference frame XYZ will have its centre in the barycentre of M_1[3]. In general, both mass distributions are inhomogeneous and have an irregular shape. Because potential energy is defined only apart from an additive constant, we make the usual convention that E_{pot} vanishes if the two masses are at an infinite distance from each other.

We can choose to calculate either the potential energy of M_2 in the field of M_1, or vice-versa. Choosing the latter possibility, we can write:

$$E_{pot} = \int_1 \rho_1(\vec{r}_1)\, V_2(\vec{r}_1)\, d\vec{r}_1 \tag{1}$$

The integral is taken over the volume occupied by M_1, or over all space. The potential V_2 of M_2 at $\vec{r}_1$ can be written as:

$$V_2(\vec{r}_1) = -G \int_2 \frac{\rho_2(\vec{r}_2)}{|\vec{r}_2 - \vec{r}_1|}\, d\vec{r}_2 \tag{2}$$

which leads to the following expression for the potential energy:

$$E_{pot} \quad = \quad -G \int_1 \int_2 \frac{\rho_1(\vec{r}_1)\rho_2(\vec{r}_2)}{|\vec{r}_2 - \vec{r}_1|}\, d\vec{r}_1\, d\vec{r}_2 \tag{3}$$

Due to the possibly irregular shapes (as will be in most general cases) of both mass distributions, the integrals in equations 1 to 3 can be hard to calculate. In order to be able to deal with simpler integrals and in order to gain simultaneously physical insight, we will make a series expansion of equation 3 using the so-called *Laplace expansion* or *multipole expansion* in spherical coordinates[4]

$$\frac{1}{|\vec{r}_2 - \vec{r}_1|} = 4\pi \sum_{n,q} \frac{r_<^n}{r_>^{n+1}} \frac{1}{2n+1}\, Y_q^{n*}(\theta_1,\, \phi_1) Y_q^n(\theta_2,\, \phi_2) \tag{4}$$

with $r_< = min\,(r_1,\, r_2)$ and $r_> = max\,(r_1,\, r_2)$. The potential energy of equation 3 then becomes:

$$E_{pot} = -4\pi\, G \int_1 \int_2 \rho_1(\vec{r}_1)\rho_2(\vec{r}_2) \left(\sum_{n,q} \frac{r_<^n}{r_>^{n+1}} \frac{1}{2n+1}\, Y_q^{n*}(\theta_1,\, \phi_1) Y_q^n(\theta_2,\, \phi_2) \right) d\vec{r}_1\, d\vec{r}_2 \tag{5}$$

[3] Any other centre will yield the same mathematics, but using this condition makes further calculations a lot easier.

[4] The Condon-Shortley phase convention for the spherical harmonics is used, see http://mathworld.wolfram.com/Condon-ShortleyPhase.html

In general, this is still a sum of very complicated integrals, as we cannot separate the integration over $\vec{r}_1$ and $\vec{r}_2$. However, if the two bodies are such that **any** r_1 **is smaller then any** r_2 [5], the separation can be made and we obtain:

$$E_{pot} = \sum_{n,q} Q_q^{n*} V_q^n \tag{6}$$

with

$$Q_q^n = \sqrt{\frac{4\pi}{2n+1}} \int_1 \rho_1(\vec{r}_1)\, r_1^n\, Y_q^n(\theta_1,\, \phi_1)\, d\vec{r}_1 \tag{7}$$

and

$$V_q^n = -G\sqrt{\frac{4\pi}{2n+1}} \int_2 \frac{\rho_2(\vec{r}_2)}{r_2^{n+1}}\, Y_q^n(\theta_2,\, \phi_2)\, d\vec{r}_2 \tag{8}$$

The Q-tensors have units $\mathrm{kg\,m}^n$, the V-tensors $\mathrm{N}/(\mathrm{kg\,m}^{n-1})$ and their products Nm or J. It is important to realize that the summation is a dot product between two spherical tensors (a different prefactor can occur if the dot product is taken between cartesian tensors).

2.2 The monopole term (n=0)

The monopole term can be read as a dot product between two tensors of rank 0 (scalars): the monopole moment Q_0^0 due to M_1 (units: kg), and the monopole field V_0^0 due to M_2 (units: Nm/kg). Explicit expressions are:

$$Q_0^0 = m_1 \tag{9}$$

$$V_0^0 = -G \int \frac{\rho_2(\vec{r}_2)}{|\vec{r}_2|}\, d\vec{r}_2 \tag{10}$$

$$E_{pot}^{(0)} = Q_0^{0*} V_0^0 \tag{11}$$

The monopole field is nothing else than the gravitational potential at the origin (where the barycentre of M_1 is) due to M_2, while the monopole moment is the total mass m_1 of M_1. The monopole contribution to the potential energy would be the only and exact contribution to the potential energy in the case where M_1 would be a point mass, situated at the origin.

[5] This excludes *a)* bodies that overlap (not possible for masses, but possible for charges: e.g. s-electron penetration in the nucleus), and *b)* a body with a hole in which a bulge on the other body enters.

2.3 The dipole term (n=1)

The dipole term can be read as a dot product between two tensors of rank 1 (vectors): the dipole moment Q_q^1 due to M_1 (units: kg m), and the dipole field V_q^1 due to M_2 (units: N/kg). Explicit expressions are:

$$Q_q^1 = \sqrt{\frac{4\pi}{3}} \int_1 \rho_1(\vec{r}_1)\, r_1\, Y_q^1(\theta_1,\, \phi_1)\, d\vec{r}_1 \tag{12}$$

$$V_q^1 = -G\sqrt{\frac{4\pi}{3}} \int_2 \frac{\rho_2(\vec{r}_2)}{r_2^2}\, Y_q^1(\theta_2,\, \phi_2)\, d\vec{r}_2 \tag{13}$$

$$E_{pot}^{(1)} = \sum_{q=-1,0,1} Q_q^{1*} V_q^1 \tag{14}$$

We can transform the dipole moment into 3 components of a cartesian vector, which will be more easily interpretable:

$$Q_x = \frac{\sqrt{2}}{2}\left(Q_{-1}^1 - Q_{+1}^1\right) \tag{15}$$

$$= \int_1 \rho_1(\vec{r}_1)\, r_1\, \sin\theta \cos\phi\, d\vec{r}_1 \tag{16}$$

$$= \int_1 \rho_1(\vec{r}_1)\, x_1\, d\vec{r}_1 \tag{17}$$

$$Q_y = \int_1 \rho_1(\vec{r}_1)\, y_1\, d\vec{r}_1 \tag{18}$$

$$Q_z = \int_1 \rho_1(\vec{r}_1)\, z_1\, d\vec{r}_1 \tag{19}$$

One recognizes the definition of the position vector of the center of mass of M_1, multiplied by the total mass m_1. As we have chosen the origin of the axis system in the center of mass, we can conclude that the three components of the dipole moment are zero, both in the cartesian and in the spherical form.

In a similar way, the following cartesian components are found for the dipole field:

$$V_x = -G \int_2 \frac{\rho_2(\vec{r}_2)}{|r_2|^3}\, x_2\, d\vec{r}_2 \tag{20}$$

$$V_y = -G \int_2 \frac{\rho_2(\vec{r}_2)}{|r_2|^3}\, y_2\, d\vec{r}_2 \tag{21}$$

$$V_z = -G \int_2 \frac{\rho_2(\vec{r}_2)}{|r_2|^3}\, z_2\, d\vec{r}_2 \tag{22}$$

One recognizes now that the dipole field vector is the opposite of the gravitational field due to M_2 at the origin[6].

2.4 The quadrupole term (n=2)

The quadrupole term can be read as a dot product between two tensors of rank 2: the quadrupole moment Q_q^2 due to M_1 (units: $\mathrm{kg\,m^2}$), and the quadrupole field V_q^2 due to M_2 (units: $\mathrm{N/(kg\,m)}$). Explicit expressions are:

$$Q_q^2 = \sqrt{\frac{4\pi}{5}} \int_1 \rho_1(\vec{r}_1)\, r_1^2\, Y_q^2(\theta_1,\, \phi_1)\, d\vec{r}_1 \tag{24}$$

$$V_q^2 = -G\sqrt{\frac{4\pi}{5}} \int_2 \frac{\rho_2(\vec{r}_2)}{r_2^3}\, Y_q^2(\theta_2,\, \phi_2)\, d\vec{r}_2 \tag{25}$$

$$E_{pot}^{(2)} = \sum_{q=-2,\ldots,2} Q_q^{2*} V_q^2 \tag{26}$$

Being given a spherical tensor field of rank 2, the corresponding 6 components of its cartesian form (only 5 of them are independent) are found by:

$$\begin{aligned} a_{11} &= \frac{\sqrt{6}}{2}\left(a_2^2 + a_{-2}^2\right) - a_0^2 \\ a_{22} &= -\frac{\sqrt{6}}{2}\left(a_2^2 + a_{-2}^2\right) - a_0^2 \\ a_{33} &= 2a_0^2 \\ a_{12} &= -\frac{\sqrt{6}}{2} i \left(a_2^2 - a_{-2}^2\right) \\ a_{13} &= -\frac{\sqrt{6}}{2}\left(a_1^2 - a_{-1}^2\right) \\ a_{23} &= \frac{\sqrt{6}}{2} i \left(a_1^2 + a_{-1}^2\right) \end{aligned} \tag{27, 28}$$

The quadrupole moment tensor can be transformed in its cartesian form: a traceless, symmetric matrix:

$${}_cQ_{sh}^{(2)} = \int_1 \rho_1(\vec{r}_1) \begin{bmatrix} 3x_1^2 - r_1^2 & 3x_1y_1 & 3x_1z_1 \\ 3x_1y_1 & 3y_1^2 - r_1^2 & 3y_1z_1 \\ 3x_1z_1 & 3y_1z_1 & 3z_1^2 - r_1^2 \end{bmatrix} d\vec{r}_1 \tag{29}$$

[6] $\vec{E}_2(\vec{0}) = -\vec{\nabla} V_2(\vec{0})$, with V_2 given by equation 2. This results in:

$$\vec{E}_2(\vec{0}) = G \int_2 \frac{\rho_2(\vec{r}_2)}{|r_2|^3}\, \vec{r}_2\, d\vec{r}_2 \tag{23}$$

It is understood that the integration over $\vec{r}_1$ is performed for all of the 9 elements. The physical interpretation of the quadrupole moment tensor is as follows: its i^{th} diagonal element will be positive if along the i^{th} axis of the reference frame the actual radius of M_1 is larger than the radius of the best-approximating sphere. In this situation M_1 is said to be *prolate* along this axis. In the inverse case, M_1 is *oblate* along this axis (see example in Fig. 6). For a perfect sphere, this tensor is zero.

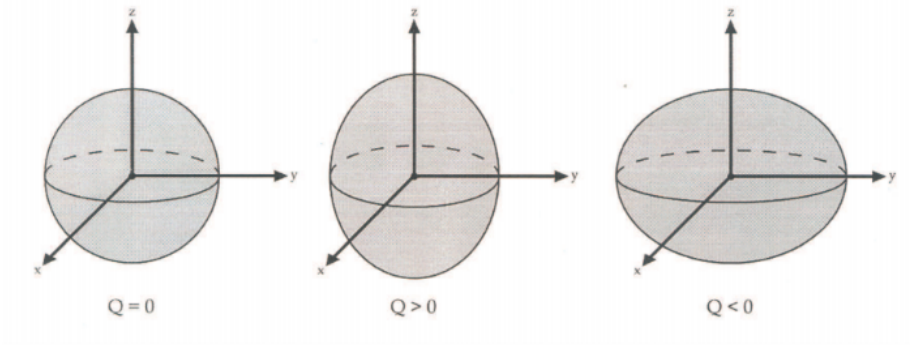

Figure 6: *A spherical, prolate and oblate mass distribution (with respect to the z-axis).*

The same transformation (using equation 27) can be done for the quadrupole field:

$$ {}_cV_{sh}^{(2)} = -G \int_2 \frac{\rho_2(\vec{r}_2)}{|\vec{r}_2|^5} \begin{bmatrix} 3x_2^2 - r_2^2 & 3x_2y_2 & 3x_2z_2 \\ 3x_2y_2 & 3y_2^2 - r_2^2 & 3y_2z_2 \\ 3x_2z_2 & 3y_2z_2 & 3z_2^2 - r_2^2 \end{bmatrix} d\vec{r}_2 \quad (30) $$

Note that the structure of this quadrupole field tensor is definitely different from the quadrupole moment tensor, due to the factor $1/|\vec{r}_2|^5$.

How to interpret the meaning of this tensor? Let us take the negative gradient of the x-component of the gravitational field:

$$ -\nabla E_{2x}(\vec{0}) = \left(-\frac{\partial E_{2x}(\vec{0})}{\partial x_1}, -\frac{\partial E_{2x}(\vec{0})}{\partial y_1}, -\frac{\partial E_{2x}(\vec{0})}{\partial z_1} \right) \quad (31) $$

$$ = \left(\frac{\partial^2 V_2(\vec{0})}{\partial x_1^2}, \frac{\partial^2 V_2(\vec{0})}{\partial y_1 \partial x_1}, \frac{\partial^2 V_2(\vec{0})}{\partial z_1 \partial x_1} \right) \quad (32) $$

Repeating this for the y- and z-components of the gravitational field leads to 9 quantities which can be arranged in a symmetric matrix:

$$\begin{bmatrix} \frac{\partial^2 V_2(\vec{0})}{\partial x_1^2} & \frac{\partial^2 V_2(\vec{0})}{\partial y_1 \partial x_1} & \frac{\partial^2 V_2(\vec{0})}{\partial z_1 \partial x_1} \\ \frac{\partial^2 V_2(\vec{0})}{\partial x_1 \partial y_1} & \frac{\partial^2 V_2(\vec{0})}{\partial y_1^2} & \frac{\partial^2 V_2(\vec{0})}{\partial z_1 \partial y_1} \\ \frac{\partial^2 V_2(\vec{0})}{\partial x_1 \partial z_1} & \frac{\partial^2 f(\vec{0})}{\partial y_1 \partial z_1} & \frac{\partial^2 V_2(\vec{0})}{\partial z_1^2} \end{bmatrix} \tag{33}$$

This matrix is also trace-less. Indeed, its trace is the Laplacian of the potential due to M_2, evaluated at the origin:

$$\Delta V_2(\vec{0}) \;=\; \frac{\partial^2 V_2(\vec{0})}{\partial x^2} + \frac{\partial^2 V_2(\vec{0})}{\partial y^2} + \frac{\partial^2 V_2(\vec{0})}{\partial z^2} \;=\; 4\pi\, G\, \rho_2(\vec{0}) \tag{34}$$

By the Poisson equation, this Laplacian can be related to $\rho_2(\vec{0})$, the mass density of M_2 at the origin. By our restriction that $\vec{r}_1 < \vec{r}_2$, $\rho_2(\vec{0})$ must necessarily be zero, and the above matrix is trace-less. You can verify now that:

$$V_{ij} \;=\; \frac{\partial^2 V_2(\vec{0})}{\partial x_{1i} \partial x_{1j}} \tag{35}$$

$$\;=\; -G \int_2 \frac{\rho_2(\vec{r}_2)}{|\vec{r}_2|^5} \left(3 x_{2i} x_{2j} - r_2^2 \delta_{ij}\right) d\vec{r}_2 \tag{36}$$

which are exactly the 9 components of the cartesian form of the quadrupole field given in equation 30. Looking at equations 31 and 33, we can therefore interpret the quadrupole field tensor as the negative gradient of the gravitational field at the origin due to M_2. Therefore the quadrupole field tensor is often called the *(gravitational-) field gradient* tensor. Its ij^{th} element expresses how strongly the i-component of the gravitational field at the origin varies if one goes along the j-direction.

2.5 Correction to Multipole Expansion.

By assuming $r_1 < r_2$ in the Laplace expansion, we made an error for those mass distributions where this condition is not fulfilled. Often this error will be small, but in the case of overlapping charge distributions as we will meet them in the following chapters, it will produce nevertheless measurable effects. The necessary corrections can be expressed as corrections to each of the multipole terms separately, but the correction to the monopole term is the most important one. In order to find this correction, we will take the opportunity to use the multipole expansion in cartesian coordinates rather than the Laplace expansion, which sheds a different light on the problem we have just solved in spherical coordinates. The full solution using spherical coordinates involves Tesseral harmonics, and can be found at many places.

We start again from equation 3. In order to avoid the complicated integral in this expression, we make a Taylor expansion of V_2 around the origin of the axis system. Such a Taylor expansion converges rapidly if the points $\vec{r}_1$ at which we need the value of V_2 are much closer to the origin than the major part of the mass of M_2 is. We assume that this is the case[7], and will truncate the series after the second order term. On how to expand a potential, consider a function

$$f(\vec{r}) \quad = \quad \int \frac{g(\vec{r}_v)}{|\vec{r}_v - \vec{r}|}\, d\vec{r}_v \tag{37}$$

The integral runs over that part of space where $g(\vec{r}_v)$ is not zero, which might be a finite or infinite region. If g is a charge or mass distribution, f gives the electric or gravitational potential in a point $\vec{r}$ (apart from an appropriate factor). That point can be either inside or outside the non-zero region of g. If it lies inside, the denominator in the integral becomes zero and we have to care about the convergence of the integral. The latter is determined by the properties of g. We assume that we know the value of f and of all its derivatives *at the origin* $\vec{0}$. What we want to know is the value of f at points $\vec{r} = (x, y, z)$ that are not far away from $\vec{0}$. This means we need a Taylor expansion of $f(\vec{r})$ around $\vec{0}$. The general form of a Taylor expansion around $\vec{0}$ for a function with vectors as argument, is:

$$f(\vec{0} + \vec{r}) \quad = \quad \sum_{j=0}^{\infty} \left[\frac{1}{j!} \left(\vec{r} \cdot \vec{\nabla}_{\vec{r}\,'} \right)^j \, f(\vec{r}\,') \right]_{\vec{r}\,'=\vec{0}} \tag{38}$$

Explicitly for our case, this gives for the zeroth order term:

$$\begin{aligned} E_{pot}^{(0)} &= \left(\int \rho_1(\vec{r}_1)\, d\vec{r}_1 \right) V_2(\vec{0}) && (39)\\ &= m_1\, V_2(\vec{0}) && (40)\\ &= m_1 \left(-G \int \frac{\rho_2(\vec{r}_2)}{|\vec{r}_2|}\, d\vec{r}_2 \right) && (41)\\ &= Q_0^0 V_0^0 && (42)\\ &= {}_sQ_{sh}^{(0)} \cdot {}_sV_{sh}^{(0)} \;=\; {}_cQ_{sh}^{(0)} \cdot {}_cV_{sh}^{(0)} && (43) \end{aligned}$$

In equation 41, we recognize the monopole moment and monopole field derived in equations 9 and 10.

[7] We will use this later for atoms, where $\vec{r}_1$ is of the order of the nuclear radius (10^{-15} m) and $\vec{r}_2$ of the order of the radius of an electron orbit (10^{-10} m).

The first order term in the expansion of E_{pot} can be written as:

$$E^{(1)}_{pot} = \left[\int \rho_1(\vec{r}_1) x_1 \, d\vec{r}_1 \quad \int \rho_1(\vec{r}_1) y_1 \, d\vec{r}_1 \quad \int \rho_1(\vec{r}_1) z_1 \, d\vec{r}_1 \right] \begin{bmatrix} \frac{\partial V_2(\vec{0})}{\partial x_1} \\ \frac{\partial V_2(\vec{0})}{\partial y_1} \\ \frac{\partial V_2(\vec{0})}{\partial z_1} \end{bmatrix} \tag{44}$$

$$= \left[\int \rho_1(\vec{r}_1) x_1 \, d\vec{r}_1 \quad \int \rho_1(\vec{r}_1) y_1 \, d\vec{r}_1 \quad \int \rho_1(\vec{r}_1) z_1 \, d\vec{r}_1 \right] \begin{bmatrix} -G \int \frac{\rho_2(\vec{r}_2)}{|\vec{r}_2|^3} x_2 \, d\vec{r}_2 \\ -G \int \frac{\rho_2(\vec{r}_2)}{|\vec{r}_2|^3} y_2 \, d\vec{r}_2 \\ -G \int \frac{\rho_2(\vec{r}_2)}{|\vec{r}_2|^3} z_2 \, d\vec{r}_2 \end{bmatrix} \tag{45}$$

$$= {}_cQ^{(1)}_{sh} \cdot {}_cV^{(1)}_{sh} = {}_sQ^{(1)}_{sh} \cdot {}_sV^{(1)}_{sh} \tag{46}$$

We recognize the cartesian forms of the dipole moment and the dipole field, as derived before.
The second order term in the expansion of E_{pot} is:

$$E^{(2)}_{pot} = \frac{1}{2} \begin{bmatrix} \int \rho_1(\vec{r}_1) x_1^2 \, d\vec{r}_1 & \int \rho_1(\vec{r}_1) x_1 y_1 \, d\vec{r}_1 & \int \rho_1(\vec{r}_1) x_1 z_1 \, d\vec{r}_1 \\ \int \rho_1(\vec{r}_1) y_1 x_1 \, d\vec{r}_1 & \int \rho_1(\vec{r}_1) y_1^2 \, d\vec{r}_1 & \int \rho_1(\vec{r}_1) y_1 z_1 \, d\vec{r}_1 \\ \int \rho_1(\vec{r}_1) z_1 x_1 \, d\vec{r}_1 & \int \rho_1(\vec{r}_1) z_1 y_1 \, d\vec{r}_1 & \int \rho_1(\vec{r}_1) z_1^2 \, d\vec{r}_1 \end{bmatrix} \cdot \begin{bmatrix} \frac{\partial^2 V_2(\vec{0})}{\partial x_1^2} & \frac{\partial^2 V_2(\vec{0})}{\partial y_1 \partial x_1} & \frac{\partial^2 V_2(\vec{0})}{\partial z_1 \partial x_1} \\ \frac{\partial^2 V_2(\vec{0})}{\partial x_1 \partial y_1} & \frac{\partial^2 V_2(\vec{0})}{\partial y_1^2} & \frac{\partial^2 V_2(\vec{0})}{\partial z_1 \partial y_1} \\ \frac{\partial^2 V_2(\vec{0})}{\partial x_1 \partial z_1} & \frac{\partial^2 f(\vec{0})}{\partial y_1 \partial z_1} & \frac{\partial^2 V_2(\vec{0})}{\partial z_1^2} \end{bmatrix} \tag{47}$$

$$= \frac{1}{2} \, {}_cK^{(2)} \cdot {}_cW^{(2)} \tag{48}$$

This is a dot product between two (Cartesian) tensors of rank 2 (mind the fact that this is no matrix multiplication, but short-hand notation for a dot product)[8]. In contrast to the zeroth and first order terms, we cannot immediately identify the two cartesian tensors in this dot product with multipole moments and multipole fields. The left tensor seems to be related to the quadrupole moment (equation 29), but is not identical to it. The right tensor seems at first

[8] We are all accustomed to the dot product for 2 vectors of dimension n. Where we multiply the first element of the first vector with the first element of the second vector and sum it with the product between the second element of the first vector and the second element of the second vector and so on to the n'th pair of elements. It is clear that both vectors need to be of the same dimention. The same holds for the dot product between two matrices (dimensions n x m). Here we will multiply element (0,0) of the first matrix with element (0,0) of the second matrix and sum it with the product between (0,1) of the first matrix and element (0,1) of the second matrix, all the way to (0,m). Then we continue summing for (1,0) to (1,m). Up to (n,0) to (n,m). Summing each product until we get our final result (a scalar).

sight identical to the cartesian form of the quadrupole field (equation 30), but it is not: its trace – the Laplacian of the potential – is not necessarily zero, because we did not need to require $r_1 < r_2$ for the Taylor expansion. By equation 34, this trace can be different from zero. But we can write in the same way both tensors as a sum of the quadrupole moment/field and a multiple of the unit 3×3 matrix (the integrations are noted in short-hand by curled {brackets}):

$$ {}_cK^{(2)} = \frac{1}{3}\begin{bmatrix} \{3x_1^2\} - \{r_1^2\} & \{3x_1y_1\} & \{3x_1z_1\} \\ \{3y_1x_1\} & \{3y_1^2\} - \{r_1^2\} & \{3y_1z_1\} \\ \{3z_1x_1\} & \{3z_1y_1\} & \{3z_1^2\} - \{r_1^2\} \end{bmatrix} + \frac{1}{3}\begin{bmatrix} \{r_1^2\} & 0 & 0 \\ 0 & \{r_1^2\} & 0 \\ 0 & 0 & \{r_1^2\} \end{bmatrix} \tag{49} $$

$$ {}_cW^{(2)} = \begin{bmatrix} \frac{\partial^2 V_2(\vec{0})}{\partial x_1^2} - \frac{\Delta V_2(\vec{0})}{3} & \frac{\partial^2 V_2(\vec{0})}{\partial y_1 \partial x_1} & \frac{\partial^2 V_2(\vec{0})}{\partial z_1 \partial x_1} \\ \frac{\partial^2 V_2(\vec{0})}{\partial x_1 \partial y_1} & \frac{\partial^2 V_2(\vec{0})}{\partial y_1^2} - \frac{\Delta V_2(\vec{0})}{3} & \frac{\partial^2 V_2(\vec{0})}{\partial z_1 \partial y_1} \\ \frac{\partial^2 V_2(\vec{0})}{\partial x_1 \partial z_1} & \frac{\partial^2 f(\vec{0})}{\partial y_1 \partial z_1} & \frac{\partial^2 V_2(\vec{0})}{\partial z_1^2} - \frac{\Delta V_2(\vec{0})}{3} \end{bmatrix} + \begin{bmatrix} \frac{\Delta V_2(\vec{0})}{3} & 0 & 0 \\ 0 & \frac{\Delta V_2(\vec{0})}{3} & 0 \\ 0 & 0 & \frac{\Delta V_2(\vec{0})}{3} \end{bmatrix} \tag{50} $$

Now make the dot product between these two sums. You end up with 4 terms, of which two will be zero: the dot product between a trace-less tensor and a multiple of a unit matrix is zero. With the two nonzero terms we can write the second order term of the Taylor expansion of E_{pot} as:

$$ \begin{aligned} E_{pot}^{(2)} = {} & \frac{1}{6}\begin{bmatrix} \{3x_1^2\} - \{r_1^2\} & \{3x_1y_1\} & \{3x_1z_1\} \\ \{3y_1x_1\} & \{3y_1^2\} - \{r_1^2\} & \{3y_1z_1\} \\ \{3z_1x_1\} & \{3z_1y_1\} & \{3z_1^2\} - \{r_1^2\} \end{bmatrix} \cdot \\ & \begin{bmatrix} \frac{\partial^2 V_2(\vec{0})}{\partial x_1^2} - \frac{\Delta V_2(\vec{0})}{3} & \frac{\partial^2 V_2(\vec{0})}{\partial y_1 \partial x_1} & \frac{\partial^2 V_2(\vec{0})}{\partial z_1 \partial x_1} \\ \frac{\partial^2 V_2(\vec{0})}{\partial x_1 \partial y_1} & \frac{\partial^2 V_2(\vec{0})}{\partial y_1^2} - \frac{\Delta V_2(\vec{0})}{3} & \frac{\partial^2 V_2(\vec{0})}{\partial z_1 \partial y_1} \\ \frac{\partial^2 V_2(\vec{0})}{\partial x_1 \partial z_1} & \frac{\partial^2 f(\vec{0})}{\partial y_1 \partial z_1} & \frac{\partial^2 V_2(\vec{0})}{\partial z_1^2} - \frac{\Delta V_2(\vec{0})}{3} \end{bmatrix} + \\ & \frac{1}{6}\begin{bmatrix} \{r_1^2\} & 0 & 0 \\ 0 & \{r_1^2\} & 0 \\ 0 & 0 & \{r_1^2\} \end{bmatrix} \cdot \begin{bmatrix} \frac{\Delta V_2(\vec{0})}{3} & 0 & 0 \\ 0 & \frac{\Delta V_2(\vec{0})}{3} & 0 \\ 0 & 0 & \frac{\Delta V_2(\vec{0})}{3} \end{bmatrix} \end{aligned} \tag{51} $$

Working it out shows that this is just a scalar product between two numbers, which we can interpret as a dot product:

$$ \frac{1}{6} {}_cQ_{sz}^{(0)} \cdot {}_cV_{sz}^{(0)} = \frac{1}{6}\Delta V_2(\vec{0}) \left\langle r_1^2 \right\rangle \tag{52} $$

$$ = \frac{4\pi G}{6}\rho_2(\vec{0}) \int \rho_1(\vec{r}_1)\, r_1^2 \, d\vec{r}_1 \tag{53} $$

This energy term is the leading correction to the multipole expansion of equation 6 for situations where r_1 can be larger than r_2. It is a dot product between two tensors of rank 0, hence this is a correction to the monopole term of the multipole expansion. The reason why we find this contribution in the Taylor expansion and not in the (approximated) Laplace expansion is that in the former we did not require $r_1 < r_2$.

3 The Double Ring

Consider a dumb-bell consisting out of two equal point masses connected by a rigid massless rod. The total mass of the dumb-bell is m_1, the length of the rod is l_1. As the dumb-bell will play the role of M_1, we fix it with its centre of mass (the middle of the rod) to the origin of an axis system XYZ, in such a way that the dumb-bell can rotate freely about this origin. As second mass distribution take 2 rings with radius R in planes parallel to XY, separated by a distance h, one $\frac{h}{2}$ above the XY-plane and one $\frac{h}{2}$ below it. The total mass of the 2 rings is m_2, and its (constant) linear mass density is ρ_2 (fig. reffig-2-3). The question we want to solve is: if also the rings are kept fixed in XYZ, what will be the preferred (= lowest-energy) orientation of the dumb-bell?

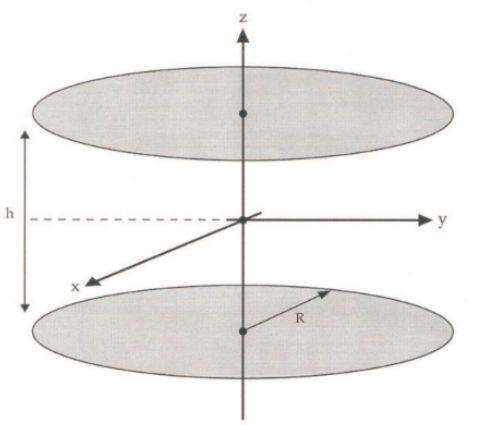

Figure 7: *A double ring system. The rings are shaded gray for clarity, but actually they are hollow and all mass is concentrated at their circumference.*

The condition $\frac{r_1}{r_2} \ll 1$ becomes here $\frac{l_1}{2} \ll \sqrt{\frac{h^2}{4} + R^2}$, which is fulfilled if the length of the dumb-bell is small enough compared to the geometry of the double ring. The problem has some circular symmetry, and it will be useful to use spherical coordinates in the cartesian tensors[9]. There is no overlap and hence

[9] An alternative is to use equation 5 up to the quadrupole term. Try this solution yourself.

no size-dependent monopole term. The shape-dependent monopole term can easily be calculated to be[10]:

$$\begin{aligned} E_{pot}^{(0)} &= V_{sh}^{(0)} \cdot Q_{sh}^{(0)} \\ &= -\frac{Gm_1m_2}{\sqrt{\frac{h^2}{4}+R^2}} \end{aligned} \tag{54}$$

For an arbitrary orientation (θ, ϕ) of the dumb-bell, its quadrupole moment is:

$${}_cQ_{sh}^{(2)} = \frac{3m_1l_1^2}{4} \begin{bmatrix} \sin^2\theta\cos^2\phi - \frac{1}{3} & \sin^2\theta\sin\phi\cos\phi & \sin\theta\cos\theta\cos\phi \\ \sin^2\theta\sin\phi\cos\phi & \sin^2\theta\sin^2\phi - \frac{1}{3} & \sin\theta\cos\theta\sin\phi \\ \sin\theta\cos\theta\cos\phi & \sin\theta\cos\theta\sin\phi & \cos^2\theta - \frac{1}{3} \end{bmatrix} \tag{55}$$

Note that this quadrupole moment does not change upon inversion of the axis system ($\theta \to \pi - \theta$, $\phi \to \phi + \pi$), which we expect as also the dumb-bell has inversion symmetry.

In order to calculate the tensor of the gradient of the gravitational field generated by the rings at the origin of XYZ, we use the following equalities:

$$\begin{cases} R = r_2 \sin\theta_0 \\ h = 2r_2\cos\theta_0 \\ \rho_2 = \frac{m_2}{4\pi\, r_2 \sin\theta_0} \\ R^2 + \frac{h^2}{4} = r_2^2 \end{cases} \tag{56}$$

and find that[11] (there is no overlap, such that $\rho_2(\vec{0}) = 0$):

$${}_cV_{sh}^{(2)} = -\frac{Gm_2\,(h^2-2R^2)}{8R(R^2+\frac{h^2}{4})^{\frac{5}{2}}} \begin{bmatrix} -1 & 0 & 0 \\ 0 & -1 & 0 \\ 0 & 0 & 2 \end{bmatrix} \tag{57}$$

The diagonal form of this equation shows that XYZ by chance (?) is a principal axis system for the tensor $V_{sh}^{(2)}$. After some straightforward goniometric manipulation, the quadrupole energy becomes:

$$\frac{1}{6}Q_{sh}^{(2)} \cdot V_{sh}^{(2)} = -\frac{3Gm_1m_2\,l_1^2\,(h^2-2R^2)}{32R(R^2+\frac{h^2}{4})^{\frac{5}{2}}}\,(2\cos^2\theta - \sin^2\theta) \tag{58}$$

This energy does not depend on the azimuthal orientation ϕ of the dumb-bell. The value of θ_{low} where the quadrupole energy is minimal will depend on the sign of $h^2 - 2R^2$:

$$\begin{cases} \sqrt{2}\,R < h & \Longrightarrow \quad \theta_{low} = 0^\circ \\ \sqrt{2}\,R = h & \Longrightarrow \quad \theta_{low} = \textit{any angle} \\ \sqrt{2}\,R > h & \Longrightarrow \quad \theta_{low} = 90^\circ \end{cases} \tag{59}$$

[10] Both centers of mass coincide at $\vec{0}$, hence $\vec{r}_0 = \vec{0}$ and one could write everything explicitly in terms of fields as $E_{pot}^{(0)}(\vec{0})$ etc.

[11] take $d\vec{r}_2 = 2\,r_2 \sin\theta_0\, d\phi$ (the factor 2 is due to the *double* ring)

If the radius is small enough compared to the distance between the rings, the dumb-bell has it lowest energy when it lies parallel to the Z-axis. Not unexpected: the limiting case are two rings which are so small that they are almost point masses on the z-axis, and obviously the dumb-bell would like to lie along the z-axis in such case, as this minimizes the distance between the dumb-bell and the masses, and hence maximizes the gravitational attraction. When the radius is large, the dumb-bell prefers an orientation in the XY-plane. Also not unexpected: the limiting case is two coinciding rings, and now distances are minimized if the dumb-bell is in the plane of the rings. One special R/h-ratio exists for which the orientation of the dumb-bell does not matter.

It is instructive to have a closer look at this. In section 2.4, we defined the *main component* of a rank 2 tensor, and mass distributions are divided into three distinct classes based on the sign of their main component (see Figure 6). With this terminology, we see that θ_{low} for the dumb-bell being 0°, anything or 90° corresponds to the main component of the double ring's field gradient being negative, zero or positive (equation 57). Three typical double ring systems belonging to each of the 3 classes are drawn below.

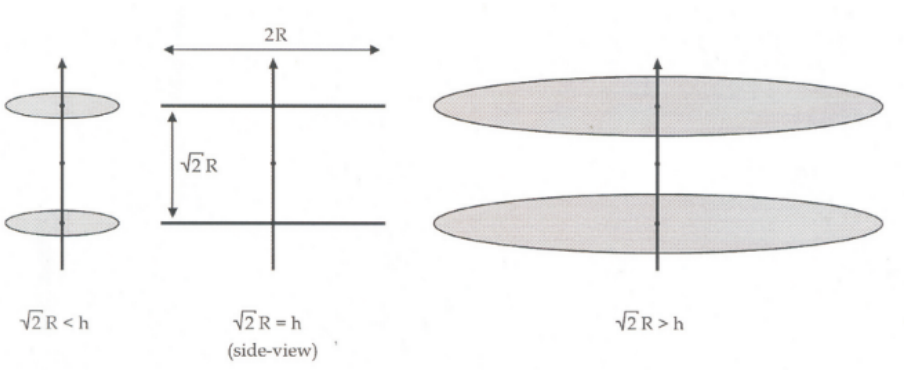

Figure 8: *The three distinct classes of double-ring systems.*

For some orientations the quadrupole correction is negative and for others positive. If the total energy is approximated by the sum of monopole and quadrupole contributions, some orientations will reduce the total energy and others will increase it. This is shown schematically in Fig. 9, a kind of picture we will meet again later in a quantummechanical situation. Note that all quadrupole energies between the two outer values are possible (i.e. all angles θ are possible).

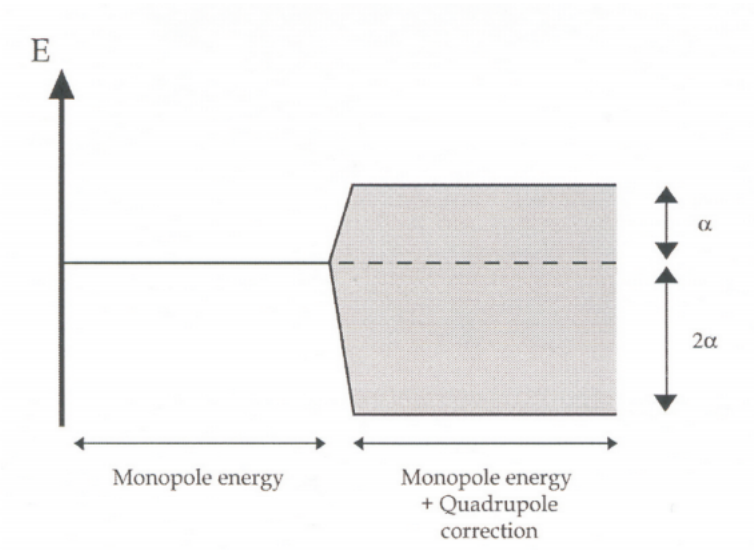

Figure 9: *Quadrupole corrections to the monopole energy for a dumb-bell in a double ring, for the case where* $h > \sqrt{2}R$. *For any orientation of the dumb-bell, a total energy between the shown outer values is found. The quantity* α *has the form* $\alpha = \frac{Gm_1m_2\ell_1^2(h^2-2R^2)}{32(R^2+\frac{h^2}{4})^{5/2}}$

Hyperfinecourse A: quantum version

February 5, 2020

Abstract

This document is meant for optional background reading when studying www.hyperfinecourse.org. It deals with one of the chapters of this course. The formal course content is defined by the website and videos. The present document does not belong to the formal course content. It covers the same topics, but usually with more mathematical background, more physical background and more examples. Feel free to use it, as long as it helps you mastering the course content in the videos. If you prefer studying from the videos only, this is perfectly fine.

The present text has been prepared by Jeffrey De Rycke (student in this course in the year 2018-2019). He started from a partial syllabus written by Stefaan Cottenier for an earlier version of this course, and cleaned, edited and elaborated upon that material. That syllabus was itself inspired by a course taught by Michel Rots at KU Leuven (roughly 1990-1995).

1 Perturbation Theory

In quantum mechanics, the central problem to be solved for stationary systems is the time independent Schrödinger equation. We want to find the eigenvalues E_i (possible E values of the system) and their eigenvalues $|n_i\rangle$ (possible wave functions of the system) of the equation $\hat{H}|n\rangle = E|n\rangle$.

Unfortunately, most systems you can image can not be solved analytically. Therefore we need approximations. In this chapter, the time independent perturbation theory will be explained. A rather powerful technique when one has a system which is a small perturbation of a system that is precisely solvable (known E_i's and $|n_i\rangle$'s). This will be done for non-degenerate and degenerate systems.

1.1 Non-degenerate Time Independent System

Suppose we have a system described by the following Hamiltonian:

$$H = H_0 + \epsilon H_1$$

With the following conditions:

- We know the eigenvalues and eigenfunctions of the Hamiltonian H_0 (the unperturbed system):
$$H_0|n_0\rangle = E_n^0|n_0\rangle$$
- ϵH_1 is a small perturbation: the energy shifts it causes are small compared to the energy differences between the unperturbed levels. ϵ is directly coupled to how strong the perturbating Hamiltonian is. We therefore want to have it small. We also assume again that the complete set of eigenfunctions for the unperturbed Hamiltonian also forms a complete set for the perturbation.

What perturbation theory does is construct approximate solutions for the perturbed system in terms of the solutions for the unperturbed system. You can compare it to the Taylor expansion of a (nicely behaving) function around a certain point (a), which can be used to find the value of the function at another point (b) without actually having to solve function at b. Just as in a Taylor expansion, it is up to the user to choose how high he or she wants its order of approximation to be. In this chapter, we will calculate corrections up to first order for the energy and the wave functions. This is in many cases an already good enough approximation, while not being difficult to calculate.

1.1.1 Equations

Assuming all the states are non-degenerate, the expansions of the eigenstates and eigenvalues of the Hamiltonian read:

$$E_i = E_i^0 + \epsilon E_i^1 + \epsilon^2 E_i^2 + ...$$

$$|n_i\rangle = |n_i^0\rangle + \epsilon\,|n_i^1\rangle + \epsilon^2\,|n_i^2\rangle + ...$$

Substituting this into the Schrödinger equation we get:

$$(H_0 + \epsilon H_1)(|n_i^0\rangle + \epsilon\,|n_i^1\rangle + \epsilon^2\,|n_i^2\rangle + ...)$$

$$= (E_i^0 + \epsilon E_i^1 + \epsilon^2 E_i^2 + ...)(|n_i^0\rangle + \epsilon\,|n_i^1\rangle + \epsilon^2\,|n_i^2\rangle + ...)$$

These solutions should hold for any value of ϵ, therefore we can decouple the big equations into small ones, for each power of ϵ. As we are only interested in solutions up to first order (proportional to ϵ) the following two equations are suffice:

$$H_0\,|n_i^0\rangle = E_i^0\,|n_i^0\rangle$$

$$H_0\,|n_i^1\rangle + H_1\,|n_i^0\rangle = E_i^0\,|n_i^1\rangle + E_i^1\,|n_i^0\rangle$$

The first set of equations are just the solutions to the unperturbed system. The second set will be used to find the first order corrections.

1.1.2 First Order Energy Corrections

Rewriting the new set of equations, we get:

$$(H_0 - E_i^0)\,|n_i^1\rangle = (E_i^1 - H_1)\,|n_i^0\rangle$$

Because we assumed that $|n_i^0\rangle$ forms a complete basis of the total problem, we can write $|n^1\rangle$ as a linear combination of the functions $|n_i^0\rangle$. This gives us:

$$(H_0 - E_i^0)\sum_j c_{ij}^1\,|n_j^0\rangle = (E_i^1 - H_1)\,|n_i^0\rangle$$

Now multiplying with $\langle n_i^0|$ and noting that the states are orthonormal we get:

$$0 = E_i^1 - \langle n_i^0|\,H^1\,|n_i^0\rangle \rightarrow E_i^1 = \langle n_i^0|\,H^1\,|n_i^0\rangle$$

Multiplying with ϵ now gives us the first order energy correction. In general we can see that the first order energy corrections can be found by calculating the diagonal matrix elements of the perturbing Hamiltonian H_1 in the basis of eigenfunctions of the unperturbed Hamiltonian H_0 (and then multiplying by ϵ).

The energy eigenvalues up to first order therefore read:

$$E_i = E_i^0 + \epsilon\,\langle n_i^0|\,H^1\,|n_i^0\rangle$$

1.1.3 First Order Wavefunction Corrections

We start from the previously found equation:

$$(H_0 - E_i^0) \sum_j c_{ij}^1 \left|n_j^0\right\rangle = (E_i^1 - H_1) \left|n_i^0\right\rangle$$

Where we multiply with $\langle n_k^0|$ where k $\neq$ i. Therefore we get:

$$\langle n_k^0| (H_0 - E_i^0) \sum_j c_{ij}^1 \left|n_j^0\right\rangle = \langle n_k^0| (E_i^1 - H_1) \left|n_i^0\right\rangle$$

$$(E_k^0 - E_i^0) c_{ik}^1 = - \langle n_k^0| H_1 \left|n_i^0\right\rangle$$

$$c_{ik}^1 = \frac{\langle n_k^0| H_1 \left|n_i^0\right\rangle}{(E_i^0 - E_k^0)}$$

Therefore, the eigenstates of the perturbed Hamiltonian up to first order are:

$$\left|n_i\right\rangle = \left|n_i^0\right\rangle + \epsilon \sum_{j \neq i} \frac{\langle n_j^0| H_1 \left|n_i^0\right\rangle}{(E_i^0 - E_j^0)} \left|n_j^0\right\rangle$$

1.1.4 Example Non-degenerate system

Suppose we have an infinitely deep potential well with width a, and a particle in said well with mass m and charge q. Taking $H_0 = -\frac{\hbar^2}{2m}\frac{d^2}{dx^2}$ we get:

$$E_i^0 = \frac{\hbar^2 \pi^2}{2ma^2} i^2$$

$$n_i^0(x) = \sqrt{\frac{2}{a}} sin \frac{i\pi x}{a}$$

Now taking $H_1 = -qK\hat{x}$ (a constant electric field in the x direction). Where we assume the corrections will be small (due to an electric field that is not too strong). The first order energy corrections can be calculated as:

$$E_i^1 = \langle n_i^0| H^1 \left|n_i^0\right\rangle = -\frac{2qK}{a} \int x \cdot sin^2 \frac{i\pi x}{a} dx = -\frac{qKa}{2}$$

Which gives us a downward shift of all levels, independent of i.

1.2 Degenerate Time Independent System

If a certain energy value E_i^0 is degenerate, the first order approximation for the wavefunctions is not valid, as the denominator can become zero. Assuming the original state is ℓ-fold degenerate, the corresponding ℓ eigen values of $H_0 + \epsilon H_1$ can be found in two steps.

- Create an orthonormal basis of states $|n_0^j\rangle$ for the ℓ-dimensional degenerate subspace.
- The ℓ corrections E_j^1 to the degenerate energy are found as eigen values of the following matrix:

$$\begin{bmatrix} <n_0^1|\,\epsilon H_1\,|n_0^1> & <n_0^1|\,\epsilon H_1\,|n_0^2> & \cdots & <n_0^1|\,\epsilon H_1\,|n_0^\ell> \\ <n_0^2|\,\epsilon H_1\,|n_0^1> & <n_0^2|\,\epsilon H_1\,|n_0^2> & \cdots & <n_0^2|\,\epsilon H_1\,|n_0^\ell> \\ \vdots & \vdots & \ddots & \vdots \\ <n_0^\ell|\,\epsilon H_1\,|n_0^1> & <n_0^\ell|\,\epsilon H_1\,|n_0^2> & \cdots & <n_0^\ell|\,\epsilon H_1\,|n_0^\ell> \end{bmatrix} \tag{1}$$

  The ℓ new eigen states $|n_0^j\rangle$ are the eigen vectors of the above matrix.

1.2.1 Example Degenerate System

Suppose we have a free electron, this electron can have two spinstates $n_\downarrow$ and $n_\uparrow$ which are degenerate. When applying a magnetic field, this degeneracy will be lifted. We can write said perturbing Hamiltonian as:

$$H_1 = -\hat{\vec{\mu}} \cdot \vec{B} = -\left(\frac{-2\mu_B \hat{\vec{S}}}{\hbar}\right) \cdot \vec{B}$$

Therefore we have:

$$\begin{bmatrix} \langle n_\uparrow|\,\hat{S}_z\,|n_\uparrow\rangle & \langle n_\uparrow|\,\hat{S}_z\,|n\rangle \\ \langle n_\downarrow|\,\hat{S}_z\,|n_\uparrow\rangle & \langle n_\downarrow|\,\hat{S}_z\,|n_\downarrow\rangle \end{bmatrix} = \begin{bmatrix} \frac{1}{2}\hbar & 0 \\ 0 & -\frac{1}{2}\hbar \end{bmatrix} \tag{2}$$

Which is already diagonal. If this was not the case, we would need to diagonalize it.

2 Quantum Multipole Expansion

We have discussed the multipole expansion for a classical system, and will now apply it to a quantum system. We will see that it is the same, except for the need for perturbation theory.

2.1 The Total Hamiltonian

When describing the energy levels of an atom, it is the energy of the total system "nucleus + electrons" that is discussed. We will now look further into formalizing said statement.

2.1.1 A Free Nucleus

Consider first a free nucleus. This system of interacting nucleons is described by a Hamiltonian, which we will call $\hat{H}_n$. This $\hat{H}_n$ contains a term $\hat{T}_n$ that describes the kinetic energy of the nucleons, and a term $\hat{U}_{nn}$ that describes the nucleon-nucleon interaction (attractive strong force and repulsive Coulomb force):

$$\hat{H}_n \quad = \quad \hat{T}_n + \hat{U}_{nn} \tag{3}$$

The different states in which the nucleus can be – call them $|I\rangle$ – are the eigen states of $\hat{H}_n$. They are elements of a function space $\mathcal{F}_I$. These states have an eigen energy E_I, such that

$$\hat{H}_n |I\rangle \quad = \quad E_I |I\rangle \tag{4}$$

As long as the nucleons are bound, the eigen energies that are allowed form a discrete set (in the order of keV/MeV).

2.1.2 A Free Electron Gas

Next, consider a fixed number of electrons that is free to occupy all space, without any other charges being present. This system of interacting electrons is described by a Hamiltonian which we will call $\hat{H}_e$:

$$\hat{H}_e \quad = \quad \hat{T}_e + \hat{U}_{ee} \tag{5}$$

$\hat{T}_e$ describes the kinetic energy of the electrons, $\hat{U}_{ee}$ the electron-electron (Coulomb) interaction. In contrast to the nucleons which are bound by the attractive strong force, the electrons are unbound due to the repulsive Coulomb force. They repel each other, and a continuous range of eigen states $|\psi_e\rangle$ and eigen energies E_ψ is possible:

$$\hat{H}_e |\psi_e\rangle \quad = \quad E_\psi |\psi_e\rangle \tag{6}$$

The functions $|\psi_e\rangle$ are elements of a function space $\mathcal{F}_\psi$.

2.1.3 An atom

Now we put the nucleons and the electrons together, but temporarily switch off the interaction between them. Nevertheless, we want to describe this system as a whole. This can be done by direct products. An eigen state of the entire system is given by $|I\rangle \otimes |\psi_e\rangle = |I \otimes \psi_e\rangle$, a function that belongs to the direct product space $\mathcal{F}_I \otimes \mathcal{F}_\psi$. The nuclear Hamiltonian should work only on the subspace $\mathcal{F}_I$, and should therefore be rewritten as $\hat{H}_n \otimes \mathbb{1}$ ($\mathbb{1}$ is a unity operator):

$$\begin{aligned} \left(\hat{H}_n \otimes \mathbb{1}\right) |I \otimes \psi_e\rangle &= \left(\hat{H}_n |I\rangle\right) \otimes (\mathbb{1} |\psi_e\rangle) && (7)\\ &= (E_I |I\rangle) \otimes (1 |\psi_e\rangle) && (8)\\ &= E_I |I \otimes \psi_e\rangle && (9) \end{aligned}$$

Similarly for $\hat{H}_e$. The entire system can now be described by

$$\begin{aligned} \left(\hat{H}_n \otimes \mathbb{1} + \mathbb{1} \otimes \hat{H}_e\right) |I \otimes \psi_e\rangle = && (10)\\ = \left(\hat{T}_n \otimes \mathbb{1} + \hat{U}_{nn} \otimes \mathbb{1} + \mathbb{1} \otimes \hat{T}_e + \mathbb{1} \otimes \hat{U}_{ee}\right) |I \otimes \psi_e\rangle && (11)\\ = (E_I + E_\psi) |I \otimes \psi_e\rangle && (12) \end{aligned}$$

In reality, nucleons and electrons do interact with each other by the Coulomb interaction. The Hamiltonian that describes this interaction must work on the entire space $\mathcal{F}_I \otimes \mathcal{F}_\psi$. We can formally represent it by an operator $\hat{Q} \otimes \hat{V}$. The full Hamiltonian is then

$$\hat{H}_n \otimes \mathbb{1} + \mathbb{1} \otimes \hat{H}_e + \hat{Q} \otimes \hat{V} \tag{13}$$

In line with the gravitational example, the idea is now that we make a Taylor expansion of the difficult term $\hat{Q} \otimes \hat{V}$ [1]:

$$\hat{Q} \otimes \hat{V} = \hat{Q}^{(0)} \otimes \hat{V}^{(0)} + \hat{Q}^{(1)} \otimes \hat{V}^{(1)} + \hat{Q}^{(2)} \otimes \hat{V}^{(2)} + \ldots \tag{14}$$

The Hamiltonian can now be rearranged and some familiar contributions show up, with a hierarchy of energy scales (see also VIP-1):

$\hat{T}_n \otimes \mathbb{1} + \hat{U}_{nn} \otimes \mathbb{1}$	$T_n + U_{nn}$	$keV - MeV$	*nuclear energy levels*
$\mathbb{1} \otimes \hat{T}_e + \mathbb{1} \otimes \hat{U}_{ee} + \hat{Q}^{(0)} \otimes \hat{V}^{(0)}$	$T_e + U_{ee} + E_{ne}^{(0)}$	eV (meV)	*atomic energy levels*
$\hat{Q}^{(1)} \otimes \hat{V}^{(1)} + \hat{Q}^{(2)} \otimes \hat{V}^{(2)}$	$E_{ne}^{(1)} + E_{ne}^{(2)}$	μeV	*hyperfine structure*

Different states of the nuclei are separated by energies of the order of keV to MeV. It is the nucleon-nucleon interaction and the kinetic energy of the nucleons that is responsible for this. The kinetic energy of the electrons, the electron-electron interaction and the monopole term of the electron-nucleus interaction

[1] In this formal discussion, we neglect size-dependent overlap contributions for a while, just for clarity.

introduce states that are separated by energies in the eV-range. Depending on how much relativity is taken into account here, also the fine structure (meV) can be present. Higher order multipole terms of the electron-nucleus interaction are responsible for the hyperfine structure, with energy differences in the μeV range.

2.2 Applying Perturbation Theory

The presentation of section 2.1 is maybe a little misleading, as it could give the impression that we know all the hamiltonians in equations 13 and 14, and that we know how to find their eigen states. That is not true. It is the goal of theoretical nuclear physics first to find $\hat{H}_n$ and secondly to solve it, but even that first goal has by far not yet been reached. The same problem holds for the nuclear operators $\hat{Q}^{(0)}$, $\hat{Q}^{(1)}$, $\hat{Q}^{(2)}$, ...: it is not known how to handle them with first principles nuclear theory. For our final equations that describe the hyperfine structure, we will have to find ways how to deal with this lack of information. Actually, the only part of the problem that can be solved to a good extent from first principles (atomic or condensed matter) theory, is the hamiltonian $\hat{H}_0 = \mathbb{1}\otimes\hat{T}_e + \mathbb{1}\otimes\hat{U}_{ee} + \hat{Q}^{(0)}\otimes\hat{V}^{(0)}$: the form of this hamiltonian is known, and there are quite accurate methods known how to solve it numerically. The real situation is hence that we can write down $|I\rangle$ only formally, while for $\left|\psi_e^{(0)}\right\rangle$ a numerical expression can be found[2]. Fortunately, our Taylor expansion guarantees that the effect of $\hat{Q}^{(1)}\otimes\hat{V}^{(1)}$, $\hat{Q}^{(2)}\otimes\hat{V}^{(2)}$, ... will be small. This means that we can make use of *first order perturbation theory*: we will solve the 'easy' hamiltonian $\hat{H}_0$, find its eigenvalues E_0 and eigenfunctions $\left|\psi_e^{(0)}\right\rangle$, and then evaluate the additional small hamiltonian for the eigenfunctions of the easy hamiltonian:

$$E_{tot} \approx E_0 + \left\langle \psi_e^{(0)}\otimes I\right| \hat{H}_1 \left| I\otimes\psi_e^{(0)}\right\rangle \tag{15}$$

with

$$E_0 = \left\langle \psi_e^{(0)}\otimes I\right| \hat{H}_0 \left| I\otimes\psi_e^{(0)}\right\rangle \tag{16}$$

The fact that not only a Taylor series but also perturbation theory is used, is the main difference between the treatment of atoms or solids and the gravitational example. In the following sections, we will derive explicit expressions for $\hat{H}_1$ in the non-relativistic case, and in the sections dealing with the monopole shift, the magnetic dipole and the electric quadrupole interactions, the energy corrections due to this new interactions will be evaluated for the cases of free atoms (ions) and solids.

[2] Actually, not necessarily for $\left|\psi_e^{(0)}\right\rangle$ itself, but for the corresponding charge density. But for methods such as Density Functional Theory, the density is all we need. At this point however, just imagine that we do know $\left|\psi_e^{(0)}\right\rangle$.

2.3 Charge-charge Interaction

We focus first on the electrostatic part of the electromagnetic potential. Consider a nucleus described by a many-body wave function $|I\rangle$, that is an eigenstate of the nuclear Hamiltonian. The latter makes that the nuclear charge density $\rho_n(\vec{r}_n)$ is time independent. This nucleus is immersed in an electron cloud with which it interacts, the electron cloud being provided either by a single atom or by a crystalline solid. This electron cloud is described by a many-body wave function $|\Psi_e\rangle$ that is an eigenstate of the Hamiltonian for the atom or the crystalline solid[3]. The corresponding electronic charge density $\rho_e(\vec{r}_e)$ is time independent as well. The many-body wave functions can be related to the charge densities as we are used to in quantum mechanics:

$$\begin{aligned} <\psi_n|\,\psi_n> &= <I|\,I> = 1 \;=\; \int_n \psi_n^*(\vec{r}_n)\psi_n(\vec{r}_n)\,d\vec{r}_n \;=\; \frac{1}{Ze}\int_n \rho_n(\vec{r}_n)\,d\vec{r}_n \\ <\psi_e|\,\psi_e> &= 1 \;=\; \int_e \psi_e^*(\vec{r}_e)\psi_e(\vec{r}_e)\,d\vec{r}_e \;=\; -\frac{1}{Ne}\int_e \rho_e(\vec{r}_e)\,d\vec{r}_e \end{aligned}$$

Z is the number of protons in the nucleus, N is the number of electrons in the unit cell of the crystal (for a free neutral atom, N=Z). Using the following conversion table:

$$\begin{aligned} G &\leftrightarrow \frac{-1}{4\pi\epsilon_0} && (17)\\ \vec{r}_1 &\leftrightarrow \vec{r}_n && (18)\\ \vec{r}_2 &\leftrightarrow \vec{r}_e && (19)\\ m_1 &\leftrightarrow eZ && (20)\\ m_2 &\leftrightarrow -eN && (21) \end{aligned}$$

we can now translate our formula for the potential energy in the gravitational analogue into

$$\begin{aligned} E_{pot}^{qq} &= \frac{1}{4\pi\epsilon_0}\int_n\int_e \frac{\rho_n(\vec{r}_n)\rho_e(\vec{r}_e)}{|\vec{r}_e-\vec{r}_n|}\,d\vec{r}_n\,d\vec{r}_e && (22)\\ &= -\frac{e^2NZ}{4\pi\epsilon_0}\,\langle\psi_e\otimes I|\,\frac{1}{|\vec{r}_e-\vec{r}_n|}\,|I\otimes\psi_e\rangle && (23) \end{aligned}$$

tacitly assuming that for crystalline solids we evaluate this expression once for every nucleus – with different choice of origin – and add the nucleus-nucleus interaction later. Again using the so-called Laplace expansion or multipole expansion in spherical coordinates, we can write the Hamiltonian $\hat{H}_{ne}^{qq}$ for the electrostatic interaction between nucleus and electrons as

$$\hat{H}_{ne}^{qq} = -\frac{e^2NZ}{\epsilon_0}\left(\sum_{n=0}^{\infty}\frac{r_n^n}{r_e^{n+1}}\,\frac{1}{2n+1}\,Y^n(\theta_n,\,\phi_n)\cdot Y^n(\theta_e,\,\phi_e)\right) \qquad (24)$$

[3]In the case of a crystalline solid, periodic boundary conditions guarantee that it is sufficient to describe the many-body wave function within one unit cell of the crystal only.

(electron penetration in the nucleus is not considered here, therefore $r_e > r_n$). This Hamiltonian corresponds to the full $\hat{Q} \otimes \hat{V}$ of equation 13 (for the case of charge-charge interaction). The total energy of the system nucleus + electrons can now be written as (operators on the direct product space are not explicitly written as such):

$$E_{tot}^{qq} = \langle \psi_e \otimes I | \underbrace{\hat{T}_n + \hat{U}_{nn}}_{} + \underbrace{\hat{T}_e + \hat{U}_{ee} + \hat{H}_{ne}^{qq}}_{} | I \otimes \psi_e \rangle \quad (25)$$

$$= (E_I + E_{el}) | I \otimes \psi_e \rangle \quad (26)$$

We don't know at all what E_I is, due to the beforementioned problems with theoretical nuclear physics. What E_{el} is we don't know either, but we can approximate it as follows[4]:

$$E_{el} = \langle \psi_e \otimes I | \underbrace{\hat{T}_e + \hat{U}_{ee} - \frac{e^2 N Z}{4\pi\epsilon_0 \, r_e}}_{\hat{H}_0} | I \otimes \psi_e \rangle + \quad (27)$$

$$\langle \psi_e \otimes I | \underbrace{- \frac{e^2 N Z}{\epsilon_0} \left(\sum_{n=1}^{\infty} \frac{r_n^n}{r_e^{n+1}} \frac{1}{2n+1} Y^n(\theta_n, \phi_n) \cdot Y^n(\theta_e, \phi_e) \right)}_{\hat{H}_{1 \to \infty}} | I \otimes \psi_e \rangle$$

(Mind the sum, which runs now from $n = 1$.) Again, we remind that the nucleus-nucleus interactions for cyrstalline solids needs to be added later. The Hamiltonian $\hat{H}_0$ in 27 contains the kinetic energy of the electrons, the electron-electron interaction, and the electrostatic interaction of the electron cloud with a point-like nucleus. In atomic physics and condensed matter physics, sufficiently accurate methods are known to find eigenvalues and eigenstates of this Hamiltonian (always $\hat{U}_{ee}$ has to be approximated, but several acceptable schemes exist for that). Call the eigenstates of this Hamiltonian $\left| \psi_e^{(0)} \right\rangle$, and the eigen energies $E_{ne}^{(0)}$. The superscript (0) indicates that these are 0^{th} order results, that will be used soon to calculated first order perturbations.

In analogy with the gravitational multipole moments, we can define the electrostatic multipole moments of the nucleus:

$$Q_q^n = eZ \sqrt{\frac{4\pi}{2n+1}} \, \langle I | \, r_1^n Y_q^n \, (\theta_n, \, \phi_n) \, | I \rangle \quad (28)$$

They have as units $\mathrm{C\,m}^n$. Some books define the multipole moments divided by the electron charge e, and then multiply the dot products $Q \cdot V$ by e. Such multipole moments have as units m^n.

[4] E_{el} is different from the E_ψ of equation 6: the latter is the eigen value of a hamiltonian that does not contain the nucleus-electron interaction.

Explicit expressions – following our definition of the multipole moments – are:

$eZ\sqrt{4\pi}\,\langle I|\,Y_0^0\,(\theta_n,\,\phi_n)\,|I\rangle$: the electrostatic monopole moment of the nucleus (shortly: the electric monopole moment, 1 component. Units: C.).

$eZ\sqrt{\frac{4\pi}{3}}\,\langle I|\,r_1 Y_q^1\,(\theta_n,\,\phi_n)\,|I\rangle$: the 3 components electrostatic dipole moment of the nucleus (units: C m). We know already from the gravitational example that this can be made to vanish by taking the origin of XYZ in the center of charge of the nucleus, and we will show below also an independent general proof.

$eZ\sqrt{\frac{4\pi}{5}}\,\langle I|\,r_1^2 Y_q^2\,(\theta_n,\,\phi_n)\,|I\rangle$: the 5 components of the electrostatic quadrupole moment of the nucleus (units: $\mathrm{C\,m^2}$ or electron barn (eb)).

One half of the n-pole moments is zero however. We can understand this by looking at the parity[5] of the operators $r_n^n\,Y^n$. Because of $Y_q^n(\pi-\theta,\,\phi+\pi) = (-1)^n\,Y_q^n(\theta,\,\phi)$ and because the parity of r_n^n is always even (r_n is a distance, which is positive in whatever axis system), the parity of $r_n^n\,Y^n$ is even for even n and odd for odd n. It is an experimentally well-established fact that also the nuclear states $|I\rangle$ have a well-defined parity, i.e. either even or odd. Therefore the parity of $r_n^n\,Y^n\,|I\rangle$ will have the parity of $|I\rangle$ if n is even, and the opposite parity if n is odd. But in the latter case $\langle I|\,r_n^n\,Y^n\,|I\rangle$ is the scalar product between two states $\langle I|$ and $r_n^n\,Y^n\,|I\rangle$ of opposite parity, which is zero. Therefore only terms with even n will survive[6].

Due to the beforementioned gaps in the theory of nuclear structure, it is not possible yet to calculate the nuclear multipole moments. They can be measured, however, and that's how we will work around our problem: we will replace the (even) multipole moments by their experimental values. Rather than having a fully computable theory of interacting systems of nuclei and electrons, we are satisfied with a theory that is computable only if the nuclear information in plugged via experimentally determined parameters. That will turn out to be sufficient to allow for and interpret a variety of experimental measurements on the interacting system (cfr. the experimental methods of type 1, 2 or 3 in the second half of this course).

[5]The parity of an operator describes its behaviour under an inversion of coordinates. An operator with even parity does not change under inversion. An operator with odd parity changes sign under inversion. Operators who behave in more complicated way can always be written as a sum of an operator with even and one with odd parity. The parity of a state of a quantum system is defined in a similar way.

[6]One can do a similar reasoning in wave mechanics, where for odd n an integral over all space of an odd function will appear, which is zero again. As seen in the course video "Why are odd electric moments zero?"

In analogy with the gravitational multipole moments we define also the electrostatic multipole fields of the electron cloud (in a crystalline solid, these are the multipole fields at the center of mass of one of the nuclei, chosen by the place where we have put the origin of the axis system):

$$V_q^n \quad = \quad -\frac{eN}{\sqrt{4\pi}\epsilon_0}\sqrt{\frac{1}{2n+1}}\left\langle\psi_e^{(0)}\right|\frac{1}{r_e^{n+1}}Y_q^n\left(\theta_e,\,\phi_e\right)\left|\psi_e^{(0)}\right\rangle \tag{29}$$

Units are $\mathrm{V/m}^n$. Some explicit expressions:

$\frac{-eN}{\sqrt{4\pi}\ \epsilon_0}\left\langle\psi_e^{(0)}\right|\frac{1}{r_e}Y_0^0\left(\theta_e,\,\phi_e\right)\left|\psi_e^{(0)}\right\rangle$: the electrostatic monopole field at the nucleus (monopole field, 1 component. Units: V).

$\frac{-eN}{\sqrt{12\pi}\ \epsilon_0}\left\langle\psi_e^{(0)}\right|\frac{1}{r_e^2}Y_q^1\left(\theta_e,\,\phi_e\right)\left|\psi_e^{(0)}\right\rangle$: the 3 components of the electrostatic dipole field at the nucleus (units: V/m)

$\frac{-eN}{\sqrt{20\pi}\ \epsilon_0}\left\langle\psi_e^{(0)}\right|\frac{1}{r_e^3}Y_q^2\left(\theta_e,\,\phi_e\right)\left|\psi_e^{(0)}\right\rangle$: the 5 components of the electrostatic quadrupole field (or electric-field gradient) at the nucleus due to the electron cloud (units: $\mathrm{V/m}^2$).

In contrast to the nuclear multipole moments, the electronic multipole fields of atoms and solids can be calculated directly from quantum mechanics by modern *ab initio* methods. By using such calculations together with the experimental input of the nuclear moments, the interaction energy (which is a measurable quantity) of the different multipole orders can be predicted.

The electron states $\left|\psi_e^{(0)}\right\rangle$ have in general no well-defined parity, we can therefore not in general prove particular multipole fields to be zero. Nevertheless, due to the beforementioned parity properties of the nuclear moments, only terms with even n will appear in the hamiltonian, which in short-hand notation looks like:

$$\hat{H} \quad = \quad \hat{T}_n + \hat{U}_{nn} + \underbrace{\hat{T}_e + \hat{U}_{ee} + \hat{Q}^{(0)}\otimes\hat{V}^{(0)}}_{\hat{H}_0} + \underbrace{\sum_{n\geq 2\ and\ even}\frac{\hat{Q}^{(n)}\otimes\hat{V}^{(n)}}{2n+1}}_{\hat{H}_{1\to\infty}} \tag{30}$$

From the gravitational example in the previous chapter, we know that the contribution to the energy by $H_{1\to\infty}$ is much smaller than the contribution from H_0, as the dimensions of the nucleus ($r_n^{max} \approx 6\cdot 10^{-15}\,m$ for already large nuclei) are much smaller than the average distance of the closest electrons ($10^{-12}\,m$). For this reason, the effect of $\hat{H}_{1\to\infty}$ is very small, and rapidly decreasing with higher n. We can therefore approximate $\hat{H}_{1\to\infty}$ by the quadrupole term:

$$H \quad \approx \quad \hat{T}_n + \hat{U}_{nn} + \underbrace{\hat{T}_e + \hat{U}_{ee} - \frac{e^2NZ}{4\pi\epsilon_0\,r_e}}_{\hat{H}_0} + \underbrace{\frac{-e^2NZ}{5\epsilon_0}\left(\frac{r_n^2}{r_e^3}\,Y^2(\theta_e,\,\phi_e)\cdot Y^2(\theta_n,\,\phi_n)\right)}_{\hat{H}_1}$$

(31)

It is therefore allowed to apply first order perturbation theory, and to evaluate $\hat{H}_1$ in the eigen states $\left|\psi_e^{(0)}\right\rangle$ of $\hat{H}_0$. We will do this in the part about the electric quadrupole interaction.

2.4 Current-current interaction

The nucleus and the electron cloud do not feel one another only by the Coulomb interaction discussed above. As the protons are moving inside the nucleus, also currents are present in there. Apart from these so-called *convection currents*, there are also currents due to the spin of the protons and the neutral neutrons (*spin currents*). The moving electrons in the electron cloud constitute a current too. The interaction between these two currents represents the dynamic part of the electromagnetic interaction, and supplements the electrostatic part from the previous paragraph[7]. From classical electromagnetism it is known that a current density distribution $\vec{j}(\vec{r})$ generates a *vector* potential $\vec{A}(\vec{r})$:

$$\vec{A}(\vec{r}) = \frac{\mu_0}{4\pi} \int \frac{\vec{j}(\vec{r}\,')}{|\,\vec{r}\,' - \vec{r}\,|}\, d\vec{r}\,' \tag{33}$$

If we call the current density inside the nucleus $\vec{j}_n(\vec{r}_n)$ and the one of the electron cloud $\vec{j}_e(\vec{r}_e)$, then the potential energy due to the current-current interaction in the full system nucleus + electrons can be expressed as the energy of the nuclear current distribution in the vector potential due to the electrons:

$$\begin{aligned} E_{pot}^{jj} &= \int_n \vec{j}_n(\vec{r}_n) \cdot \vec{A}_e(\vec{r}_n)\, d\vec{r}_n \\ &= \frac{\mu_0}{4\pi} \int_n \int_e \frac{\vec{j}_n(\vec{r}_n) \cdot \vec{j}_e(\vec{r}_e)}{|\,\vec{r}_e - \vec{r}_n\,|}\, d\vec{r}_n\, d\vec{r}_e \end{aligned} \tag{34}$$

This expression is similar to equation 22, except for the fact that in the numerator a dot product between vectors appears, instead of a product between scalars. We will therefore not be able to make the same kind of multipole expansion as we did for the static part of the electromagnetic interaction: an expansion in *vector* spherical harmonics will be needed. This is mathematically much more

[7] In previous sections, we always used static mass and charge contributions, and we will continue to do so as we still work with pure eigenstates. A static charge distribution does not imply however that there would be no currents. This can be understood from classical electromagnetism by means of the continuum equation ($\vec{j}$ is the current distribution)

$$\frac{\partial \rho}{\partial t} + \vec{\nabla} \cdot \vec{j} = 0 \tag{32}$$

If $\vec{\nabla} \cdot \vec{j} = 0$, then $\frac{\partial \rho}{\partial t} = 0$ and the charge distribution is static. But $\vec{\nabla} \cdot \vec{j} = 0$ does not imply that $\vec{j} = \vec{0}$! Currents that fulfill the relation $\vec{\nabla} \cdot \vec{j} = 0$ are called *steady currents* in classical electromagnetism. Stationary states in quantum mechanics correspond to steady currents.

involved, and we will not do this[8]. The current-current interaction hamiltonian for a single electron and a nucleus – provided the two current distributions *do not overlap* – turns out to be:

$$\hat{H}_{jj} \quad = \quad \sum_{n=0}^{\infty} \frac{B^{(n)} \cdot M^{(n)}}{2n+1} \tag{35}$$

The tensor $M^{(n)}$ depends on nuclear properties only, and is called the n^{th} magnetic multipole moment of the nucleus. It can be shown to have odd parity for even n, and even parity for odd n. The tensor $B^{(n)}$ is determined completely by properties of the electron cloud. Because of the well-defined parity of the nuclear states $\mid I >$, all expectation values of $M^{(n)}$ for a state $\mid I >$ will vanish if n is even. This makes the term with $n = 1$ the leading term in 35.

The dimensions of $M^{(1)}$ are J/T (Joule per Tesla), and it can be identified with the magnetic moment[9] of the nucleus $\vec{\mu}_I$ (a vector). $B^{(1)}$ has as dimension T, and is the opposite of the magnetic field at the nucleus, generated by the electrons. The latter field is called the *magnetic hyperfine field* $\vec{B}(0)$ [10].

2.5 Summary

We can now finally write down the approximate[11] hamiltonian expressing the hyperfine corrections to the potential energy of a nucleus and an electron cloud:

$$\hat{H} \quad \approx \quad \hat{T}_n + \hat{U}_{nn} + \underbrace{\hat{T}_e + \hat{U}_{ee} - \frac{e^2 N Z}{4\pi\epsilon_0\, r_e}}_{\hat{H}_0} + \tag{36}$$

$$\underbrace{\frac{-\,e^2 N Z}{5\epsilon_0} \left(\frac{r_n^2}{r_e^3}\, Y^2(\theta_e,\, \phi_e) \cdot Y^2(\theta_n,\, \phi_n) \right) - \hat{\vec{\mu}}_I \cdot \hat{\vec{B}}(\vec{0})}_{\hat{H}_1}$$

Where the first part in $\hat{H}_1$ is the electronic quadrupole term, and the second part is the magnetic dipole term.

[8] The derivation can be found at various places, for instance in *Theory of Hyperfine Structure*, Charles Schwartz, Physical Review 92(2) (1955) 380-395, in *Electron Paramagnetic Resonance of Transition Ions*, A. Abragam and B. Bleany, Clarendon Press - Oxford, 1970, chapter 17, and in *Theory of the Hyperfine Structure of Free Atoms*, L. Armstrong, 1971, Wiley (Interscience), New York.

[9] Note that again we have no reliable tools to calculate this nuclear dipole moment: it has to be replaced by experimental values.

[10] The lowest order term in the current-current interaction is calculated explicitly and elegantly in *Classical Electrodynamics*, J.D. Jackson, 3^{rd} edition 1998, John Wiley & Sons, sections 5.6 and 5.7

[11] We emphasize that the approximation is due to i) using first order perturbation theory and ii) truncating the multipole expansions.

In the next 3 chapters we will discuss in a quantitative way the effect of the charge and current (or electric and magnetic) hyperfine interaction on the energy. As before, we will stick to a non-relativistic treatment. We will also pay attention to what happens when the two charge or current distributions overlap, and size contributions will appear. The scheme of our discussion is shown in Fig. 1: both for the charge-charge and current-current interactions there are contributions that are zero by symmetry. The non-zero contributions have a shape-dependent and size-dependent part, which might or might not be negligible.

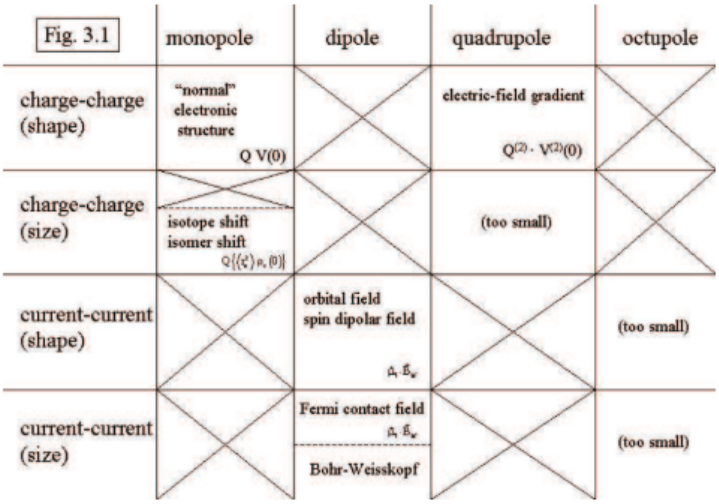

Figure 1: *A schematic overview of all contributions to electric (charge-charge) and magnetic (current-current) hyperfine fields, ordered according to their multipole order, and split into shape-dependent and size-dependent contribution. Contributions that do not exist are barred, contributions that are too small to be relevant are indicated. When a dashed line is present in a box, the contribution above the line does not vanish for a point nucleus, while the contribution below the line does. Explaining this scheme is the topic of the following 3 chapters*

Hyperfinecourse A: electric monopole shift

February 5, 2020

Abstract

This document is meant for optional background reading when studying www.hyperfinecourse.org. It deals with one of the chapters of this course. The formal course content is defined by the website and videos. The present document does not belong to the formal course content. It covers the same topics, but usually with more mathematical background, more physical background and more examples. Feel free to use it, as long as it helps you mastering the course content in the videos. If you prefer studying from the videos only, this is perfectly fine.

The present text has been prepared by Jeffrey De Rycke (student in this course in the year 2018-2019). He started from a partial syllabus written by Stefaan Cottenier for an earlier version of this course, and cleaned, edited and elaborated upon that material. That syllabus was itself inspired by a course taught by Michel Rots at KU Leuven (roughly 1990-1995).

1 Monopole Shift

1.1 Interaction Energy Nucleus And Electrons

In the previous chapter, we have seen that we can Taylor-expand the interaction term between the nucleons and the electrons as follows:

$$\hat{Q} \otimes \hat{V} = \hat{Q}^{(0)} \otimes \hat{V}^{(0)} + \hat{Q}^{(1)} \otimes \hat{V}^{(1)} + \hat{Q}^{(2)} \otimes \hat{V}^{(2)} + \dots \quad (1)$$

With the following expressions:

$$Q_q^n = eZ\sqrt{\frac{4\pi}{2n+1}} \langle I| r_1^n Y_q^n (\theta_n, \phi_n) |I\rangle \quad (2)$$

$$V_q^n = -\frac{eN}{\sqrt{4\pi}\epsilon_0} \sqrt{\frac{1}{2n+1}} \left\langle \psi_e^{(0)} \right| \frac{1}{r_e^{n+1}} Y_q^n (\theta_e, \phi_e) \left| \psi_e^{(0)} \right\rangle \quad (3)$$

Where we made the agreement to treat all nuclear properties as phenomenological parameters, whilst keeping the electronic properties as operators. As well as keeping $r_e > r_n$. Suppose we now want to calculate the first term for a nucleus with one electron. We will get the following expressions:

$$Q_{00} = \frac{\sqrt{4\pi}}{\sqrt{4\pi}} \int \rho_n(\vec{r}) d\vec{r} = eZ \quad (4)$$

$$V_{00} = \frac{1}{4\pi\epsilon_0} \frac{\sqrt{4\pi}}{\sqrt{4\pi}} \int \frac{\rho_n(\vec{r})}{r} d\vec{r} = \frac{-e}{4\pi\epsilon_0} \langle \Psi_e| \frac{1}{r} |\Psi_e\rangle \quad (5)$$

$$E_0^0 = Q_{00} V_{00} = \frac{-e^2 Z}{4\pi\epsilon_0} \langle \Psi_e| \frac{1}{r} |\Psi_e\rangle \quad (6)$$

As you can see, these are just the non-relativistic energy levels of a point charge Ze in the potential of an electron.

Order	Multipole moment or field	First-order quasimoment or quasifield	Second-order quasimoment or quasifield	...
$O(0)$	MI:	$\mathrm{MS}^{(1)}$:	$\mathrm{MS}^{(2)}$:	...
	$M \propto r^0 Y_{00}$	$\tilde{M}^{(1)} \propto \{r^2 Y_{00}\}$	$\tilde{M}^{(2)} \propto \{r^4 Y_{00}\}$	
	$V \propto v(0)$	$\tilde{V}^{(1)} \propto \Delta v(0)$	$\tilde{V}^{(2)} \propto \Delta^2 v(0)$	
$O(2)$	QI:	$\mathrm{QS}^{(1)}$:	$\mathrm{QS}^{(2)}$:	
	$Q \propto r^2 Y_{20}$	$\tilde{Q}^{(1)} \propto \{r^4 Y_{20}\}$	$\tilde{Q}^{(2)} \propto \{r^6 Y_{20}\}$	...
	$V_{ij} \propto \partial_{ij} v(0)$	$\tilde{V}^{(1)}_{ij} \propto \partial_{ij} \Delta v(0)$	$\tilde{V}^{(2)}_{ij} \propto \partial_{ij} \Delta^2 v(0)$	
$O(4)$	HDI:	$\mathrm{HDS}^{(1)}$:	$\mathrm{HDS}^{(2)}$:	
	$H \propto r^4 Y_{40}$	$\tilde{H}^{(1)} \propto \{r^6 Y_{40}\}$	$\tilde{H}^{(2)} \propto \{r^8 Y_{40}\}$	...
	$V_{ijkl} \propto \partial_{ijkl} v(0)$	$\tilde{V}^{(1)}_{ijkl} \propto \partial_{ijkl} \Delta v(0)$	$\tilde{V}^{(2)}_{ijkl} \propto \partial_{ijkl} \Delta^2 v(0)$	
...	...	...	...	...

Figure 1: *Systematic overview of nuclear multipole and quasi-multipole-moments and electric multipole and quasi-multipole-fields that appear in the multipole expansion of two interacting (and overlapping) classical charge distributions. The first column gives the regular multipole expansion for point nuclei: the monopole, quadrupole, and hexadecapole interactions. The next columns give the quasi-multipole-moments/fields for every multipole interaction, denoted by a tilde: these are corrections to the multipole interactions due to electron penetration into an extended nucleus. Entries in the large round brackets are by generalization only, and are not systematically derived in this course. The objects in each line are spherical tensors of a given rank (rank 0 for line 1, rank 2 for line 2, and rank 4 for line 3).*

A nucleus is, however, not a point charge. Further multipole moments can be calculated to further correct the energy levels due to the shape of the nucleus. In case of charge-charge interactions, these can be found via the quadrupole moment, the hexadecapole moment,... Not only does the shape of the nucleus amount to corrections, so does the fact that the nucleus and the electrons can overlap. In a fully exact description of the multipole expansion with overlapping charged distributions, every individual multipole term itself becomes a series expansion in powers of a quantity that is characteristic for the amount of overlap. Most of the effect of overlap is usually captured already in the first non-leading term of each of those expansions. The first order correction to the monopole moment is called the "first order monopole-shift" and will be the topic of this chapter. The first order correction to the quadrupole moment is called the "first order quadrupole shift", and so on and so forth. Each higher order moment having a smaller value then the previous one. The same goes for the order of the overlap correction. The second order monopole shift will be much smaller then the first order monopole shift.

1.2 First-order Monopole Shift Without Overlap

On the previous page, we have calculated the monopole correction due to the interaction between the nucleus and the electrons. The full energy level up to this correction (with N electrons) is as follows:

$$E_{sh}^{qq\,(0)} = E_I + \left\langle \psi_e^{(0)} \otimes I \right| \hat{T}_e + \hat{U}_{ee} - \frac{e^2 NZ}{4\pi\epsilon_0\, r_e} \left| I \otimes \psi_e^{(0)} \right\rangle \tag{7}$$

$$= \underbrace{E_I + E_e + E_{ee}}_{E_\alpha} - \frac{e^2 NZ}{4\pi\epsilon_0} \langle I|\, I\rangle \underbrace{\left\langle \psi_e^{(0)} \left| \frac{1}{r_e} \right| \psi^{(0)} \right\rangle}_{\left\langle \frac{1}{r_e} \right\rangle} \tag{8}$$

$$= E_\alpha - \frac{e^2 NZ}{4\pi\epsilon_0} \left\langle \frac{1}{r_e} \right\rangle \tag{9}$$

E_α is just shorthand notation for some contributions that will always be the same. In the second term we again have the (dot) product between the monopole moment of the nucleus eZ and the monopole field at the origin due to the electrons, $\frac{-eN}{4\pi\epsilon_0} \left\langle \frac{1}{r_e} \right\rangle$ (as usual, we either consider a neutral atom (N=Z) or one of the nuclei of a solid, with the origin chosen at that nucleus). Note that we again use the fact that we have no knowledge of the nuclear many-body wave function $|I\rangle$): instead of calculating the monopole moment from the nuclear many-body wave function, we replace it by the experimentally known total charge of the nucleus.

This shape-dependent monopole contribution of the charge-charge interaction, is by far the largest contribution to the electrostatic energy of the system nucleus + electrons. It is insensitive to details of the nuclear charge distribution, but through $< \frac{1}{r_e} >$ sensitive to details of the electronic charge distribution. Different states $|\psi_e^{(0)}>$ will lead to different $< \frac{1}{r_e} >$ and therefore to the distinct atomic levels with their eV-separation in the first zoomed in part of VIP-1.

1.3 First-order Monopole Shift With Overlap

Let us now look at the monopole term, with a first order correction due to overlap. Looking back at the gravitational result, the size-dependent monopole contribution is:

$$E_{sz}^{qq\,(0)} = \frac{eZ}{6} \begin{bmatrix} \langle r_n^2 \rangle & 0 & 0 \\ 0 & \langle r_n^2 \rangle & 0 \\ 0 & 0 & \langle r_n^2 \rangle \end{bmatrix} \cdot \begin{bmatrix} \frac{\Delta V(\vec{0})}{3} & 0 & 0 \\ 0 & \frac{\Delta V(\vec{0})}{3} & 0 \\ 0 & 0 & \frac{\Delta V_e(\vec{0})}{3} \end{bmatrix} \tag{10}$$

$$= \frac{eZ}{6}\, \Delta V(\vec{0})\, \underbrace{\langle I|\, r_n^2\, |I\rangle}_{\langle r_n^2 \rangle} \tag{11}$$

Using Poisson's equation:

$$\Delta V_e(\vec{r}_e) \quad = \quad -\frac{\rho_e(\vec{r}_e)}{\epsilon_0} \tag{12}$$

the energy including shape- and size-dependent monopole contributions becomes[1]:

$$E_{qq}^{(0)} \quad = \quad E_\alpha \, - \, \frac{e^2 N Z}{4\pi\epsilon_0} \left\langle \frac{1}{r_e} \right\rangle \, - \, \frac{eZ}{6\epsilon_0} \, \rho_e(\vec{0}) \, \left\langle r_n^2 \right\rangle \tag{13}$$

Note that the size-dependent contribution is always positive. Equation 13 can be rewritten as:

$$E_{qq}^{(0)} \quad = \quad E_\alpha \, + \, \tilde{\mathrm{Q}} \left\{ -\frac{eN}{4\pi\epsilon_0} \left\langle \frac{1}{r_e} \right\rangle \right\} \, + \, \tilde{\mathrm{Q}} \left\{ -\frac{1}{6\epsilon_0} \, \rho_e(\vec{0}) \, \left\langle r_n^2 \right\rangle \right\} \tag{14}$$

with $\tilde{\mathrm{Q}} = eZ$ the nuclear charge. This notation shows explicitly that both the shape- and size-dependent monopole contributions are a product between the nuclear charge (the nuclear monopole moment) and a potential at the nucleus. The potential that appears in the shape-dependent contribution depends entirely on properties of the electrons (it is the electronic monopole field). The effect of the overlap between nuclear and electronic charge distributions can be interpreted as due to an extra positive potential $-\frac{1}{6\epsilon_0} \, \rho_e(\vec{0}) \, \left\langle r_n^2 \right\rangle$ at the nucleus. This potential depends not only on the electronic property $\rho_e(\vec{0})$, but also on the nuclear property $\left\langle r_n^2 \right\rangle$. The latter is not really surprising. If electrons penetrate into the nucleus, they will interact differently with a nuclear charge that is contained into a small or a large volume. This difference is expressed by the mean square nuclear radius. In the limiting case of a point nucleus ($\left\langle r_n^2 \right\rangle \to 0$), this size-dependent correction becomes zero, as we intuitively expect. The same is true when electrons can/do not enter the nucleus. Then this term is zero as well.

1.4 Electrons Inside The Nucleus

We have said that the size-dependent monopole term arises from electrons penetrating the nucleus. The questions we now have to ask ourselves is: do electrons penetrate the nucleus? In other words, does this term even exist in reality? In a non-relativistic treatment, s-electrons do have a non-zero probability at the position of the nucleus $\vec{r} = \vec{0}$. This happens even if the nucleus is a single mathematical point, as the s-electron wave function does not vanish at $\vec{r} = \vec{0}$. In a relativistic treatment also the $p_{\frac{1}{2}}$ electrons (= relativistic quantum number $\kappa = 1$, from the Dirac equation) can penetrate into the nucleus. Can we estimate the size of said size-dependent term? Only[2] s-electrons will contribute to the overall charge density ρ_e at $\vec{0}$. For a fully filled s-shell, we can therefore write

[1] Check that all terms have dimensions of energy.

[2] in the non-relativistic treatment

$\rho_e(\vec{0}) = -2e \left|\psi_s(\vec{0})\right|^2$, where ψ_s is a (single particle) s-electron wave function. Filling out values for the Be-atom ($Z = 4$, $r_n = 1.4 \cdot 10^{-15} A^{\frac{1}{3}}$ m, $|\psi_{2s}(\vec{0})|^2 = \frac{2Z^3}{a_0^3 \pi}$) yields 3.5 μeV. Overlap corrections to the monopole term are therefore of the order of magnitude of μeV. In order to calculate numerical values for these corrections, experimental values for $\langle r_n^2 \rangle$ must be known (they cannot yet be calculated from first principles nuclear theory). Alternatively, if energies are measured, this equation can be used to determine $\langle r_n^2 \rangle$.

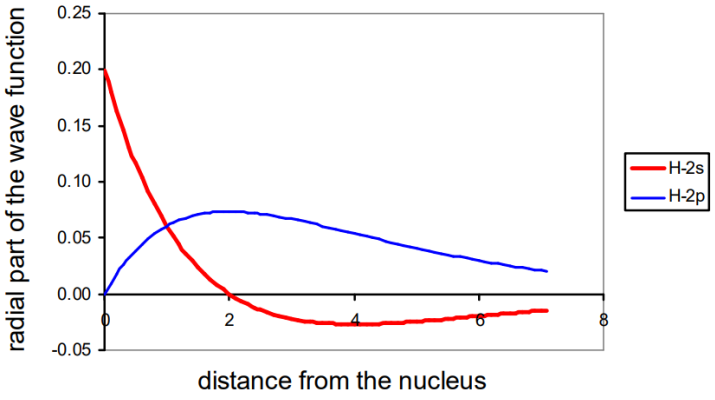

Figure 2: *Difference between radial part of the wave function for 2s and 2p electrons of the H-atom. One can cleary see that the 2s electrons have a change >0 to be at the origin.*

1.5 Isotope and Isomer Shift

The correction to the monopole energy due to the penetration of electrons into the nucleus does not lift any degeneracy, but only shifts the levels by a positive amount which depends on the amount of penetration and the mean square radius of the nucleus. The nuclei of different isotopes of the same element can be expected to have different nuclear radii, and hence different corrections. This effect is well-known in atomic spectroscopy as one of the contributions to the *isotope shift*, namely the *field shift*. There is another contribution to this isotope shift, which is due to the fact that different isotopes can have different masses: the *mass shift*. The observed isotope shift (in Fig. 2 on the next page) is the sum of field shift and mass shift. Two states (isomers, excited nuclei) of the same nucleus can have different radii a well, this is called the isomer shift. To be clear, this is not illustrated in Fig. 2.

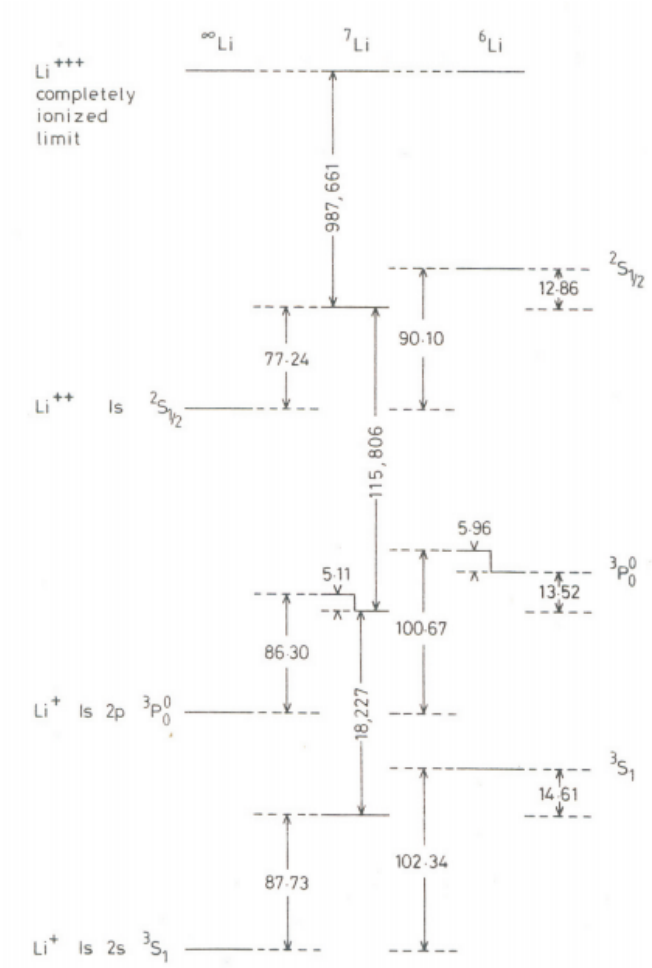

Figure 3: *Calculated mass shifts in free Li ions. All energies are relative to the completely ionized limit. Energies are expressed in* cm^{-1} *(multiply by 0.5809 to get values in* μeV*). For instance, the* $^3S_1$ *configuration (*$1s^1$ $2s^1$ *with the two spins parallel) in infinitely heavy* Li^+ *has an energy which is 87.73* cm^{-1} *(50.96* μeV*) lower than the same configuration in* $^7Li^+$*, and 102.34* cm^{-1} *(59.44* μeV*) lower than in* $^6Li^+$*. Comparisons with an infinitely heavy ion cannot be checked experimentally, but the difference of 14.61* cm^{-1} *(8.48* μeV*) between the* $^3S_1$ *configurations of* $^7Li^+$ *and* $^6Li^+$ *is present in experiments. Similar interpretations can be made for the* $^2S_{1/2}$ *configuration, while the* $^3P_0$ *configuration contains complications not discussed in this text. (Picture taken from* Isotope Shifts in Atomic Spectra*, W. H. King, Plenum Press, 1984.)*

1.6 Second Order Monopole Shift

We have just discussed the first order monopole shift, but what about the second order monopole shift? This correction is, as previously stated, much smaller then the first order shift (4^{th} power of nuclear radius instead of 2^{nd}). It will nonetheless pop up when dealing with so called "muonic atoms". These are atoms where one of the electrons is replaced by a muon, which is about 207 times heavier than the electron. Therefore it will circle much closer to the nucleus and have a larger overlap with said nucleus.

2 A Toy Model For The Monopole Shift

The writer of this document didn't think there was more background to add in addition to the course video about this topic. Writing about what is discussed in the video would be a literal translation from video to text, and this is not the purpose of these documents. For additional background on this video, please read https://biblio.ugent.be/publication/2988716/file/2988720.pdf. This is the paper from where said toy model originates and is writen by K. Rose and S. Cottenier (the lecturer of this course). The paper is free to download for everybody with a UGent account.

Hyperfinecourse A: magnetic hyperfine interaction

February 5, 2020

Abstract

This document is meant for optional background reading when studying www.hyperfinecourse.org. It deals with one of the chapters of this course. The formal course content is defined by the website and videos. The present document does not belong to the formal course content. It covers the same topics, but usually with more mathematical background, more physical background and more examples. Feel free to use it, as long as it helps you mastering the course content in the videos. If you prefer studying from the videos only, this is perfectly fine.

The present text has been prepared by Jeffrey De Rycke (student in this course in the year 2018-2019). He started from a partial syllabus written by Stefaan Cottenier for an earlier version of this course, and cleaned, edited and elaborated upon that material. That syllabus was itself inspired by a course taught by Michel Rots at KU Leuven (roughly 1990-1995).

1 Prologue

We have seen that the leading term in the Hamiltonian for the current-current interaction is:

$$\hat{H}_{jj} \;=\; -\,\hat{\vec{\mu}}_I \cdot \hat{\vec{B}}(\vec{0}) \tag{1}$$

In first order perturbation, we have to evaluate this in the eigenstates $\left| I \otimes \Psi_e^{(0)} \right\rangle$ of the monopole Hamiltonian:

$$E_{jj} \quad = \quad -\left\langle \Psi_e^{(0)} \otimes I \right| \hat{\vec{\mu}}_I \cdot \hat{\vec{B}}(\vec{0}) \left| I \otimes \Psi_e^{(0)} \right\rangle \tag{2}$$

We will examine this expression for the case of a free atom and a solid. The approach will be different in both cases. For a free atom, it will be possible to rewrite $\hat{H}_{jj}$ as a sum of operators for which the states of the total atom (electrons + nucleus) are eigen states. For a solid this is not possible. There we will let $\hat{\vec{\mu}}_I$ operate on the nuclear space and $\hat{\vec{B}}(\vec{0})$ on the electron space separately.

2 Free atoms

If we take spin-orbit coupling into account, the electron cloud of a free atom or ion is in a state $\left| \Psi_e^{(0)} \right\rangle = |J\rangle$ that has a well-defined, single value of J (Hyperfinecoure A: framework, 1.2.3 Spin-Orbit Coupling (fine splitting)). Without hyperfine interaction, the orientation of the nuclear angular momentum – indicated by I – is independent from the orientation of the electronic angular momentum – indicated by J. Therefore the $(2I+1)(2J+1)$ possible mutual orientations are all degenerate. Each such a state can be described either by I, m_I, J, m_J, or by I, J, F, m_F, with F given by

$$F \;=\; I{+}J,\, I{+}J{-}1,\, \ldots,\, |\, I{-}J| \tag{3}$$

F is a new angular momentum quantum number, that gives the angular momentum of the entire atom or ion. Each value of F indicates another mutual orientation of I and J, ranging from parallel ($F = I + J$) to antiparallel ($F = |I - J|$). As long as the hyperfine interaction is not taken into account, there is no need to use F.

The nuclear magnetic moment operator is parallel and related to the nuclear angular momentum operator via:

$$\hat{\vec{\mu}}_I \;=\; \frac{\mu}{I\,\hbar}\,\hat{\vec{I}} \tag{4}$$

The scalar quantity μ ('the' magnitude of the magnetic moment of the nucleus in the state $|I\rangle$) is experimentally known. Similarly also $\hat{\vec{B}}(\vec{0})$ – which we note

now explicitly as $\hat{\vec{B}}_J(\vec{0})$ – is parallel to $\hat{\vec{J}}$, say $\hat{\vec{B}}_J = \alpha\hat{\vec{J}}$[1]. If we now define the experimentally accessible quantity B_J as:

$$\begin{aligned} B_J &= <J,\, m_J = J|\, \hat{B}_{Jz}|\, J,\, m_J = J> & (5)\\ &= \alpha\hbar J & (6)\end{aligned}$$

we can write similarly to 4:

$$\hat{\vec{B}}_J = \frac{B_J}{J\hbar}\,\hat{\vec{J}} \tag{7}$$

The Hamiltonian 1 can be written now as[2]:

$$\begin{aligned} \hat{H}_{jj} &= -\frac{\mu B_J}{\hbar^2\, IJ}\,\hat{\vec{I}}\cdot\hat{\vec{J}} \\ &= -\frac{\mu B_J}{2\hbar^2\, IJ}\,(\hat{F}^2 - \hat{I}^2 - \hat{J}^2) & (8)\end{aligned}$$

We evaluate matrix elements of this hamiltonian in states specified by I, J, F, m_F, noted shortly as $|\, F>$. Because I, J and F are good quantum numbers for such a state, the matrix elements are:

$$\begin{aligned} <F|\, \hat{H}_{jj}|\, F> &= -\frac{\mu B_J}{2\hbar^2\, IJ}\, <F|\, \hat{F}^2 - \hat{I}^2 - \hat{J}^2|\, F> \\ &= -\frac{\mu B_J}{2\hbar^2\, IJ}\,\hbar^2\, \underbrace{(F(F+1) - I(I+1) - J(J+1))}_{C} \\ &= -\frac{1}{2}\, a\, C & (9)\end{aligned}$$

Here we defined the *hyperfine coupling constant* a as:

$$a = \frac{\mu\, B_J}{IJ} \tag{10}$$

Equation 9 tells that for a free atom with the nucleus in a state $|\, I>$ and the electron cloud in a state $|\, J>$ the energy contribution due to the current-current interaction depends on the mutual orientation of $\vec{I}$ and $\vec{J}$ as specified by F. The $(2I+1)(2J+1)$-fold degenerate level splits into different levels with each another value of F. The degeneracy is not completely lifted, as each F-level is still $(2F+1)$-fold degenerate (m_F does not appear in equation 9, this is due to the overall spherical symmetry [section 2.1]). The hyperfine coupling constant sets the scale for the energy differences between the F-levels. An example for $|\, I = 3/2>$ and $|\, J = 3/2>$ is shown in fig. 1. In this example, the energy between levels with a different F varies, which can be proven in general to be true. Similar to Land's interval rule:

$$\frac{E_F - E_{F-1}}{E_{F-1} - E_{F-2}} = \frac{F(F+1) - (F-1)F}{(F-1)F - (F-2)(F-1)} = \frac{F}{F-1} \tag{11}$$

[1] This can be understood classically: the magnetic field at the center of a planar circular current loop is parallel to the angular momentum of the moving charges.

[2] Use $\hat{\vec{F}}^2 = \hat{F}^2 = \left(\hat{\vec{I}} + \hat{\vec{J}}\right)^2 = \hat{I}^2 + \hat{J}^2 + 2\hat{\vec{I}}\cdot\hat{\vec{J}}$

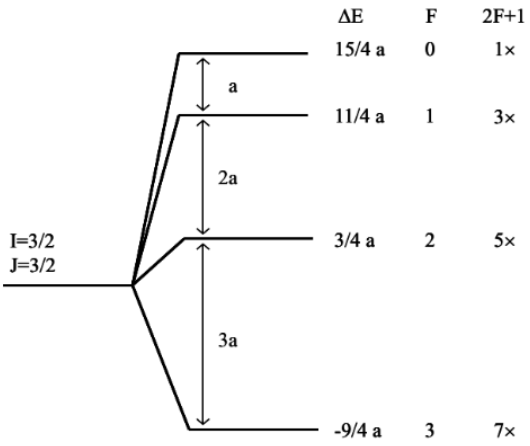

Figure 1: *Magnetic hyperfine splitting for an atom with nuclear spin $I = 3/2$ and electronic spin $J = 3/2$. The energy of the total system depends on how I and J are oriented with respect to each other, which is given by the new total spin F. The picture uses a correct scale. The right column gives the degeneracy of each level. The hyperfine variant of the Landé interval rule is illustrated as well.*

An order of magnitude estimate for the amount of splitting can be found by evaluating a for the typical values of $I = 3/2$, $J = 3/2$, $\mu = \mu_N$ and $B = 100$ T, which yields $a = 2.2 \cdot 10^{-25}\, J = 1.4\ \mu eV$. Note that we have again circumvented the lack of first principles knowledge of the nuclear magnetic dipole moment by substituting it by an experimental value (μ or g).

The hyperfine coupling constant a is a useful quantity. Measuring the energy splitting by either nuclear or atomic spectroscopy for a nucleus with known μ is an experimental way to determine the hyperfine field. Once the hyperfine field is known, the measurement can be repeated on another isotope of the same element. As the electron cloud is the same, also the hyperfine field will be the same[3]. Measuring the energy splitting therefore makes it possible to determine the magnetic moment of the new isotope (I can be determined because 11 has to be fulfilled). The hyperfine field can also be calculated by theory, which makes it possible to determine an unknown μ and I without a previous calibrating experiment.

[3]Some caution has to be given to the hyperfine anomaly.

The formalism we described here is applicable to free atoms and free ions only. In order to study free atoms or ions experimentally, they have to be measured while flying in a beam through vacuum. Qualitatively, the formalism can be used also to describe ions in ionic compounds (salts), as the Na^+ ion in NaCl.

Finally, note that the above formalism can be applied in exactly the same way to describe the coupling of the electronic L and S to J by the spin-orbit interaction. In the spin-orbit coupling constant an electronic magnetic moment of the order of μ_B instead of μ_N will appear. Because the latter is 3 orders of magnitude smaller than the former, and because the relevant magnetic field in the spin-orbit case is certainly not larger than a typical hyperfine field, typical spin-orbit splittings are in the meV-range. The distance between levels with different J will be given by 11, with J instead of F. This is called the *Landé interval rule*.

2.1 Breaking rotational invariance

After having taken into account the magnetic dipole term, not all degeneracy in the states of the atom or ion has been lifted: every state characterized by some F is still $2F + 1$-fold degenerate due to m_F (the orientation of the total angular momentum). The reason of this is obvious. The J-degeneracy was lifted because not every orientation of the angular momentum of the electron cloud *with respect to the angular momentum of the nucleus* was equivalent. We have taken into account this orientation of $\vec{J}$ with respect to $\vec{I}$ by considering the total angular momentum $\vec{F}$: different values for F indicate different relative orientations of $\vec{J}$ with respect to $\vec{I}$. But as soon as we consider the total angular momentum, we can again ask about its orientation. Now there is spherical symmetry again (or rotational invariance, in other words), as there is no special direction with respect to which we can specify the direction of $\vec{F}$. If we would introduce an external magnetic field, that would provide the special direction and the different m_F-levels would be Zeeman-split.

It will be convenient for later use to discuss here another (imaginary) way of breaking the rotational invariance of the atom. Imagine we could 'freeze' the electronic subsystem in a state with both $J = 3/2$ and $m_J = 3/2$ fixed. This implies that somehow we could determine a special z-direction, along which the z-component of $\vec{J}$ is taken. Instead of precessing about $\vec{F}$, $\vec{J}$ now precesses about the z-axis and yields a *static* magnetic field at the nucleus. A nucleus with $I = 3/2$ has 4 allowed orientations with respect to the same z-axis. They are given in fig. 2 as pictorial representations. For each of these 4 situations, the state of the entire system (nucleus + electrons) is given as a decomposition in states $|F, m_F>$. We can calculate the energy of these 4 states, as we know by fig. 1 the energies of individual F-states. Clearly, the 4 orientations of the nucleus correspond now to an equidistant Zeeman-splitting (fig. 3).

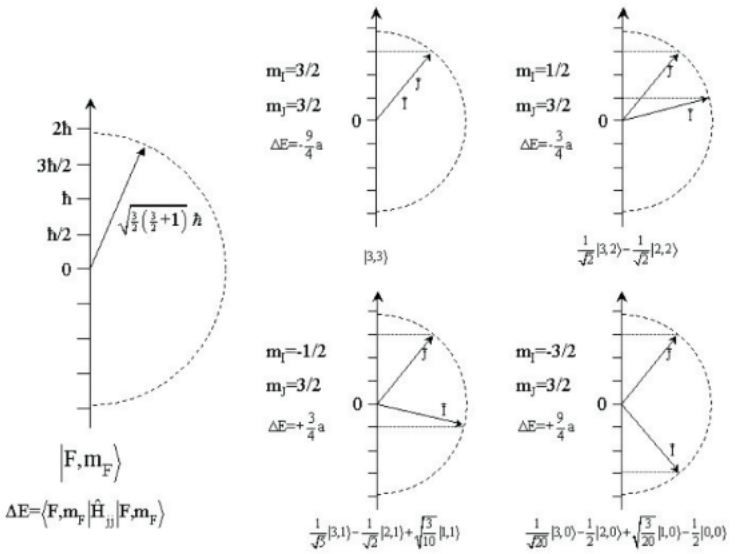

Figure 2: *Vector representation of the coupling of two spins I and J, being both 3/2. In units of ħ, their z-components are restricted to* $\pm\frac{3}{2}$ *and* $\pm\frac{1}{2}$*. The magnitude is* $\sqrt{\frac{3}{2}\left(\frac{3}{2}+1\right)}\hbar = 1.93\ \hbar$*. We consider the 4 different situations with* m_J *fixed to* $3/2$*, and* m_I *taking all of its 4 different values. In all 4 situations, the wave function and its energy are given.*

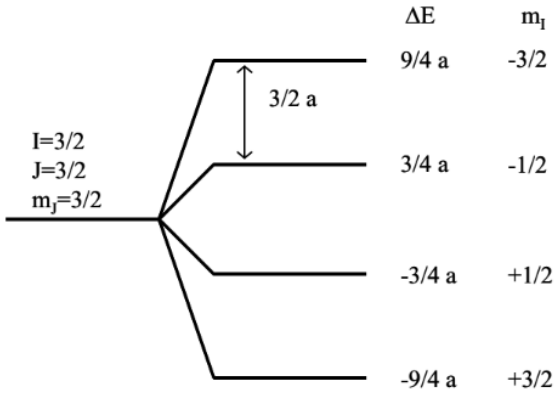

Figure 3: *Energy diagram of the 4 states given in fig. 2. Note that this is an equidistant (Zeeman) splitting.*

This is an important result. Our discussion with the total angular momentum $\vec{F}$ is valid only for atoms and ions, where $\vec{J}$ has a meaning. The entire system 'nucleus+electrons' is rotationally invariant. If this rotational invariance is broken by forcing the electron cloud with respect to some special direction, we cannot use $\vec{J}$ any more, and hence also not $\vec{F}$. In that case the energy of the system for a given state of the electron cloud (= for a given hyperfine field) is determined by the orientation of $\vec{I}$ with respect to the field. This will lead to a Zeeman splitting of the states of the system. Such a splitting is equidistant, in contrast to the situation for an atom or ion (fig. 1). This situation will appear for solids.

3 Solids

Consider an ideal solid, i.e. a perfect crystalline lattice that covers all space, without boundaries. The presence of the crystal breaks the isotropy of space: there is no rotational invariance in this case. The electron cloud is described by a many body wave function $\left|\psi_e^{(0)}\right\rangle$, but the concept of a well-defined angular momentum $\vec{J}$ is not valid any more. We are in the case described in section 2.1, where the electron cloud generates a magnetic field at the origin – where we have put our nucleus of interest – that has a well-determined direction in space. We will take the z-axis of our axis system along this magnetic field[4]. In this axis system, the magnetic hyperfine field therefore has a z-component only[5], and we can write it as $B(\vec{0}) = \left\langle \Psi_e^{(0)} \right| \hat{B}(\vec{0}) \left| \Psi_e^{(0)} \right\rangle$. The dot product of equation 2 can now be written as:

$$\begin{aligned} E_{jj} &= -\langle I|\,\hat{\vec{\mu}}_I\,|I\rangle \cdot \left\langle \psi_e^{(0)} \right| \hat{\vec{B}}\left(\vec{0}\right) \left| \Psi_e^{(0)} \right\rangle && (12)\\ &= -\langle I|\,\hat{\vec{\mu}}_I\,|I\rangle \cdot \vec{B}(\vec{0}) && (13)\\ &= -\langle I|\,\hat{\mu}_{I,z}\,|I\rangle\; B(\vec{0}) && (14) \end{aligned}$$

A numerical value for the hyperfine field $B(\vec{0})$ can be found if an explicit form of the operator $\hat{B}(\vec{0})$ is known, and if the ground state many body wave function $\left|\Psi_e^{(0)}\right\rangle$ for the solid is known. The problem of obtaining $\left|\Psi_e^{(0)}\right\rangle$ in order to find a numerical value for the hyperfine field will not be discussed, but is computable via point-nucleus DFT. The operator $\hat{\vec{\mu}}_I$ has been written explicitly in equation 4. We will see later how we can transform it into a sum of operators for which the $|I\rangle$ are eigenstates, after which the matrix elements are numerically found.

[4] This does not impose restriction: in case one wants to choose another axis, you can still solve the problem first with z parallel to the hyperfine field, and then transform back to the wanted axis system.

[5] Such an axis system is a *Principle Axis System* (PAS) for the magnetic hyperfine field.

3.1 The nuclear magnetic moment operator

In equation 4, we wrote the magnetic moment operator by means of the nuclear angular momentum operator. The three components of the latter vector operator

$$\hat{\vec{I}} \;=\; \hat{I}_x\vec{e}_x \,+\, \hat{I}_y\vec{e}_y \,+\, \hat{I}_z\vec{e}_z \tag{15}$$

can be written entirely in terms of the operator $\hat{I}_z$ and the raising and lowering operators $\hat{I}_\pm$, with the properties:

$$\hat{I}_+ \,=\, \hat{I}_x + i\hat{I}_y \qquad\qquad \hat{I}_+\,|I,\,m_I\rangle \,=\, \sqrt{I(I+1) \,-\, m_I(m_I+1)}\,\hbar\;|I,\,m_I+1\rangle \tag{16}$$

$$\hat{I}_- \,=\, \hat{I}_x - i\hat{I}_y \qquad\qquad \hat{I}_-\,|I,\,m_I\rangle \,=\, \sqrt{I(I+1) \,-\, m_I(m_I-1)}\,\hbar\;|I,\,m_I-1\rangle \tag{17}$$

This can be done as follows:

$$\hat{\vec{\mu}}_{Ix} \;=\; \frac{\mu}{2I\hbar}\left(\hat{I}_+ \,+\, \hat{I}_-\right) \tag{18}$$

$$\hat{\vec{\mu}}_{Iy} \;=\; \frac{\mu}{2I\hbar}\,\frac{1}{i}\left(\hat{I}_+ \,-\, \hat{I}_-\right) \tag{19}$$

$$\hat{\vec{\mu}}_{Iz} \;=\; \frac{\mu}{I\hbar}\,\hat{I}_z \tag{20}$$

Now we can easily find all matrix elements between states $|I,\,m_I\rangle$:

$$\langle m_I',\,I|\,\hat{\mu}_x\,|I,\,m_I\rangle \;=\; \frac{\mu}{2I}\left(\sqrt{I(I+1) \,-\, m_I(m_I+1)}\,\delta_{m_I',m_I+1} \,+\, \sqrt{I(I+1) \,-\, m_I(m_I-1)}\,\delta_{m_I',m_I-1}\right) \tag{21}$$

$$\langle m_I',\,I|\,\hat{\mu}_y\,|I,\,m_I\rangle \;=\; \frac{\mu}{2iI}\left(\sqrt{I(I+1) \,-\, m_I(m_I+1)}\,\delta_{m_I',m_I+1} \,-\, \sqrt{I(I+1) \,-\, m_I(m_I-1)}\,\delta_{m_I',m_I-1}\right) \tag{22}$$

$$\langle m_I',\,I|\,\hat{\mu}_z\,|I,\,m_I\rangle \;=\; \frac{\mu}{I}\,m_I\,\delta_{m_I',m_I} \tag{23}$$

As soon as we know the values of μ and I from experiment, these matrix elements are known – without the need for explicit expressions of $|I\rangle$ or $|I,\,m_I\rangle$.

3.2 Operator description of $\hat{\vec{\mu}}$

We have just introduced states $|\, I,\, m_I >$ of the nucleus, which are eigen states of the nuclear spin angular momentum operator $\hat{\vec{I}}$ and its z-component $\hat{I}_z$. We can get an idea about how fast a nucleus is spinning by treating its spin classically. A nucleus in the state $|\, I = \frac{1}{2} >$ has an expectation value of $\frac{\sqrt{3}}{2}\,\hbar = 9.1{\cdot}10^{-34}\ Js$ for the magnitude of its spin angular momentum. In order to obtain a similar value, a particle with the mass of a proton orbiting in a circle with radius equal to a typical nuclear radius (about 10^{-15} m) needs according to the classical equation $2\pi\, mr^2\nu$ to make the tremendous number of $9 \cdot 10^{21}$ revolutions per second.

The equivalent feature in quantum physics of the classical magnetic moment vector, is the magnetic moment (vector) *operator* $\hat{\vec{\mu}}$. The magnitude $\mu(I,\, m_I)$ of the magnetic moment of a nucleus in a state $|\, I,\, m_I >$ is the expectation value of the operator $\hat{\vec{\mu}}$ in that state:

$$\mu(I,\, m_I) \;=\; |\, \vec{\mu}(I,\, m_I)| \;=\; |\; <I,\, m_I|\, \hat{\vec{\mu}}|\, I,\, m_I > |\qquad (24)$$

In general, $\hat{\vec{\mu}}$ is built from the operators $\hat{\vec{L}}$ and $\hat{\vec{S}}$ working on the individual nucleons, and from the g_l and g_s of this nucleons. This microscopic approach is worked out in detail in the theory of nuclear models. Here we use the practical approach to define $\hat{\vec{\mu}}$:

$$\hat{\vec{\mu}} \;=\; \frac{g\,\mu_N}{\hbar}\,\hat{\vec{I}}\qquad (25)$$

where the dimensionless *g factor* is experimentally determined for every state of every nucleus[6]. This can also be expressed by the *gyromagnetic ratio* γ:

$$\hat{\vec{\mu}} \;=\; \gamma\,\hat{\vec{I}} \qquad \gamma \;=\; \frac{g\,\mu_N}{\hbar}\qquad (26)$$

If one speaks about 'the' magnetic moment μ of a nucleus with spin I, one refers by convention to the following quantity:

$$\begin{aligned}
\mu \;&=\; <I,\, m_I = I|\, \hat{\mu}_z|\, I,\, m_I = I> &(27)\\
&=\; \gamma\hbar I &(28)\\
&=\; g\mu_N I &(29)
\end{aligned}$$

Typical experimental values of g are of the order of unity, with either sign. Note that μ is an observable quantity, while $\hat{\mu}_z$ and $\hat{\vec{\mu}}$ are operators.

[6] When applied to a classical planar current loop, we retrieve the desired property that – because of the angular momentum which is normal to the plane of the loop – the magnetic moment is perpendicular to the loop.

3.3 Energy levels of the magnetic dipole hamiltonian for solids

Equation 14 gives the first order perturbations to the total energy due to the magnetic dipole interaction, where the matrix elements of the magnetic moment operator are given by equation 23, and the matrix element of the magnetic hyperfine field operator by equation 60. Assuming for a while that we already can obtain numerical values for the latter, we can write these corrections explicitely as the matrix elements of a nuclear Hamiltonian $\hat{H}^{nuc}_{jj}$:

$$E_{jj} = \langle I,\, m_I |\, \hat{H}^{nuc}_{jj}\, | I,\, m_I \rangle \tag{30}$$

$$\hat{H}^{nuc}_{jj} = -\frac{\mu\, B(\vec{0})}{I\,\hbar}\,\hat{I}_z \tag{31}$$

These nuclear matrix elements are sensitive to the *orientation* of the nucleus, as they depend on the quantum number m_I. The original, unperturbed Hamiltonian $\hat{T}_n + \hat{U}_{nn} + \hat{H}_0$ does not depend on m_I. We must therefore use first order perturbation theory for the degenerate case. Fortunately, the matrix formed by $\langle m'_I,\, I |\, \hat{H}^{nuc}_{jj}\, | I,\, m_I \rangle$ is already diagonal (use equation 23), and the eigenvalues – which are the first order corrections to the energy – can be read immediately from the diagonal (that will not be the case for the quadrupole interaction):

$$E^{m_I}_{jj} = -\frac{\mu\, m_I}{I}\, B_{hf} \tag{32}$$

(write B_{hf} for $B(\vec{0})$ from now on). These corrections depend on the orientation of the nuclear magnetic moment with respect to the hyperfine field, as specified by m_I. Using equation 29, this energy can be expressed in terms of the g-factor g_I of the nuclear state $|I\rangle$:

$$E^{m_I}_{jj} = -\, g_I\, \mu_N\, B_{hf}\, m_I \tag{33}$$

Verify that the orientation of $\vec{\mu}_I$ with the lowest energy is always parallel to $\vec{B}_{hf}$ ($m_I = \pm I$), independent on the sign of g_I. The nuclear spin I can be parallel or antiparallel to $\vec{B}_{hf}$, dependent on the sign of g_I.

The nuclear spin I can take $2I + 1$ different orientations with respect to $\vec{B}_{hf}$. The energy difference between two subsequent orientations is:

$$E^{m_I+1}_{hf} - E^{m_I}_{hf} = -\, g_I\, \mu_N\, B_{hf} = \hbar\, \omega_L \tag{34}$$

This is independent of m_I, and we thus find the familiar equidistant Zeemansplitting (fig. 4).

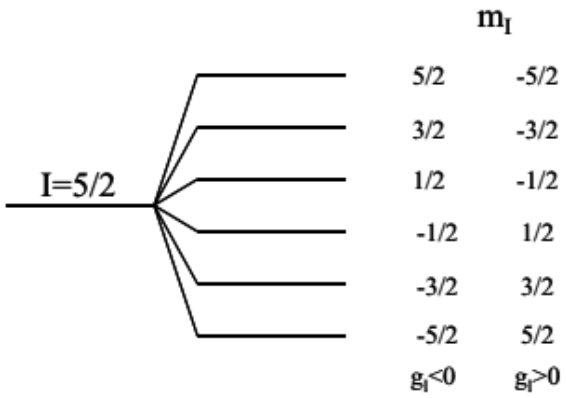

Figure 4: *Zeeman splitting under influence of a magnetic hyperfine field.*

For rather large values of $g_I = 1$ and $B_{hf} = 100\ T$, the energy between two subsequent levels is about $5 \cdot 10^{-25}\ J$ or 3 μeV, which is a very small value. Even at a quite low temperature of 1 K, the thermal energy kT is still 86 μeV. Therefore, at 1 K (and any higher temperature) a collection of nuclei subject to a hyperfine field will not settle in its lowest-energy orientation, but will by thermal agitation populate all m_I-levels and will hence have no preferred orientation. In order to obtain spontaneous orientation, temperatures in the mK-range are needed.

Provided one can in one way or another prepare an oriented collection of nuclei, will the hyperfine splitting then be observable? The typical splitting between two states $|\, I_1 >$ and $|\, I_2 >$ is roughly 100 keV. If one of these is split by a magnetic hyperfine field, we could in principle observe this splitting by detection of the radiation which is emitted in the radioactive decay from the higher into the lower level. However, detecting variations of the order of μeV on radiation with an energy of the order of 100 keV needs a resolution which is way beyond the capabilities of radiation detectors. More involved detection methods are needed to observe hyperfine splittings, and some of them will be discussed in the second part of this course.

The experimentally observable quantity is the hyperfine splitting ΔE, which depends on the product of two other observable quantities B_{hf} and g_I (or μ). Therefore, by measuring ΔE, we will not know B_{hf} and g_I (or μ) separately, only their product. If by an independent measurement the observable magnetic moment μ of the nucleus is known[7], a ΔE-measurement can be used to determine B_{hf}. On the other hand, if B_{hf} is somehow known[8], a ΔE-measurement determines μ.

[7] Several techniques for this exist in nuclear physics.

[8] By a direct calculation of the matrix elements of equation 60 for instance.

3.4 The magnetic hyperfine field operator

We will now construct an explicit expression for the operator $\hat{B}(\vec{0})$ (or $\hat{\vec{B}}(\vec{0})$). We will do this not by the general way of vector spherical harmonics, but by a much less general *ad hoc* approach.

WARNING: the following derivation – up to the line just before *equation 60 – might contain some inconsistencies.* Instead of considering the currents inside the nucleus interacting with the magnetic field due to the electrons – which is the way of thinking we adopted up to now – we will take the alternative but equivalent point of view of the current due to the electrons interacting with the magnetic field due to the nucleus. The latter point of view is mathematically somewhat more convenient, but both approaches would result in the same final expression.

The nuclear magnetic moment $\vec{\mu}_I$ at the origin of an axis system generates a vector potential $\vec{A}_n(\vec{r})$ at a position $\vec{r}$ equal to[9]:

$$\vec{A}_n(\vec{r}) \;=\; \vec{\nabla} \times \left(\frac{\mu_0 \, \vec{\mu}_I}{4\pi \, r} \right) \;=\; \frac{\mu_0}{4\pi} \, \frac{\vec{\mu}_I \times \vec{r}}{r^3} \tag{35}$$

The corresponding magnetic field at this position $\vec{r}$ is then

$$\vec{B}_n(\vec{r}) \;=\; \vec{\nabla} \times \vec{A}_n(\vec{r}) \tag{36}$$

It is clearly seen that this magnetic field is due to $\vec{\mu}_I$. The classical hamiltonian for a single electron $|\,\psi_e>$ moving in the scalar Coulomb potential V_n and vector potential $\vec{A}_n$ of the nucleus is:

$$\begin{aligned} H^{clas} &= \frac{\left(\vec{p} + e\vec{A}_n\right)^2}{2m} - eV_n \\ &= \left(-\frac{\hbar^2}{2m}\vec{\nabla}^2 - eV_n \right) + \frac{e}{2m}\left(\vec{p}\cdot\vec{A}_n + \vec{A}_n \cdot \vec{p} \right) + \frac{e^2}{2m}\vec{A}_n^2 \end{aligned} \tag{37}$$

with the linear momentum operator $\vec{p} = -i\hbar\vec{\nabla}$. In the last equation we recognize the hamiltonian of the electron in the absence of the magnetic field, plus a correction due to the presence of $\vec{B}_n$ (or equivalently, $\vec{A}_n$). We are interested in first order corrections only, and therefore neglect the term with $\vec{A}_n^2$.

$\vec{p}$ is an operator and can work both on $\vec{A}_n$ and on the wave function. Therefore

$$\begin{aligned} \left(\vec{p}\cdot\vec{A}_n\right)\,|\,\psi_e> &= -i\hbar\vec{\nabla}\cdot\left(\vec{A}_n\,|\,\psi_e>\right) \\ &= -i\hbar\left(\vec{\nabla}\cdot\vec{A}_n\right)|\,\psi_e> -i\hbar\vec{A}_n\cdot\vec{\nabla}|\,\psi_e> \\ &= \left(\vec{A}_n\cdot\vec{p}\right)|\,\psi_e> \end{aligned} \tag{38}$$

[9] This equation implies we adopt the Coulomb gauge $\vec{\nabla}\cdot\vec{A}_n = 0$.

because of the Coulomb gauge $\vec{\nabla} \cdot \vec{A}_n = 0$. The first order correction due to the magnetic field (current-current interaction) is therefore:

$$\begin{aligned} H_{jj}^{clas} &= \frac{e}{m}\,\vec{A}_n \cdot \vec{p} \\ &= \frac{e}{m}\,\frac{\mu_0}{4\pi\, r^3}\,(\vec{\mu}_I \times \vec{r}) \cdot \vec{p} \\ &= \frac{e}{m}\,\frac{\mu_0}{4\pi\, r^3}\,\vec{\mu}_I \cdot (\vec{r} \times \vec{p}) \qquad (39) \\ &= \frac{\mu_B \mu_0}{2\pi\,\hbar\, r^3}\,\vec{\mu}_I \cdot \vec{L}_i \qquad (40) \end{aligned}$$

with μ_B the Bohr magneton and $\vec{L}_i$ the orbital angular momentum operator for a single electron. For clarity, we stress here that $\vec{r}$ is the position vector of the electron in an axis system with the nucleus in the origin.

But in reality, we are *not* dealing with a classical problem. To describe relativistic effects (such as spin), we could of course resort to the Dirac hamiltonian to substitute equation 37. This is difficult however. An often used simpler approach is the Pauli approximation, which adds spin to the hamiltonian '*by hand*'[10]:

$$H^{Pauli} = \left(-\frac{\hbar^2}{2m}\vec{\nabla}^2 - eV\right) + \underbrace{\frac{\mu_B \mu_0}{2\pi\,\hbar\, r^3}\,\vec{\mu}_I \cdot \vec{L}_i \,+\, \mu_B\left(\vec{\sigma} \cdot \left(\vec{\nabla} \times \vec{A}_n\right)\right)}_{H_{jj}^{Pauli}} \qquad (41)$$

The vector $\vec{\sigma}$ is the vector of Pauli matrices:

$$\vec{\sigma} = (\sigma_x,\, \sigma_y,\, \sigma_z) \quad , \quad \sigma_x = \begin{bmatrix} 0 & 1 \\ 1 & 0 \end{bmatrix} \quad \sigma_y = \begin{bmatrix} 0 & -i \\ i & 0 \end{bmatrix} \quad \sigma_z = \begin{bmatrix} 1 & 0 \\ 0 & -1 \end{bmatrix} \qquad (42)$$

$$\vec{S} = \frac{\hbar}{2}\,\vec{\sigma} \qquad (43)$$

$\vec{S}$ is the spin angular momentum operator. In the Pauli formulation, a state $|\,\psi_e>$ is specified by a 2×1-matrix containing a spin up and spin down contribution:

$$|\,\psi_e> \sim \begin{bmatrix} \psi_+ \\ \psi_- \end{bmatrix} \qquad (44)$$

$$<\psi_e|\ \sim \begin{bmatrix} \psi_+ & \psi_- \end{bmatrix} \qquad (45)$$

As a result, H_{jj}^{Pauli} should be a 2×2-matrix[11]. This is obviously true for the second term in 41, while for the first term it is understood that both $\vec{\mu}_I$ and

[10] Verify that all terms in this hamiltonian have the dimension of energy.

[11] Verify that the eigenvalue of σ_z for a pure up-state $\begin{bmatrix} \psi_+ \\ 0 \end{bmatrix}$ is +1, and -1 for a pure down-state. The same you can prove from considering that the eigenvalues of S_z are $\pm\frac{\hbar}{2}$ and combining this with 43

$\vec{L}_I$ are notation for a diagonal matrix with on both diagonal positions the same vector operator $\vec{\mu}_I$ or $\vec{L}_I$. Now work out the spin dependent part of 41:

$$\mu_B\,\vec{\sigma}\cdot\left(\vec{\nabla}\times\vec{A}_n\right) = \frac{\mu_B\mu_0}{4\pi}\,\vec{\sigma}\cdot\left(\vec{\nabla}\times\left(\vec{\nabla}\times\frac{\vec{\mu}_I}{r}\right)\right) \tag{46}$$

$$= \frac{\mu_B\mu_0}{4\pi}\,\left[\left(\vec{\sigma}\cdot\vec{\nabla}\right)\left(\vec{\mu}_I\cdot\vec{\nabla}\right)-\left(\vec{\sigma}\cdot\vec{\mu}_I\right)\vec{\nabla}^2\right]\,\frac{1}{r} \tag{47}$$

$$= \frac{\mu_B\mu_0}{4\pi}\,\left[\left(\vec{\sigma}\cdot\vec{\nabla}\right)\left(\vec{\mu}_I\cdot\vec{\nabla}\right)-\frac{1}{3}\left(\vec{\sigma}\cdot\vec{\mu}_I\right)\vec{\nabla}^2\right]\,\frac{1}{r}\;-\;\frac{\mu_B\mu_0}{6\pi}\,\left(\vec{\sigma}\cdot\vec{\mu}_I\right)\vec{\nabla}^2\,\frac{1}{r} \tag{48}$$

The reason for the trivial step in the last line will become clear below. You can readily verify that $\vec{\nabla}^2\left(\frac{1}{r}\right)=0$ if $r\neq 0$. We will soon need to evaluate the expectation value $<\psi_e|\,H^{Pauli}\,|\,\psi_e>$, which involves an integral over the region of space where the electron can be. If the electron does not penetrate the nucleus, i.e. if $\vec{r}\neq\vec{0}$, then all terms with $\vec{\nabla}^2\left(\frac{1}{r}\right)$ will disappear from 46. No penetrations means no overlap of the nuclear and electronic current distributions. But even when sticking to a non-relativistic treatment, s-electrons – and only they – can penetrate the nucleus (as seen in hyperfine course A: electric monopole shift 1.4), making the two current distributions to overlap. We should therefore treat s- and non-s electrons seperately. For non-s electrons the magnetic contribution to the Pauli hamiltonian becomes:

$$H_{jj}^{Pauli} = \frac{\mu_B\mu_0}{2\pi\,\hbar\,r^3}\,\vec{\mu}_I\cdot\vec{L}_i\;+\;\frac{\mu_B\mu_0}{4\pi}\,\left(\vec{\sigma}\cdot\vec{\nabla}\right)\left(\vec{\mu}_I\cdot\vec{\nabla}\right) \tag{49}$$

$$= \frac{\mu_B\mu_0}{2\pi\,\hbar\,r^3}\,\vec{\mu}_I\cdot\vec{L}_i\;+\;\frac{\mu_B\mu_0}{4\pi}\,\left(\frac{-\vec{\sigma}\cdot\vec{\mu}_I+3\left(\vec{\sigma}\cdot\vec{e}_r\right)\left(\vec{\mu_I}\cdot\vec{e}_r\right)}{r^3}\right) \tag{50}$$

For s-electrons, the same hamiltonian will apply, but with an extra contribution at the point $r=0$ in the integration. We calculate now this extra overlap contribution (size contribution), for which we need the Poisson equation for the potential $V_e(\vec{r}\,')$, the latter being the Coulomb potential at $\vec{r}\,'$ due to an electron at $\vec{r}$ [12]:

$$\vec{\nabla}^2 V_e(\vec{r}\,') = \frac{e\rho_e(\vec{r}\,')}{\epsilon_0} \tag{51}$$

$$\vec{\nabla}^2\int\frac{-e\rho_e(\vec{r})}{4\pi\,\epsilon_0\,|\,\vec{r}-\vec{r}\,'|}\,d\vec{r} = \frac{e\rho_e(\vec{r}\,')}{\epsilon_0} \tag{52}$$

$$\vec{\nabla}^2\int\frac{\rho_e(\vec{r})}{|\,\vec{r}-\vec{r}\,'|}\,d\vec{r} = -4\pi\,\rho_e(\vec{r}\,') \tag{53}$$

[12] Sticking to our convention, we use the notation $\rho_e(\vec{r})$ for the probability density of an electron at the position $\vec{r}$. In most texts on classical electricity, this symbol is used for the *charge density*, however. Our notation $e\rho_e(\vec{r})$ is therefore equivalent with $-\rho_e(\vec{r})$ in traditional notation

Apply this general expression at the position $\vec{r}\,' = \vec{0}$, where the nucleus is:

$$\vec{\nabla}^2 \int \frac{\rho_e(\vec{r})}{r}\, d\vec{r} \;=\; -4\pi\, \rho_e(\vec{0}) \tag{54}$$

$$< \psi_e |\, \vec{\nabla}^2 \left(\frac{1}{r}\right) |\, \psi_e > \;=\; -4\pi\, \rho_e(\vec{0}) \tag{55}$$

Because we know that for every $r \neq 0$ the integral must yield a zero contribution, we conclude:

$$< \psi_e |\; \vec{\nabla}^2 \left(\frac{1}{r}\right)\Big|_{r=0} |\, \psi_e > \;=\; -4\pi\, \rho_e(\vec{0}) \;=\; -4\pi\, |\, \psi_e(\vec{0})|^2 \;=\; -4\pi\; < \psi_e |\, \delta(\vec{r}) |\, \psi_e > \tag{56}$$

$$\vec{\nabla}^2 \left(\frac{1}{r}\right) \;=\; -4\pi\, \delta(\vec{r}) \tag{57}$$

It can be proven – but we don't do it – that the first two terms in equation 48 cancel to a good approximation at $\vec{r} = \vec{0}$. Therefore for s-electrons the magnetic contribution to the Pauli hamiltonian becomes:

$$H_{jj}^{Pauli} \;=\; \frac{\mu_B \mu_0}{2\pi\, \hbar\, r^3}\; \vec{\mu}_I \cdot \vec{L}_i \;+\; \frac{\mu_B \mu_0}{4\pi}\; \left(\frac{-\vec{\sigma} \cdot \vec{\mu}_I + 3\, (\vec{\sigma} \cdot \vec{e}_r)\, (\vec{\mu_I} \cdot \vec{e}_r)}{r^3} \right) \;+\; \frac{2\mu_B \mu_0}{3}\, (\vec{\sigma} \cdot \vec{\mu}_I)\; \delta(\vec{r}) \tag{58}$$

Because non-s electrons will never appear at $\vec{r} = \vec{0}$, the term with the Dirac δ-function will not contribute for these electrons, and therefore equation 58 is our final and unambiguous expression for the magnetic contribution the the hamiltonian for any type of electrons in the Pauli approximation.

Finally, we now change back to the point of view of currents inside the nucleus, interacting with the magnetic field at the position of the nucleus due to the electrons. This is easily done because in equation 58 we recognize a dot product between the operator $\hat{\vec{\mu}}_I$ and another operator which we now identify with $\hat{\vec{B}}(\vec{0})$:

$$\hat{H}_{jj}^{Pauli} \;=\; -\hat{\vec{\mu}}_I \cdot \hat{\vec{B}}(\vec{0}) \tag{59}$$

The explicit form for the expectation value of $\hat{\vec{B}}(\vec{0})$ is:

$$\begin{aligned} \vec{B}(\vec{0}) \;=\; & -\frac{\mu_B \mu_0}{2\pi\hbar} \left\langle \psi_e^{(0)} \right| \frac{\vec{L}_i}{r^3} \left| \psi_e^{(0)} \right\rangle \;+ \\ & \frac{\mu_B \mu_0}{4\pi} \left\langle \psi_e^{(0)} \right| \frac{\vec{\sigma} - 3\, (\vec{\sigma} \cdot \vec{e}_r)\, \vec{e}_r}{r^3} \left| \psi_e^{(0)} \right\rangle \;+ \\ & -\frac{2\mu_B \mu_0}{3} \left\langle \psi_e^{(0)} \right| \vec{\sigma}\, \delta(\vec{r}) \left| \psi_e^{(0)} \right\rangle \end{aligned} \tag{60}$$

After having discussed the energy levels of the magnetic dipole hamiltonian in section 3.3 – the task we started with at the beginning of section 3 – some properties of the 3 contributions in equation 60 will be discussed in section 3.5.

3.5 Properties of 3 contributions to the magnetic hyperfine field

In equation 60 we obtained an expression for the magnetic hyperfine field $\vec{B}_{hf}$ at a site in an infinitely large crystal, an expression that consists of three contributions. With modern methods and computers, these contributions can be calculated from first principles, without experimental input (remember: this was not the case for the nuclear magnetic moment). We will not do this here yet, but rather discuss some of the properties of these three contributions to the magnetic hyperfine field.

3.5.1 The orbital contribution

Due to our choice of Z-axis on page 7, we know that $-\vec{\mu}_I \cdot \vec{B}_{hf} = -\mu_z B_{hf}$. The *orbital contribution* to the hyperfine field becomes:

$$B_{hf}^{orb} = -\frac{\mu_B \mu_0}{2\pi\hbar} < \psi_e | \frac{L_z}{r^3} | \psi_e > \tag{61}$$

This expression is valid both for solids[13] and for atoms. For atoms, it can be worked out further. First consider the contribution due to a single electron, indexed i:

$$B_{hf}^{orb,i} = -\frac{\mu_B \mu_0}{2\pi} m_{L,i} < \psi_{e,i} | \frac{1}{r^3} | \psi_{e,i} > \tag{62}$$

$$= -\frac{\mu_B \mu_0}{2\pi} m_{L,i} < \frac{1}{r^3} > \tag{63}$$

Restricting ourselves to cases where the LS-coupling scheme is valid, and where therefore $\sum_i m_{L,i} = L$, the contribution due to a given shell is:

$$B_{hf}^{orb} = -\frac{\mu_B \mu_0}{2\pi} < \frac{1}{r^3} > L \tag{64}$$

where $\left\langle \frac{1}{r^3} \right\rangle$ is now averaged over all electrons in the shell. From equation 64 we conclude that the orbital hyperfine field is zero when L is zero, i.e. for completely filled and half-filled shells, and for situations where 'quenching' of the orbital angular momentum occurs. 'Quenching' happens for ions with incompletely filled d-shells, incorporated in metals: due to the influence of the crystal field on the d-electrons, L turns out to become zero and the orbital hyperfine field vanishes. For lanthanide ions in metals, the valence 6s and 5d shells strongly reduce the influence of the crystal field on the incomplete 4f shell, which is nearer to the nucleus. Therefore the orbital hyperfine field due to the

[13] Common implementations of this term in computer codes will take into account only contributions from electrons in a region of space occupied by the atom to which the nucleus at which the orbital field is calculated belongs. Or in other words: we consider the orbital moment only of those electrons that orbit the nucleus under consideration. For a reliable calculation of the contribution due to orbital moments at other atoms in the crystal, quantum mechanics is less needed.

4f shell will survive.

We can estimate the size of the orbital hyperfine field for a lanthanide element where the f-electron sits at a typical distance of $a_0/2$ to be $(-100 \cdot L)$ T, with L ranging from 0 to 6. For ions with d-electrons at a typical distance of a_0, the orbital hyperfine field is about $(-10 \cdot L)$ T, with L often zero due to quenching.

In practical implementations in computer codes, the proper quantummechanical expression for the orbital contribution will be evaluated only for electrons that appear within the volume occupied by the atom to which the nucleus under consideration belongs. For electrons that appear on other atoms, a quantum mechanical treatment is not so much needed, and a classical summation is usually made.

The orbital hyperfine field can easily be understood in a classical way: it is the magnetic field at the nucleus due to the current loop of the electrons orbiting the nucleus. Consider a single electron in a circular orbit with radius r in the XY-plane. The magnetic field at the nucleus due to this electron is classically:

$$\vec{B} = \frac{\mu_0 I}{2r}\,\vec{e}_z \qquad I = -\frac{ev}{2\pi r} \tag{65}$$

The classical orbital angular momentum is $m_e\,\vec{r}\times\vec{v}$, with magnitude $m_e r v$ and z-component $m_e r v\,\vec{e}_z$. In classical mechanics, the magnitude of the total orbital angular momentum vector and its z-component are equal, in quantum mechanics both quantities are $\sqrt{l(l+1)}\,\hbar$ and $l\hbar$ respectively[14]. By using the 'equality' $m_e r v\,\vec{e}_z = l\hbar\,\vec{e}_z$ [15] one sees immediately that

$$\vec{B} = -\frac{\mu_0 e v}{4\pi r^2}\,\vec{e}_z \tag{66}$$

$$= -\frac{\mu_0 \mu_B}{2\pi}\,\frac{l}{r^3}\,\vec{e}_z \tag{67}$$

which is equal to 63 if also there the electron is taken to be in the XY-plane.

Finally, we prove that the orbital contribution to the hyperfine field is zero, when the electron cloud has cubic (or higher) symmetry. This can be seen e.g. by deducing from equation 39 the classical $\vec{B}_{hf}^{\,orb,\,class}$:

$$\vec{B}_{hf}^{\,orb,\,class} = -\frac{e}{m}\,\frac{\mu_0}{4\pi}\int \frac{\vec{r}\times\vec{p}}{r^3}\,\rho(\vec{r})\,d\vec{r} \tag{68}$$

For cubic symmetry, x-, y- and z-coordinates play the same role. If the electron therefore appears at a position $(x_0,\ y_0,\ z_0)$, it must by symmetry pass also

[14] Just for curiosity: note that in the classical limit ($l \to \infty$) both become equal again, as it should be.

[15] It is a correspondence between classical and quantum mechanics, rather than an equality.

at the positions ($\pm x_0$, $\pm y_0$, $\pm z_0$), with corresponding velocities. These are 8 positions in total. You can quickly check that the contribution of these 8 points to equation 68 is zero[16]. For every other point of the orbit you can find a corresponding set of 8 equivalent positions as well, and the integral in equation 68 will yield zero.

3.5.2 The spin dipolar contribution

To give a correct quantummechanical treatment of the *spin dipolar contribution* to the hyperfine field is somewhat more cumbersome than it was for the orbital contribution[17]. We are therefore satisfied with a classical interpretation only. The classical interaction energy between two magnetic dipoles $\vec{\mu}_I$ (which can be the nuclear spin) and $\vec{\mu}_s$ (which can be the electron spin) of Fig. 5 is given by:

$$E_{dip} = \frac{\mu_0}{4\pi} \frac{\vec{\mu}_I \cdot \vec{\mu}_s - 3\,(\vec{\mu}_I \cdot \vec{e}_r)\,(\vec{\mu}_s \cdot \vec{e}_r)}{r^3} \tag{69}$$

$$= -\vec{\mu}_I \cdot \vec{B}_s \tag{70}$$

The magnetic field at the position of the dipole $\vec{\mu}_I$ is then:

$$\vec{B}_s = -\frac{\mu_0}{4\pi} \frac{\vec{\mu}_s - 3\,(\vec{\mu}_s \cdot \vec{e}_r)\;\vec{e}_r}{r^3} \tag{71}$$

Using

$$\vec{\mu}_s = \frac{g_{S_{e^-}}\;\mu_B}{\hbar}\,\vec{S}_i \tag{72}$$

and 43 one sees that:

$$\vec{\mu}_s = -\mu_B\,\vec{\sigma} \tag{73}$$

which yields after taking the expectation value in a state $|\,\psi_e>$ the second term of equation 60. The spin dipolar hyperfine field $\vec{B}_{hf}^{\,dip,spin}$ can therefore be understood as generated by the intrinsic magnetic moment of the electrons.

In practical implementations in computer codes, the proper quantummechanical expression for the spin dipolar contribution will be evaluated only for electron spins that appear within the volume occupied by the atom to which the nucleus under consideration belongs. For electron spins that appear on other atoms, a quantum mechanical treatment is not so much needed, and a classical summation is usually made.

[16] Use e.g. that if $x_0 \to -x_0$, then $p_x = m\;\frac{dx}{dt}\Big|_{x_0} \to -p_x$.

[17] The reason is that the dot product $\vec{\sigma} \cdot \vec{r}$ is a 2×2 matrix of scalars: after taking the z-component of equation 60 we are still left with all three components of $\vec{\sigma}$ and the troubles they carry with them.

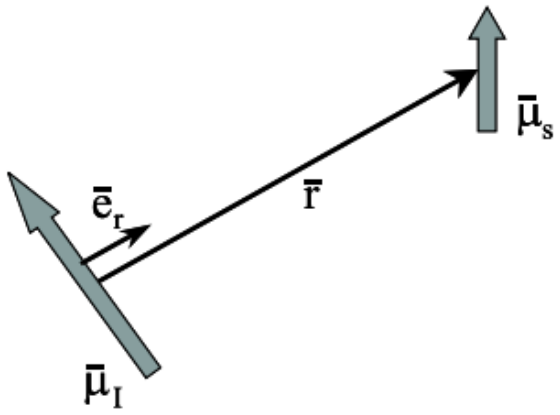

Figure 5: *Geometry for a dipole-dipole interaction between two magnetic moments.*

As for the orbital contribution, we can prove that the dipolar contribution due to a spin distribution with cubic (or higher) symmetry is zero. Consider a magnetic moment μ, distributed over space with a probability density $\rho_m(\vec{r})$ (the latter has as dimension $1/m^3$). At any point in space, the infinitesimal moment $\mu\rho_m(\vec{r})$ is pointing in the z-direction. Classically, the z- and xy-components of the magnetic field at the origin due to this distribution can be shown to be

$$B_z^{dip,\,class} = \frac{\mu_0}{4\pi}\,\mu \int \frac{3\cos^2\theta - 1}{r^3}\,\rho_m(\vec{r})\,d\vec{r} = \frac{\mu_0}{4\pi}\,\mu \int \frac{3z^2 - r^2}{r^5}\,\rho_m(\vec{r})\,d\vec{r} \tag{74}$$

$$B_{xy}^{dip,\,class} = \frac{\mu_0}{4\pi}\,\mu \int \frac{3\cos\theta\,\sin\theta}{r^3}\,\rho_m(\vec{r})\,d\vec{r} = \frac{\mu_0}{4\pi}\,\mu \int \frac{3z\,\sqrt{x^2+y^2}}{r^5}\,\rho_m(\vec{r})\,d\vec{r} \tag{75}$$

For $\rho_m(\vec{r})$ with cubic symmetry, the integral can be considered as an infinitesimal sum over sets of 8 equivalent (= same $\rho_m(\vec{r}_0)$) points ($\pm x_0$, $\pm y_0$, $\pm z_0$). It is easy to check that the contribution due to each such set is zero, and hence B_z and B_{xy} are zero too. When the symmetry is lower than cubic, but there is still axial symmetry about the z-axis, the xy-component will be zero. To obtain the z-component, the *opposite* contributions of $\rho_\uparrow(\vec{r})$ and $\rho_\downarrow(\vec{r})$ have to be summed.

A spin distribution with cubic symmetry is realized at a lattice site with a cubic point group[18], or in the case of a completely or half-filled shell in an atom. A special case of a half-filled shell is a single s-electron: this will have neither an orbital or a spin dipolar contribution. A typical value for $\vec{B}_s$ in cases where it does not vanish you can find by evaluating 71 with $\mu_s \approx \mu_B$ and $r \approx a_0$, which gives about 25 T.

3.5.3 The Fermi contact contribution

The *Fermi contact contribution* to the hyperfine field is:

$$B^f_{hf} = -\frac{2\mu_B\mu_0}{3} \left[\begin{array}{cc} \langle\Psi_{e,\uparrow}| & \langle\Psi_{e,\downarrow}| \end{array} \right] \sigma_z\, \delta(\vec{r}) \left[\begin{array}{c} |\Psi_{e,\uparrow}\rangle \\ |\Psi_{e,\downarrow}\rangle \end{array} \right] \tag{76}$$

$$= -\frac{2\mu_B\mu_0}{3} \left(\left|\psi_{e,\uparrow}(\vec{0})\right|^2 - \left|\psi_{e,\downarrow}(\vec{0})\right|^2 \right) \tag{77}$$

(note the appearance of the δ-function, which is the density operator we encountered before, but now applied to electrons with a specific spin). This celebrated equation due to Enrico Fermi[19] gives the most important contribution to the hyperfine field at spd-impurities in metals, where the orbital contribution is quenched, and the dipolar field is small (or zero due to symmetry). As an example we calculate the contribution to B^f_{hf} by a single 2s up electron, of which the probability density at $\vec{r} = \vec{0}$ is $|\psi_{2s}(\vec{0})|^2 = \frac{2Z^3}{a_0^3\pi}$:

$$B^f_{hf,\uparrow} = -\frac{4\mu_B\mu_0}{3\pi\, a_0^3}\, Z^3 = -33.4 \cdot Z^3 \text{ Tesla} \tag{78}$$

For Z=1 to 92, this yields contact fields from -33 T till -26 MT (Mega-Tesla). For 1s electrons, the contact fields are even 8 times higher, for $n \geq 3$ they are lower[20]. Such huge fields are normally not observed however, as most often in the same shell an s-electron with the opposite spin is present, that yields a contact field of different sign. At first sight, both fields would exactly cancel each other. This is often not the case, however, due to an effect called 'core polarization', which will shortly be touched in Sec. 5.2.

[18] Some attention is required here. Although at a given lattice site there can be *crystallographic* cubic point symmetry, this need not be the case for the electron distribution. Indeed, if spin-orbit coupling is important, the spin introduces a preferential direction which breaks the cubic symmetry. For instance, a substitutional Ca-impurity in bcc Fe sits at a site with cubic symmetry. Both orbital and dipolar contributions vanish, it feels a hyperfine field due to the Fermi contact contribution only (see soon). But for a much heavier U-impurity at the same site, spin orbit coupling is important. For this case, there will be orbital and dipolar fields, on top of the Fermi contact field.

[19] E. Fermi, Z. Phys. 60 (1930) 320

[20] Note once more that non-s electrons have a zero probability at the nucleus, and will not contribute to the contact field.

Be aware that the presence of a Fermi contact field is *not* a quantum effect, as is sometimes said, but rather a manifestion in a quantum system of a classical effect. The fundamental origin of the contact field lies in the overlap of two current distributions (size contribution), and can happen therefore also in classical electromagnetism. In the quantum system electrons+nucleus, such an overlap occurs, with a contact field as a result. Some elaborations on this point can be found in Manfred Bucher, *European Journal of Physics* 21 (2000) p. 19-22.

We just used the word 'size contribution' again. Indeed, the orbital and spin dipolar contributions to the magnetic dipole term are present whenever we deal with two current distributions. They depend on the details of the shape of the current distributions, and are therefore shape dependent terms in the sense of the multipole expansion. The Fermi contact contribution stems from the overlap of the two current distributions, just as the size dependent part of the monopole term stems from the overlap of two charge distributions. The Fermi contact contribution is part of a dipole term and is therefore a dot product between two vectors, while the size dependent part of the monopole term was a (dot) product between two scalars (look back at Hyperfinecourse A: quantum version Fig.1 to see the systematics).

There is one important difference, however, between the size-dependent charge-charge monopole contribution and the size-dependent current-current dipole contribution. The additional potential that was generated due to the charge-charge overlap depends on electronic *and* nuclear properties (Hyperfinecourse A: quantum version eq. 14), while the additional field (Fermi contact field) generated by the current-current overlap depends on electronic properties only. This has as a consequence that even in the limit of a point nucleus, the Fermi contact field will exist (as long as there is a net spin density at that point). In other words: the Fermi contact field is not sensitive to how exactly the nuclear magnetic moment is distributed over the volume of the nucleus. It is clear that the details of this distribution must have an influence. This (small) effect is called the *Bohr-Weisskopf effect*, and it will be discussed qualitatively in section 6.

4 Symmetry properties of magnetic hyperfine interactions in solids

When talking about symmetry, we need to make sure we specify which property we are discussing (and from which point of view). Take image 6.a, which is a 2D analogon of a body centred cubic unit cell. From the perspective of the central atom, there is 'cubic' symmetry (more strictly: the point group of the central atom has the same symmetry operations as a square). There are no magnetic moments involved in this example, in contrast to the next two examples. Therefore, we can consider this cubic symmetry as being a chemical symmetry property.

Apart from chemical symmetry, there might be symmetry related to magnetic properties as well. In fig. 6.b, a 2D analogon of a ferromagnetic cubic unit cell is shown. The four magnetic moments on the neighbouring atoms point in the same direction. A rotation over 90 degrees is now not a symmetry operation any longer, as it changes the orientation of the moments. This is an example of magnetic symmetry that is different from chemical symmetry. In fig. 6.c, the orientation of the magnetic moments is different, and is such that the fourfold rotation symmetry is restored. Here chemical and magnetic symmetry are identical.

The role of symmetry in HFF is as follows. If there is chemical and magnetic cubic symmetry (image on the right), the orbital and spin dipolar contributions to the magnetic HFF disappear. If there is only chemical symmetry, these parts only approximately disappear. This is seen in the next section when talking about the magnetic hyperfine contributions to the HFF field of Fe in Fe_4N.

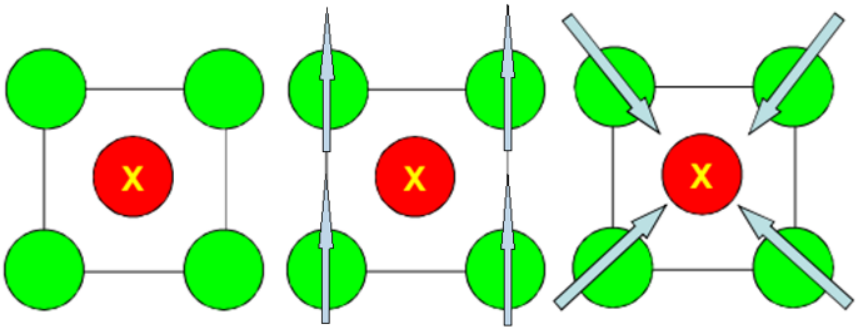

Figure 6: On the left: chemical cubic symmetry. In the centre: chemical cubic symmetry but no magnetic symmetry. On the right: chemical and magnetic cubical symmetry.

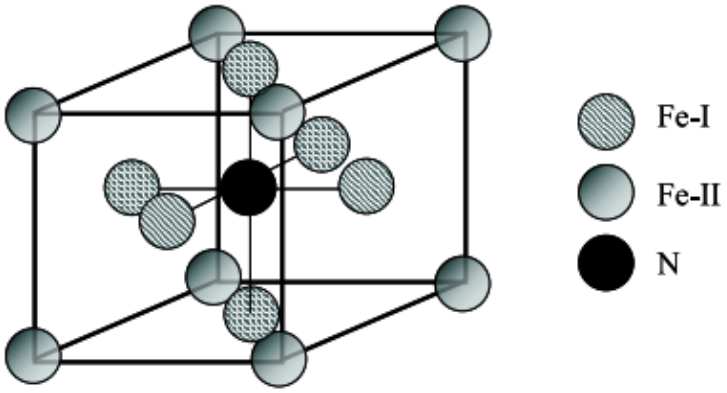

Figure 7: Unit cell of Fe_4N (a=b=c).

5 Examples of magnetic hyperfine fields in solids

5.1 The HFF of Fe in Fe_4N

We will discuss the HFF of Fe in ferromagnetic Fe_4N. The Fe sublattice has fcc structure, and in the center of a conventional fcc cube sits one Nitrogen atom. We will discuss this example, but in a more qualitative measure (such as symmetry etc.) (Fig. 7).

Already at the level of crystallographic symmetry, there are two inequivalent Fe sites in this structure: six Fe-I atoms, which are at the face centers of the cube and are separated from N by one half of the lattice constant, and eight Fe-II atoms, which are at the corners of the cube and are at $\sqrt{3}/2$ times the lattice constant from N. An Fe nucleus at these sites 'sees' different surroundings, depending whether it sits on site I or II. Therefore, different magnetic fields at this nucleus can be expected. The point symmetry groups for both sites are listed in Tab. 1. Furthermore, orientation of the magnetic moments of the Fe-atoms may further reduce the symmetry by the spin-orbit coupling. If the direction of ferromagnetic alignment is (001), then for two of the six Fe-I atoms the two N-neighbours lie along the magnetic moment direction (Fe-Ia), while for the other four Fe-I the two N-neighbours are connected by a line that is perpendicular to the moment direction (Fe-Ib). If, on the other hand, the magnetic moments would point along the (111) direction, then all six Fe-I atoms remain equivalent.

As can be seen in Tab. 1, whenever the direction of the moments is taken into account, the point groups of the different Fe-sites are noncubic. As a consequence, there will be orbital and spin dipolar contributions to the hyperfine field, and these contributions can be different for each inequivalent Fe-site.

crystallography only	Pm$\bar{3}$m (221)
Fe-I	4/mmm
Fe-II	m$\bar{3}$m
moments ∥ (001)	P4/mmm (123)
Fe-Ia	4/mmm
Fe-Ib	mmm
Fe-II	4/mmm
moments ∥ (111)	R$\bar{3}$m (166)
Fe-I	2/m
Fe-II	$\bar{3}$m1

Table 1: *Space groups and point groups for Fe_4N with different orientations of the magnetic moments of Fe.*

A Mössbauer experiment[21] on Fe_4N [22] shows 3 inequivalent sites. This is consistent with an orientation of the magnetic moments along the (001) direction, a conclusion which is supported by transverse Magneto-Optical Kerr Effect experiments ('transverse MOKE'). The electric-field gradient plays a role in this story as well, and we will therefore come back to this example in Hyperfinecourse A: electric quadrupole interaction.

Fig. 8 lists which sites have cubic or non-cubic symmetry, when considering the chemical symmetry only or including magnetic symmetries:

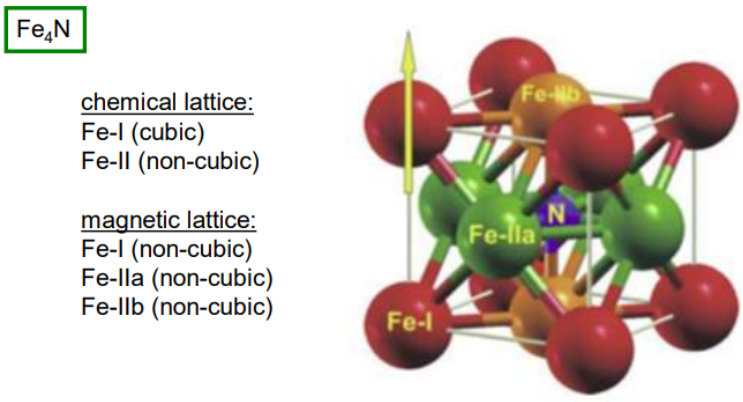

Figure 8: *Different directions and their symmetries.*

[21] Mössbauer Spectroscopy is an experimental method that will be discussed in the second part of this book.

[22] J.L. Costa-Krämer, D.M. Borsa, J.M. García-Martín, M.S. Martín-González, D.O. Boerma and F. Briones, *Physical Review B* **69** (2004) 144402

Direction	Fermi contact hff
Fe-I	-29.7
Fe-IIa	-21.0
Fe-IIb	-21.1
Direction	orbital hff
Fe-I	3.7
Fe-IIa	0.4
Fe-IIb	2.7
Direction	dipolar hff
Fe-I	0.0
Fe-IIa	3.0
Fe-IIb	-6.3

Table 2: *Values of the different magnetic HFF contributions for different directions and different contributions.*

When using figure 5 and table 2 side by side, one can see the effects of the symmetries (chemical and magnetic) on the values of the different HFF contributions.

5.2 The HFF of impurities in bcc Fe

Take the HFF of an Fe atom in bcc-Fe. What would happen with this field if one Fe atom in the entire crystal is replaced by an atom of another element? The nucleus of this other element will see an entirely different electronic surrounding then the Fe nucleus did: instead of the 26 electrons of Fe, it is surrounded by Z electrons (Z=1-100) of this new element. The valence electrons among them will make bonds with the surrounding Fe host lattice. These valence electrons are not necessarily 4s3d-electrons as for Fe: s-, sp- and sdf-electrons are possible as well, with different principal quantum numbers (1s-7s, 2s2p-6s6p, 4s3d-6s5d, 6s5d4f-7s6d5f). This will result in a variety of types of bonds, each with their own characteristic consequences for the hyperfine fields (Fig. 9). To name a few:

- Up to about Xe, the Fermi contact field is by far the major contribution to the total hyperfine field. For heavier elements, orbital and spin dipolar contributions can become important as well (spin-obit coupling!). For lanthanides and actinides, the orbital contribution from 4f or 5f electrons is overwhelmingly dominant.

- The Fermi contact contribution is negative in the beginning of an sp-series, and much larger and positive at the end of it. This effect can be understood[23] through the exchange interaction between the impurity-s and Fe-3d electrons.

[23] H. Akai, M. Akai, S. Blügel, R. Zeller, and P.H. Dederichs, *Journal of Magnetism and Magnetic Materials* **45** (1984) 291, V. Bellini, S. Cottenier, M. Çakmak, F. Manghi and M. Rots, *Physical Review B* **70** (2004) 155419.

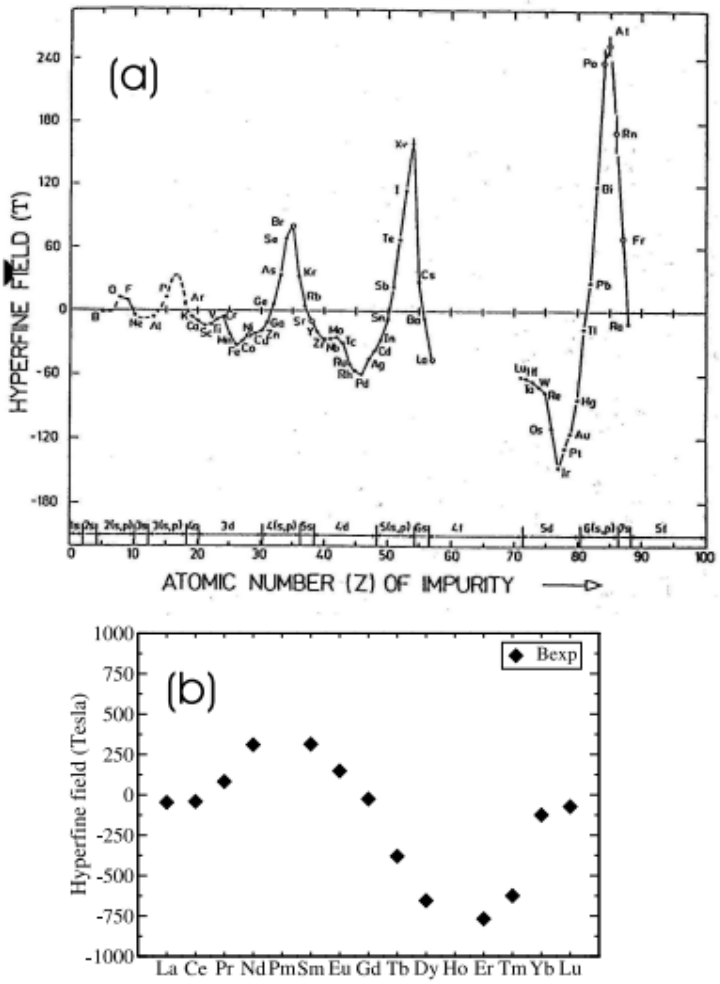

Figure 9: *Experimental hyperfine fields for (a) all spd-elements, and (b) all lanthanides, always as substitutional impurities in bcc-Fe. Mind the difference in the vertical scales between (a) and (b). Not for all elements experimental data are available. Some of the measured values are very accurate, others carry large error bars (not shown). Only in a minority of cases the sign is experimentally determined, the signs shown in these pictures are often guessed from systematics. The source of (a) is N. Severijns, J. Wouters, J. Vanhaverbeke, W. Vanderpoorten and L. Vanneste,* Hyperfine Interactions ***60*** *(1990) 889, (b) is taken from D. Torumba, S. Cottenier, V. Vanhoof and M. Rots. PRB 74 (2006) 014409 (https://dx.doi.org/10.1103/PhysRevB.74.014409) .*

- The Fermi contact field at the end of the sp-series becomes larger if one moves down along a column in the periodic table. This is due to the Z-dependence of the s-electron penetration in the nucleus: while moving down a column, the spin-polarization is more or less constant, but due to the Z-dependence the resulting contact field grows.

- While going through a d-series, the contact field in the second half of any d-series is somewhat larger than in the first half, which is referred to as an "S-shaped curve". This "S" is a result of two effects: core-polarization and the coupling between the impurity d-moment and the Fe-3d moment of the host lattice. The d-moment of the impurity will induce a core Fermi field that is strictly proportional to the magnitude of the d-moment, and has the opposite sign. Also the total Fermi field (core+valence) will be more or less proportional to this d-moment, still with the opposite sign. The d-moment is almost exclusively a spin moment (due to quenching of the orbital moment), and will therefore be largest in the middle of the d-series. For the first half of a d-series, the impurity d-moment will couple antiparallelly[24] to the Fe-3d moment. The sign of the impurity moment is therefore negative, the sign of the Fermi field is positive, and this will (in absolute value) reduce the negative Fermi field from the sp-electrons (which is there since d-elements have the same sp-configuration as early sp-elements). In the second half of a d-series, the coupling is parallel: now the sp-contribution to the Fermi field and the core polarization due to the impurity d-electrons will have the same negative sign, and the absolute value of the total field will therefore be larger (=more negative).

The Z-dependence of the impurity hyperfine fields in an Fe host lattice form an intriguing case study in condensed matter physics. Either when going through a period or through a group of the periodic table, the systematics of these impurity hyperfine fields illustrate basic concepts about electronic bonding in solids. Measuring these hyperfine fields requires a variety of specialized experimental methods, and gathering the data shown in Fig. 9 took 30 years of efforts by many research groups. Knowledge of the values of these hyperfine fields is of practical importance for the determination of nuclear magnetic moments, for which the interaction with strong magnetic fields – such as the hyperfine fields – is needed. This experimental data set has also been an important testing ground for *ab initio* calculations, which are now able to reproduce the values and – even more important – to explain the physical mechanisms behind these observed hyperfine fields[25].

[24] See the earlier reference to H. Akai (1984)

[25] M. Akai, H, Akai and J. Kanamori, *Journal of the Physical Society of Japan* **54** (1985) 4246, T. Korhonen, A. Settles, N. Papanikolaou, R. Zeller and P.H. Dederichs, *Physical Review B* **62** (2000) 452, S. Cottenier and H. Haas, *Physical Review B* **62** (2000) 461, D. Torumba, S. Cottenier and M. Rots, [submitted to PRB].

6 An extended nucleus (Bohr-Weisskopf effect)

It has been pointed out in section 3.5.3 that the Fermi contact field is independent of nuclear properties. This would lead for two isotopes with the same $\vec{\mu}_I$ to an identical interaction energy, independent of how the moment is distributed over the nuclear volume. Clearly, this is in contradiction with intuition: the electrons that penetrate the nuclear volume should somehow be affected by the details of the nuclear moment distribution. In this section, we will show more precisely how this is visible in experiments. We will not derive quantitative formulae, however, as this would lead us too deep into nuclear theory.

An extended nucleus has its dipole moment distributed over some volume of space. The interaction energy for a nuclear dipole moment of an extended nucleus and the magnetic hyperfine field is written as an extension of equation 13 as:

$$E_{mag} = -\int_{nuc} \vec{B}_{hf} \cdot d\vec{\mu}_I \tag{79}$$

where the integral is taken over the nuclear volume. If $\vec{B}_{hf}$ is constant over the nuclear volume, it can be taken out of the integral and we find equation 13 again. But in general, $\vec{B}_{hf}$ is not constant. For example, $|\,\psi_{e,\uparrow}(\vec{r})\,|^2$ for an s-electron is maximum at $\vec{r} = \vec{0}$ and drops for larger $\vec{r}$. If the nucleus is rather large (i.e. for large Z), the drop becomes appreciable and the contact hyperfine field might vary over the nuclear volume. One can therefore expect that experimental hyperfine fields will deviate somewhat from the formulae we calculated above, especially in heavy nuclei. However, for heavy nuclei a relativistic treatment is more appropriate, and therefore most deviations will be due to our non-relativistic approach rather than to the extended nucleus[26].

An experimentally more important influence of the nuclear size occurs when the distribution of the magnetic moment is different for different isotopes of the same element. Two different isotopes will have in general two different nuclear magnetic moments $\vec{\mu}_{I1}$ and $\vec{\mu}_{I2}$. If one is able to bring both types of atoms in a situation where no hyperfine field is present, one can determine the ratio of the magnetic moments experimentally as follows. Apply a homogeneous external magnetic field. This will be constant over the nuclear volume and thus $\vec{B}_{hf}$ can be extracted from the integral in equation 79. Provided one can measure the energy associated with the hyperfine interaction[27] (we will see methods for this

[26] In a correct relativistic treatment, it turns out that the integration in equation 79 has to be done over a volume *larger* than the nuclear volume. Its radius r is one half of the Thomson radius ($r = \frac{r_T}{2} = \frac{Z\,e^2}{2m_e\,c^2}$, which is roughly 10 times larger than the nuclear radius $r = r_0\,A^{\frac{1}{3}}$ ($r_0 = 1.4 \cdot 10^{-15}\ m$). (see S. Blügel, H. Akai, R. Zeller and P. H. Dederichs, Physical Review B **35** (1987) 3271)

[27] Although there is no *internal* hyperfine field, we call the interaction of the nuclear magnetic moment with the *externally* applied magnetic field also a hyperfine interaction.

in the second part of this course), the ratio $\vec{\mu}_{I1}/\vec{\mu}_{I2}$ is known:

$$\frac{E_1}{E_2} = \frac{\vec{\mu}_{I1}}{\vec{\mu}_{I2}} \tag{80}$$

because the constant field at the nucleus is the same applied field.

The situation becomes different when an internal hyperfine field is present in both measurements. Then the effective $\vec{B}$ at the nucleus (hyperfine field and possibly an applied field) is not constant and now the extendedness of the nuclei of both isotopes will play a role. The ratio between both measured energies will be:

$$\frac{E_1}{E_2} = \frac{\vec{\mu}_{I1}}{\vec{\mu}_{I2}} (1 + \Delta) \tag{81}$$

where Δ is a small correction factor due to the extendedness of the the nuclei. One calls Δ the *hyperfine anomaly*, and the fact that it can be different from zero is called the *Bohr-Weisskopf effect*[28]. Experimentally determined hyperfine anomalies are below 2%, and are highest in heavy (and hence large) nuclei where the s-electrons can spend an appreciable time inside the nucleus. In very light nuclei an *apparent* hyperfine anomaly can seem to be present, which is due however to the quantummechanical zero-point motion of the nucleus.

One could attribute the Bohr-Weisskopf effect to an extra field that is generated at the nucleus, on top of the Fermi contact field. That extra field – let us call it the Bohr-Weisskopf field – is zero for a point nucleus, and depends on how the nuclear magnetic moment is distributed over the nuclear volume. Formally, we can write the interaction energy due to the size-dependent dipole term as:

$$E_{sz}^{jj\,(1)} = -\vec{\mu}_I \cdot \vec{B}_{Fermi} - \vec{\mu}_I \cdot \vec{B}_{BW}\,[\vec{\mu}_I(\vec{r})] \tag{82}$$

where $\vec{B}_{BW}$ is a functional of the magnetic moment distribution. (Look back at Hyperfinecourse A: a quantum version Fig. 1 to put $\vec{B}_{Fermi}$ and $\vec{B}_{BW}$ in relation with the other interactions.)

Because Δ depends on the detailed distribution of the nuclear magnetic moment, it is sensitive to for instance the ratio of orbital to spin contribution to the moment. Δ-measurements can therefore be used to test nuclear models.

[28] See S. Büttgenbach, *Hyperfine Interactions* **20** (1984) 1-64 for a detailed review.

Hyperfinecourse A: electric quadrupole interaction

February 6, 2020

Abstract

This document is meant for optional background reading when studying www.hyperfinecourse.org. It deals with one of the chapters of this course. The formal course content is defined by the website and videos. The present document does not belong to the formal course content. It covers the same topics, but usually with more mathematical background, more physical background and more examples. Feel free to use it, as long as it helps you mastering the course content in the videos. If you prefer studying from the videos only, this is perfectly fine.

The present text has been prepared by Jeffrey De Rycke (student in this course in the year 2018-2019). He started from a partial syllabus written by Stefaan Cottenier for an earlier version of this course, and cleaned, edited and elaborated upon that material. That syllabus was itself inspired by a course taught by Michel Rots at KU Leuven (roughly 1990-1995).

1 From toy model to quantum physics

The writer of this document didn't think there was more background to add in addition to the course video about this topic. Writing about what is discussed in the video would be a literal translation from video to text, and this is not the purpose of these documents. For additional background on this video, please read https://biblio.ugent.be/publication/2988716/file/2988720.pdf. This is the paper from where said toy model originates and is writen by K. Rose and S. Cottenier (the lecturer of this course). The paper is free to download for everybody with a UGent account.

2 Quadrupole operator

As developed in Hyperfinecourse A: quantum version (equation 31), the leading correction term in the hamiltonian for the charge-charge interaction is:

$$\hat{H}_1 \;=\; \hat{H}_{qq} \;=\; -\frac{e^2 N Z}{5\epsilon_0}\left(\frac{1}{r_e^3}Y^2(\theta_e,\,\phi_e)\right)\cdot\left(r_n^2\,Y^2(\theta_n,\,\phi_n)\right) \tag{1}$$

In first order perturbation theory, we have to evaluate this in the eigenstates $\left|I\otimes\psi_e^{(0)}\right\rangle$ of the monopole hamiltonian $\hat{H}_0 \,=\, \hat{T}_n + \hat{U}_{nn} + \hat{H}_0$:

$$E_{qq} \;=\; -\left\langle\psi_e^{(0)}\otimes I\right|\frac{e^2 N Z}{5\epsilon_0}\left(\frac{1}{r_e^3}Y^2(\theta_e,\,\phi_e)\right)\cdot\left(r_n^2\,Y^2(\theta_n,\,\phi_n)\right)\left|I\otimes\psi_e^{(0)}\right\rangle \tag{2}$$

We do not consider charge-charge overlap, therefore we can separate the expression into:

$$E_{qq}^{(2)} \;=\; \langle I|\,{}_s\hat{Q}_{sh}^{(2)}\,|I\rangle\,\cdot\,\left\langle\psi_e^{(0)}\right|{}_s\hat{V}_{sh}^{(2)}\left|\psi_e^{(0)}\right\rangle \tag{3}$$

where we defined the nuclear electric quadrupole moment tensor operator (dimension Cm^2 or electron barn (eb))

$$\hat{Q}_q^2(\vec{r}_n) \,=\, eZ\sqrt{\frac{4\pi}{5}}\,r_n^2\,Y_q^2(\theta_n,\,\phi_n) \tag{4}$$

which operates on the nuclear space, and the electric quadrupole field tensor operator (or electric-field gradient tensor operator, dimension $\mathrm{V/m}^2$)

$$\hat{V}_q^2(\vec{r}_e) \,=\, -\frac{eN}{\sqrt{20\pi}\,\epsilon_0}\,\frac{1}{r_e^3}\,Y_q^2(\theta_e,\,\phi_e) \tag{5}$$

which operates on the electron space.

Let us not forget that expression 3 is a matrix. More precisely the matrix for the degenerate case of first order perturbation. It gives us information of the behaviour of the nucleus in the presence of the electric field gradient from the electrons.

2.1 The electric-field gradient operator

The matrix on the right in equation 3 is a tensor of rank two. It is symmetric and traceless and can therefore be described by 5 numbers. These 5 values can be calculated via ab initio code (which we do not discuss here), we will consider these 5 values as known. The 5 values depend on the choice of our axis system. Explicit expressions for the components of the cartesian forms of $Q_{sh}^{(2)}$ and $V_{sh}^{(2)}$ can be found by making the substitutions Hyperfinecourse A: quantum version (equation 17-21) in:

$$E_{pot}^{(2)} = \frac{1}{6}\int_1\int_2 \begin{bmatrix} 3x_1^2-r_1^2 & 3x_1y_1 & 3x_1z_1 \\ 3x_1y_1 & 3y_1^2-r_1^2 & 3y_1z_1 \\ 3x_1z_1 & 3y_1z_1 & 3z_1^2-r_1^2 \end{bmatrix} \cdot \frac{1}{r_2^5} \begin{bmatrix} 3x_2^2-r_2^2 & 3x_2y_2 & 3x_2z_2 \\ 3x_2y_2 & 3y_2^2-r_2^2 & 3y_2z_2 \\ 3x_2z_2 & 3y_2z_2 & 3z_2^2-r_2^2 \end{bmatrix} d\vec{r}_1 d\vec{r}_2 \tag{6}$$

or in (first dot product):

$$\begin{aligned} E_{pot}^{(2)} = {} & \frac{1}{6}\begin{bmatrix} \{3x_1^2\}-\{r_1^2\} & \{3x_1y_1\} & \{3x_1z_1\} \\ \{3y_1x_1\} & \{3y_1^2\}-\{r_1^2\} & \{3y_1z_1\} \\ \{3z_1x_1\} & \{3z_1y_1\} & \{3z_1^2\}-\{r_1^2\} \end{bmatrix} \cdot \\ & \begin{bmatrix} \frac{\partial^2 V_2(\vec{0})}{\partial x_1^2}-\frac{\Delta V_2(\vec{0})}{3} & \frac{\partial^2 V_2(\vec{0})}{\partial y_1 \partial x_1} & \frac{\partial^2 V_2(\vec{0})}{\partial z_1 \partial x_1} \\ \frac{\partial^2 V_2(\vec{0})}{\partial x_1 \partial y_1} & \frac{\partial^2 V_2(\vec{0})}{\partial y_1^2}-\frac{\Delta V_2(\vec{0})}{3} & \frac{\partial^2 V_2(\vec{0})}{\partial z_1 \partial y_1} \\ \frac{\partial^2 V_2(\vec{0})}{\partial x_1 \partial z_1} & \frac{\partial^2 f(\vec{0})}{\partial y_1 \partial z_1} & \frac{\partial^2 V_2(\vec{0})}{\partial z_1^2}-\frac{\Delta V_2(\vec{0})}{3} \end{bmatrix} + \\ & \frac{1}{6}\begin{bmatrix} \{r_1^2\} & 0 & 0 \\ 0 & \{r_1^2\} & 0 \\ 0 & 0 & \{r_1^2\} \end{bmatrix} \cdot \begin{bmatrix} \frac{\Delta V_2(\vec{0})}{3} & 0 & 0 \\ 0 & \frac{\Delta V_2(\vec{0})}{3} & 0 \\ 0 & 0 & \frac{\Delta V_2(\vec{0})}{3} \end{bmatrix} \end{aligned} \tag{7}$$

Using either expressions produces identical results only if there is no electron penetration in the nucleus. That was to be expected, as equation 4 was derived for the situation without penetration. The more general result obtained by equation 5 is:

$$\hat{V}_{ij} = -\frac{eN}{4\pi\epsilon_0}\frac{3x_{ie}x_{je}-r_e^3\delta_{ij}}{r_e^5} - \frac{\rho_e(\vec{0})}{3\epsilon_0}\delta_{ij} \tag{8}$$

The result for the quadrupole moment tensor does not depend on penetration being present or not:

$$\hat{Q}_{ij} = eZ\left(3x_{in}x_{jn}-r_n^3\delta_{ij}\right) \tag{9}$$

If we note $\left\langle \Psi_e^{(0)} \middle| \hat{V}_{ij} \middle| \Psi_e^{(0)} \right\rangle \equiv V_{ij}$, we can express the matrix elements of $\hat{V}^2$ as follows:

$$\left\langle \psi_e^{(0)} \middle| \hat{V}_0^2 \middle| \psi_e^{(0)} \right\rangle = \frac{1}{2}V_{zz}$$

$$\begin{aligned}
\left\langle \psi_e^{(0)} \right| \hat{V}_{\pm 1}^2 \left| \psi_e^{(0)} \right\rangle &= \mp \frac{1}{\sqrt{6}} \left(V_{xz} \pm V_{yz} \right) \\
\left\langle \psi_e^{(0)} \right| \hat{V}_{\pm 2}^2 \left| \psi_e^{(0)} \right\rangle &= \frac{1}{2\sqrt{6}} \left(V_{xx} - V_{yy} \pm i V_{xy} \right)
\end{aligned} \tag{10}$$

These matrix elements can be considerably simplified if we work in a principal axis system (PAS) for the electric-field gradient. For a crystalline solid this is something meaningful, as the lattice breaks the isotropy of space and provides special directions relative to which the PAS can be defined. The PAS is chosen such that the electric-field gradient tensor[1] at the point of the crystal we are interested in (the nucleus of the considered atom) is as simple as possible.

2.2 Intermezzo: Principal axis system rank 2 tensor

A principal axis system for a spherical tensor of rank 2 is an axis system in which the 3×3-matrix of the cartesian form of this tensor is diagonal (for symmetric matrices this is always possible). Once XYZ is rotated such that the matrix is diagonal, the axes are renamed by convention such that $|a_{zz}| \geq |a_{yy}| \geq |a_{xx}|$. The cartesian form in the PAS is now:

$$\begin{bmatrix} a_{xx} & 0 & 0 \\ 0 & a_{yy} & 0 \\ 0 & 0 & a_{zz} \end{bmatrix} \tag{11}$$

The trace of matrix is invariant upon rotation of the axis system and therefore remains zero. It means we have only 2 degrees of freedom in 11. Because there are also 3 degrees of freedom needed to specify the PAS with respect to the original XYZ (e.g. 3 Euler angles), we retain the 5 degrees of freedom expected for a spherical tensor of rank 2. Using the foreseen relations between cartesian and spherical components (Hyperfinecourse A: framework. Inverse relations of equations 27 and 28), we see that the spherical components in the PAS are:

$$\begin{aligned}
a_0^2 &= \frac{1}{2} a_{zz} \\
a_{\pm 1}^2 &= 0 \\
a_{\pm 2}^2 &= \frac{1}{2\sqrt{6}} \left(a_{xx} - a_{yy} \right)
\end{aligned} \tag{12}$$

Because $a_{+2}^2 = a_{-2}^2$ also in the spherical components only 2 apparent degrees of freedom are left. Again because of the 3 degrees of freedom needed to specify the PAS, we find back the 5 degrees of freedom which are needed.

$$\left\langle \psi_e^{(0)} \right| \hat{V}_0^2 \left| \psi_e^{(0)} \right\rangle = \frac{1}{2} V_{zz}$$

[1] Attention: not the *tensor operator*, which is something we cannot change (it is as it is), but the electric-field gradient *tensor* itself, i.e. the expectation value of the electric-field gradient tensor operator.

$$\begin{aligned} \left\langle \psi_e^{(0)} \right| \hat{V}_{\pm 1}^2 \left| \psi_e^{(0)} \right\rangle &= 0 \\ \left\langle \psi_e^{(0)} \right| \hat{V}_{\pm 2}^2 \left| \psi_e^{(0)} \right\rangle &= \frac{1}{2\sqrt{6}} \left(V_{xx} - V_{yy} \right) \end{aligned} \tag{13}$$

The 3 axes of the PAS are named such that $|V_{zz}| \geq |V_{yy}| \geq |V_{xx}|$. Be aware that the PAS is dependent on $\left|\psi_e^{(0)}\right\rangle$: it is not something universal, but depends on the particular compound you examine! Because of the condition on the trace of the cartesian form (traceless), only two degrees of freedom are left in 13. We can write this explicitly by defining a parameter η:

$$\eta = \frac{V_{xx} - V_{yy}}{V_{zz}} \tag{14}$$

which fulfills the relation $0 \leq \eta \leq 1$. With this definition we can write the spherical components in the PAS as:

$$\begin{aligned} \left\langle \psi_e^{(0)} \right| \hat{V}_0^2 \left| \psi_e^{(0)} \right\rangle &= \frac{1}{2} V_{zz} \\ \left\langle \psi_e^{(0)} \right| \hat{V}_{\pm 1}^2 \left| \psi_e^{(0)} \right\rangle &= 0 \\ \left\langle \psi_e^{(0)} \right| \hat{V}_{\pm 2}^2 \left| \psi_e^{(0)} \right\rangle &= \frac{1}{2\sqrt{6}} \eta V_{zz} \end{aligned} \tag{15}$$

Only η and V_{zz} determine the electric-field gradient, indeed 2 degrees of freedom. The 3 other degrees of freedom expected for a spherical tensor of rank 2 are used to specify the PAS with respect to the original axis system, e.g. by 3 Euler angles. One calls η the *asymmetry parameter* of the electric-field gradient. The reason is that for $\eta = 0$ the xx- and yy-components of the cartesian form are equal: the gradient of the electric field is the same in all directions in the XY-plane, hence the electric-field gradient has axial symmetry about the Z-axis[2]. The more η deviates from 0 and approaches 1, the more the gradient of the electric field becomes stronger in the y-direction compared to the x-direction (the gradient in the z-direction remains the strongest of course).

[2]This can be seen also in the spherical component: only V_0^2 is not zero, hence there is axial symmetry.

2.3 The nuclear electric quadrupole moment operator

Let us now look to the first term in equation 3. Again we are faced with the problem that we do not know explicit expressions for the nuclear many-body wave functions $|I\rangle$. As for the 3 components of the magnetic dipole operator, we will transform the 5 components of the electric quadrupole moment operator $\hat{Q}^2_q(\vec{r}_n)$ into expressions that involve an experimentally observable scalar – 'the' quadrupole moment Q – and operators for which we can calculate the matrix elements in the $|I\rangle$ basis. They will depend on the (experimentally known) value of I. In contrast to the magnetic case, the $|I, m\rangle$ will not be eigen states of the hamiltonian, such that non-diagonal matrix elements will be present. The transformation takes somewhat more effort than for the magnetic case, and starts from the Wigner-Eckart theorem. This famous theorem states that the matrix elements of all spherical tensors of rank n are proportional, because they can be written as:

$$<I',\, m'_I|\, T^n_q|\, I,\, m_I> = (-1)^{I'-m'_I} \begin{pmatrix} I' & n & I \\ -m'_I & q & m_I \end{pmatrix} <I' \,||\, T^n \,||\, I> \qquad (16)$$

(The so-called reduced matrix element $< I' \,||\, T^n \,||\, I >$ is independent of m'_I, m_I and q, and the Wigner $3j$-symbol between large parentheses has a close relationship[3] to the Clebsch-Gordan coefficients.) Indeed, the same type of matrix element of a spherical tensor A^n of the same rank is:

$$<I',\, m'_I|\, A^n_q|\, I,\, m_I> = (-1)^{I'-m'_I} \begin{pmatrix} I' & n & I \\ -m'_I & q & m_I \end{pmatrix} <I' \,||\, A^n \,||\, I> \qquad (18)$$

and therefore

$$\frac{<I',\, m'_I|\, T^n_q|\, I,\, m_I>}{<I',\, m'_I|\, A^n_q|\, I,\, m_I>} = \frac{<I' \,||\, T^n \,||\, I>}{<I' \,||\, A^n \,||\, I>} = C \qquad (19)$$

with C a constant depending on I', I and n, but not on m_I, m'_I and q.

The tensor operators $r^2_n\, Y^2(\theta_n,\, \phi_n)$ and $I^2\, Y^2(\vec{I})$ can be shown to be both[4] spherical tensor operators of rank 2. Applying equation 19 we get:

$$<I',\, m'_I|\, r^2_n\, Y^2(\theta_n,\, \phi_n)\,|\, I,\, m_I> = C\ <I',\, m'_I|\, I^2\, Y^2(\vec{I})\,|\, I,\, m_I> \qquad (20)$$

With this equation, we can write the matrix elements of $\hat{Q}^2_q(\vec{r}_n)$ in terms of $I^2\, Y^2(\vec{I})$. But then we need explicit expressions for $Y^2_q(\vec{I})$. For $q = 0$ and with

[3] The exact relation is:

$$\begin{pmatrix} j_1 & j_2 & j_3 \\ m_1 & m_2 & m_3 \end{pmatrix} = (-1)^{j_1 - j_2 - m_3}\, \frac{1}{\sqrt{2j_3+1}}\, (j_1\, j_2\, m_1\, m_2\,|\, j_1\, j_2\, j_3\, m_3) \qquad (17)$$

One often uses $3j$-symbols instead of Clebsch-Gordan coefficients because the former have nicer symmetry properties.

[4] Interpret the notation $Y^2(\vec{I})$ as follows: in $Y^2(\theta_n,\, \phi_n)$ (or $Y^2(\vec{r})$), θ_n and ϕ_n give the direction of $\vec{r}_n$. Use therefore in $Y^2(\vec{I})$ as argument for Y^2 the angles which specify the direction of $\vec{I}$.

θ and ϕ giving the direction of a position vector $\vec{r}$, we can with $\cos\theta = z/r$ write Y_0^2 as[5]:

$$Y_0^2(\theta,\,\phi) \;=\; Y_0^2(\vec{r}) \,=\, \frac{1}{2}\sqrt{\frac{5}{4\pi}}\,\left(\frac{3z^2\,-\,r^2}{r^2}\right) \tag{23}$$

$$r^2\,Y_0^2(\vec{r}) \;=\; \frac{1}{2}\sqrt{\frac{5}{4\pi}}\,\left(3z^2\,-\,r^2\right) \tag{24}$$

x, y an z are the x-, y- and z-components of $\vec{r}$. If we note the x-, y- and z-components of $\vec{I}$ as I_x, I_y and I_z, we can by analogy write:

$$I^2\,Y_0^2(\vec{I}) \;=\; \frac{1}{2}\sqrt{\frac{5}{4\pi}}\,\left(3I_z^2\,-\,I^2\right) \tag{25}$$

Show yourself that:

$$I^2\,Y_{\pm1}^2 \;=\; \mp\sqrt{\frac{15}{8\pi}}\,\frac{1}{2}\,\left(I_zI_\pm + I_\pm I_z\right) \tag{26}$$

$$I^2\,Y_{\pm2}^2 \;=\; \frac{1}{4}\sqrt{\frac{15}{2\pi}}\,I_\pm^2 \tag{27}$$

The operators $\hat{I}_+$ and $\hat{I}_-$ are defined in hyperfinecourse A: magnetic hyperfine interaction (equations 16 and 17).

Our last task before having found the nuclear matrix elements, is to search for the value of the proportionality constant C. First we define similarly the *observable* quadrupole moment Q of the nucleus:

$$Q \;=\; Z\,<I,\,m_I = I|\,3z^2 - r^2|\,I,\,m_I = I> \tag{28}$$

$$\;=\; Z\,2\sqrt{\frac{4\pi}{5}}\,<I,\,I|\,r_n^2 Y_0^2(\vec{r})|\,I,\,I> \tag{29}$$

Note the difference between this definition (just a number) and the quadrupole tensor (5 components). Following general practice, we define this observable quadrupole moment in units of m^2, and not in units of Cm^2 as we did for the quadrupole moment tensor (equation 4). Numerical values for Q are usually given in *barn* (1 barn = 1 b = 10^{-28} m^2, typical values are 0 - 100 b). The corresponding unit for the tensor $Q_q^{(2)}$ is the *electron barn* (eb)[6].

[5]

$$Y_0^2\,(\theta,\,\phi) \;=\; \sqrt{\frac{5}{4\pi}}\,\left(\frac{3}{2}\cos^2\theta - \frac{1}{2}\right) \tag{21}$$

(22)

[6]Do not confuse the electron barn with the *Coulomb barn* (Cb), which is not used in practice. 1 eb = $1.602\cdot10^{-19}$ Cb = $1.602\cdot10^{-47}$ Cm^2.

Apply now Wigner-Eckart to the definition of Q:

$$Q = Z\,2\sqrt{\frac{4\pi}{5}} \begin{pmatrix} I & 2 & I \\ -I & 0 & I \end{pmatrix} <I \,||\, r_n^2 Y^2(\vec{r})||\, I> \tag{30}$$

and hence:

$$<I \,||\, r_n^2 Y^2(\vec{r})||\, I> = \frac{Q}{Z\,2\sqrt{\frac{4\pi}{5}} \begin{pmatrix} I & 2 & I \\ -I & 0 & I \end{pmatrix}} \tag{31}$$

which expresses the reduced matrix element of $r_n^2\, Y^2(\vec{r_n})$ as a function of observable quantities. Now apply Wigner-Eckart again, on the following matrix element of the other operator:

$$<I,\, I|\, I^2 Y_0^2(\vec{I})|\, I, I> = \begin{pmatrix} I & 2 & I \\ -I & 0 & I \end{pmatrix} <I \,||\, I^2 Y^2(\vec{I})||\, I> \tag{32}$$

On the other hand, also this is true:

$$<I,\, I|\, I^2 Y_0^2(\vec{I})|\, I, I> = \frac{1}{2}\sqrt{\frac{5}{4\pi}}\; <I,\, I|\, 3I_z^2 - I^2|\, I, I> \tag{33}$$

$$= \frac{1}{2}\sqrt{\frac{5}{4\pi}}\,\hbar^2\left(3I^2 - I(I+1)\right) \tag{34}$$

$$= \frac{1}{2}\sqrt{\frac{5}{4\pi}}\,\hbar^2\;\left(I\,(2I-1)\right) \tag{35}$$

Combining 32 with 35 gives the reduced matrix element of $I^2\, Y^2(\vec{I})$, which together with 31, 19 and 20 finally yields the desired constant:

$$C = \frac{Q}{Z\,\hbar^2\,(I(2I-1))} \tag{36}$$

We can now finally express the quadrupole moment operator in terms of Q and the operators $\hat{I}^2$, $\hat{I}_z$ and $\hat{I}_\pm$:

$$\hat{Q}_q^2 = \sqrt{\frac{4\pi}{5}}\frac{eQ}{I\,(2I-1)\,\hbar^2}\,\hat{\vec{I}}^2\, Y_q^2(\hat{\vec{I}}) \tag{37}$$

with $\hat{\vec{I}}^2\, Y_q^2(\hat{\vec{I}})$ given by equations 25 to 27.

All this enables us to write down explicitly the nuclear matrix elements:

$$<I,\, m_I'|\, Q_0^2\,|\, I,\, m_I> = \tag{38}$$
$$\frac{1}{2}\,\frac{e\,Q}{I(2I-1)}\;\left(3m^2 - I(I+1)\right)\;\delta_{m_I,\, m_I'}$$

$$<I,\, m'_I|\, Q^2_{\pm 1}\,|\, I,\, m_I> = \tag{39}$$
$$\mp\,\frac{1}{2}\,\sqrt{\frac{3}{2}}\,\frac{e\,Q}{I(2I-1)}\,\sqrt{I(I+1)\,-\,m_I(m_I\pm 1)}\,(2m_I\,\pm 1)\,\delta_{m'_I,\,m_I+1}$$
$$<I,\, m'_I|\, Q^2_{\pm 2}\,|\, I,\, m_I> = \tag{40}$$
$$\frac{1}{2}\,\sqrt{\frac{3}{2}}\,\frac{e\,Q}{I(2I-1)}\,\sqrt{(I(I+1)-m_I(m_I\pm 1))\,(I(I+1)-(m_I\pm 1)(m_I\pm 2))}\,\delta_{m'_I,\,m_I+2}$$

The observable nuclear quadrupole moment Q as defined by equation 29 is an experimentally accessible measure for the deviation from spherical symmetry of the nucleus. We can make the observation that due to equations 20, 29 and 35, Q is zero for $I = 0$ and $I = 1/2$, which means that these nuclei are always spherically symmetric. As a result, all nuclear matrix elements are zero in these two cases, and the quadrupole hamiltonian will not yield any energy contribution. The lowest spin for which a quadrupole contribution to the total energy is observable is therefore $I = 1$. Similar arguments can be used to prove that the lowest spin for which a hexadecapole moment can exist is $I = 3/2$.

2.4 Energy levels of the electric quadrupole hamiltonian for solids

By inserting equations 37 and equations 15 into equation 3, we obtain the equivalent of equation 31 in hyperfinecourse A: magnetic hyperfine interaction: a Hamiltonian that describes the energy contribution due to the interaction between a specific electric-field gradient tensor (specified by V_{zz}, η and the orientation of its PAS with respect to the crystal) and the nuclear quadrupole moment tensor, depending on the orientation of the latter with respect to the PAS:

$$H^{nuc}_{qq} \;=\; \frac{e\,Q\,V_{zz}}{4\,I(2I-1)\,\hbar^2}\,\left[(3I_z^2-I^2)\,+\,\frac{\eta}{2}\,(I_+^2+I_-^2)\right] \tag{41}$$

This hamiltonian depends on the electric-field gradient through V_{zz} and η, and on the spin of the nucleus through I. It also depends on the orientation of the nucleus (m_I), through $\hat{I}_z$ and $\hat{I}^2_{\pm}$. As the unperturbed Hamiltonian $\hat{T}_n + \hat{U}_{nn} + \hat{H}_0$ does not depend on m_I, we should use first order perturbation theory for the degenerate case. In contrast to the magnetic case, the matrix formed by $\langle m'_I,\, I|\, H^{nuc}_{qq}\,|I,\, m_I\rangle$ is not diagonal, due to the presence of $\hat{I}_{\pm}$. Therefore, it must be diagonalized in order to find the eigenvalues and eigenfunctions. The only – and important – exception is when the electric-field gradient has axial symmetry ($\eta = 0$). We examine now the eigenstates and eigenvalues of H^{nuc}_{qq} with and without axial symmetry of the electric-field gradient.

3 Case studies & symmetry

3.1 Analytical example 1: I = 3/2

We will search now explicit and analytical expressions for eigen values and eigen functions of a non-axially symmetric quadrupole hamiltonian for the case $I = 3/2$. These eigen states $|N>$ are not the $|I, m_I>$, but because the latter form a basis the equality

$$\sum_{m_I} |I, m_I><I, m_I| \;=\; 1 \tag{42}$$

holds, and this we can use to decompose $|N>$ in the $|I, m_I>$-basis:

$$|N> = \sum_{m_I} \underbrace{<I, m_I|N>}_{c_{m_I}} |I, m_I> \tag{43}$$

Our goal is to find the coefficients c_{m_I} [7].

The non-zero matrix elements of H^{nuc}_{qq} in the $|I, m_I>$-basis are[8]:

$$<\pm\frac{1}{2}|\, H^{nuc}_{qq}|\, \pm\frac{1}{2}> \;=\; -3\,\frac{eQ\,V_{zz}}{12} \tag{44}$$

$$<\pm\frac{3}{2}|\, H^{nuc}_{qq}|\, \pm\frac{3}{2}> \;=\; +3\,\frac{eQ\,V_{zz}}{12} \tag{45}$$

$$<\pm\frac{3}{2}|\, H^{nuc}_{qq}|\, \mp\frac{1}{2}> \;=\; \sqrt{3}\,\eta\,\frac{eQ\,V_{zz}}{12} \tag{46}$$

The full matrix reads:

$$E_Q \;=\; \frac{eQ\,V_{zz}}{12} \begin{array}{c} [+\frac{3}{2} \quad +\frac{1}{2} \quad -\frac{1}{2} \quad -\frac{3}{2}] \\ \left[\begin{array}{cccc} 3 & 0 & \sqrt{3}\,\eta & 0 \\ 0 & -3 & 0 & \sqrt{3}\,\eta \\ \sqrt{3}\,\eta & 0 & -3 & 0 \\ 0 & \sqrt{3}\,\eta & 0 & 3 \end{array}\right] \end{array} \tag{47}$$

One can find now the eigen vectors and eigen values of this matrix in the usual way. The secular equation would be a fourth order polynomial. We can reduce the complexity however just by making a rearrangement of the basis states in the following way:

$$E_Q \;=\; \frac{eQ\,V_{zz}}{12} \begin{array}{c} [+\frac{3}{2} \quad -\frac{1}{2} \quad -\frac{3}{2} \quad +\frac{1}{2}] \\ \left[\begin{array}{cccc} 3 & \sqrt{3}\,\eta & 0 & 0 \\ \sqrt{3}\,\eta & -3 & 0 & 0 \\ 0 & 0 & 3 & \sqrt{3}\,\eta \\ 0 & 0 & \sqrt{3}\,\eta & -3 \end{array}\right] \end{array} \tag{48}$$

[7] Clearly, if $\eta = 0$ all c_{m_I} are zero except for one which equals 1.
[8] We note for a while $|I, m_I>$ as $|m_I>$.

In this notation we clearly see that the new eigen states will be combinations of either $|\frac{3}{2}, +\frac{3}{2}>$ and $|\frac{3}{2}, -\frac{1}{2}>$ only, or $|\frac{3}{2}, -\frac{3}{2}>$ and $|\frac{3}{2}, +\frac{1}{2}>$ only. The problem is reduced now to finding the eigenvalues and eigenstates of two identical smaller matrices (the secular equations will be twice a second order polynomial here). We will see soon that this kind of reduction is a general property. Verify that both submatrices have as eigen values:

$$E_a \;=\; E_{\pm\tilde{\frac{3}{2}}} \;\;=\;\; \frac{eQ\,V_{zz}}{4}\sqrt{1+\frac{\eta^2}{3}} \tag{49}$$

$$E_b \;=\; E_{\pm\tilde{\frac{1}{2}}} \;\;=\;\; -\,\frac{eQ\,V_{zz}}{4}\sqrt{1+\frac{\eta^2}{3}} \tag{50}$$

As both eigenvalues appear twice in the full 4×4-matrix, we say they have a multiplicity of 2.

3.2 Analytical example 1: I = 1

By a suitable rearrangement, we can write the full matrix – similarly to equation 48 – as follows:

$$E_Q \;=\; \frac{eQ\,V_{zz}}{4} \begin{array}{c} \begin{array}{ccc} [+1 & -1 & 0] \end{array} \\ \begin{bmatrix} 1 & \eta & 0 \\ \eta & 1 & 0 \\ 0 & 0 & -2 \end{bmatrix} \end{array} \tag{51}$$

We immediately recognizes an eigenvalue $E_{\tilde{0}}$ which is identical to the eigenvalue $E_{m_I=0}$ for the case of axial symmetry, and which does not depend on η. The eigen state belonging to $E_{\tilde{0}}$ is identical to $|\,0>$:

$$E_{\tilde{0}} \;=\; -\,\frac{eQ\,V_{zz}}{2} \qquad |\,\tilde{0}> = \,|\,0> \tag{52}$$

Non-axial symmetry will therefore not change this state.

The eigenvalues of the 2×2 submatrix do depend on η:

$$E_\pm \;\;=\;\; \frac{eQ\,V_{zz}}{4}\,(1 \pm \eta) \tag{53}$$

$$|\pm> \;\;=\;\; \frac{1}{\sqrt{2}}\,(|+1> \pm |-1>) \tag{54}$$

The difference

$$E_+ - E_- \;=\; \frac{eQ\,V_{zz}}{2}\,\eta \tag{55}$$

is linear in η.

3.3 Symmetry properties and classes

We observe the following two facts:

- The expectation values of $|\, I,\, \pm m_I >$ are identical under H_{qq}^{nuc}. Indeed, the following symmetry relations are valid:

$$<I,\, m_I + 2|\, I_+^2\,|\, I, m_I> \;=\; <I,\, -m_I - 2|\, I_-^2\,|\, I, -m_I> \qquad (56)$$

$$<I,\, m_I|\, 3I_z^2 - I^2|\, I,\, m_I> \;=\; <I,\, -m_I|\, 3I_z^2 - I^2|\, I,\, -m_I> \qquad (57)$$

  and therefore:

$$<I,\, m_I|\, H_{qq}^{nuc}|\, I,\, m_I> \;=\; <I,\, -m_I|\, H_{qq}^{nuc}|\, I,\, -m_I> \qquad (58)$$

- Because H_{qq}^{nuc} connects only states with $\Delta m_I = 0$ and $\Delta m_I = \pm 2$, the states can be divided in 2 classes, such that no state of one class can ever be connected to a state of the other class. The situation is different for integer and half integer spin:

  – integer spin:

$$\textit{Class 1}: \quad m_I \;=\; \textit{even} \qquad (59)$$

$$\textit{Class 2}: \quad m_I \;=\; \textit{odd} \qquad (60)$$

  – half integer spin

$$\textit{Class 1}: \quad m_I \;=\; -I,\; -I+2,\; \ldots,\; +\frac{1}{2},\; +\frac{5}{2},\; \ldots, I-1 \qquad (61)$$

$$\textit{Class 2}: \quad m_I \;=\; -I+1,\; -I+3,\; \ldots,\; -\frac{1}{2},\; +\frac{3}{2},\; \ldots, +I \qquad (62)$$

The existence of these two classes means that it is always possible to rearrange the eigenstates in such a way that H_{qq}^{nuc} is in block form, because the block form explicitly shows that only states belonging to the same class can be mixed. In our two examples above, we did indeed observe that this was possible. The situation is qualitatively different however for integer and half integer spin:

half integer spin: The number of states in both classes is the same, the two submatrices have therefore the same dimension. Even better, by virtue of the symmetry properties 56 and 57, both submatrices are identical[9] The states $|\, m_I >$ and $|\, -m_I >$ play exactly the same role, each for their one submatrix.

Consider now an eigenstate $|\, N_1 >$ of H_{qq}^{nuc}. It must be built from states $|\, m_I >$ belonging to one and the same class, and according to equation 43 the coefficients c_{m_I} with m_I belonging to the other class are zero. For half

[9] You can convince yourself about this by looking at 48, and by making the matrix for $I = 5/2$. It is not necessary to write down explicit matrix elements, just use 56 and 57 to identify identical ones.

integer spin, m_I and $-m_I$ belong to different classes. Therefore, if $c_{m_I}^{N_1}$ appears in the development of $|\, N_1>$, $c_{-m_I}^{N_1}$ must be zero. But because the two submatrices are identical and because $|\, \pm m_I>$ play the same role, there must exist an eigenstate $|\, N_2>$ of H_{qq}^{nuc} built from the corresponding states of the other class, with the same coefficients: $c_{-m_I}^{N_2} = c_{m_I}^{N_1}$ and $c_{m_I}^{N_2} = 0 = c_{-m_I}^{N_1}$.

Because $|\, N_1>$ and $|\, N_2>$ are eigenstates of identical submatrices, they must have identical eigenvalues (-energies) and are therefore degenerate. This reasoning does not depends on the value of η, and we can conclude: *the eigenstates of H_{qq}^{nuc} for half integer I are two-fold degenerate (Kramers-degeneracy).* The degeneracy which was present for axial symmetry is never lifted for half integer spin.

integer spin: In this case, there will always be a different number of states in each class. The two submatrices will have a different dimension and can hence never be the identical. The states $|\, \pm m_I>$ now belong to the same class. Therefore there is no reason why they must lead to degenerate states (although they still can do so). In general, the $\pm m_I$-degeneracy will be lifted for integer spin.

If I becomes larger, the dimension of the submatrices grows and hence also the degree of the secular equation. From $I = 4$ onwards, one deals with secular equations of the fifth degree and higher. It is well known from algebra that only for polynomials up to the fourth degree analytical formulae for their roots exist. For higher orders numerical procedures are the only possibility. This means that $I = 7/2$ is the highest spin for which the eigenvalues can be given analytically (although already from $I = 5/2$ onwards the analytical solution becomes quite involved). In fig. 1 the eigenvalues of H_{qq}^{nuc} (found either analytically or numerically) for some values of I are given as a function of η. Note the Kramers degeneracy for half integer spin, and the fast lifting of degeneracy for $m_I = \pm 1$ (remember it was present already in first order perturbation theory!). The larger $|\, m_I|$, the higher η needs to be in order to produce a sufficiently large splitting.

One can compare these pictures of fig. 1 to fig. 2 of the gravitational example. There all possible orientations of the dumb-bell (= nucleus) were allowed. In the quantummechanical case only a limited number of orientations remains, which means that we must select a discrete number of energies from the continuous range of fig. 2.

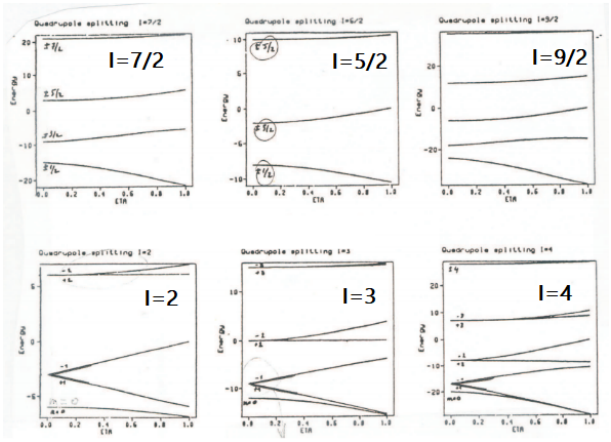

Figure 1: *Quadrupole splittings for half integer (top, 7/2, 5/2, 9/2) and integer (bottom, 2, 3, 4) spins. The vertical energy axis is in units of* $eQV_{zz}/I(2I-1)$*, while the horizontal axis scans all possible values of the asymmetry parameter* η $(0 \rightarrow 1)$*.*

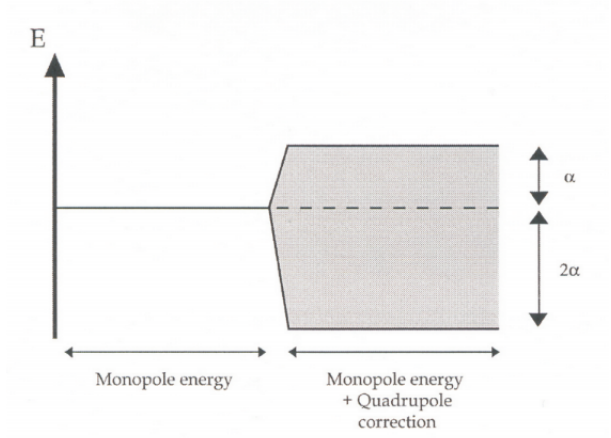

Figure 2: *See hyperfinecourse A: framework, Figure 9*

3.4 Symmetry properties of the electric-field gradient

For the magnetic hyperfine field we were able to identify where in a crystal such a field can exist and what will be its direction, just by using symmetry arguments. In the present section we will show how the crystallographic symmetry can be used to identify sites where an electric-field gradient exists, and what is the direction of the Z-axis of its PAS.

3.5 Theorem 1: an n-fold rotation axis

Consider a spherical tensor of rank 2 V^2 in an axis system $S1$. Its 5 components $V^2_{q'}(S1)$ are related to the component $V^2_q(S2)$ in an axis system $S2$ in the following way:

$$V^2_q(S2) \;=\; \sum_{q'} D^{(2)}_{q'q}\,(\alpha,\,\beta,\,\gamma)\,V^2_{q'}(S1) \tag{63}$$

The quantities $D^{(2)}_{q'q}\,(\alpha,\,\beta,\,\gamma)$ are components of the *Wigner rotation matrix* of dimension $2\cdot 2+1$ which can be found in tables. The angles α, β and γ are the Euler angles which specify $S2$ with respect to $S1$.

Consider now a position in a crystal of whom the point group contains an n-fold rotation axis. Imagine we know the 5 electric field gradient components in an axis system $S1$ with its z-axis along the n-fold axis (n is a positive integer). The components in an axis system $S2$ which is obtained by rotating $S1$ over an angle $2\pi/n$ about the z-axis will be identical to the ones in $S1$:

$$V^2_q(S2) \;=\; \sum_{q'} D^{(2)}_{q'q}\left(\alpha=\frac{2\pi}{n},\,0,\,0\right)V^2_{q'}(S1) \;=\; V^2_q(S1) \tag{64}$$

Because of the following property of the Wigner rotation matrix elements:

$$D^{(2)}_{q'q}\,(\alpha,\,0,\,0) \;=\; e^{-iq\alpha}\,\delta_{q'q} \tag{65}$$

we find

$$e^{-iq\frac{2\pi}{n}}\,V^2_q(S1) \;=\; V^2_q(S1) \qquad or \qquad e^{-iq\frac{2\pi}{n}} \;=\; 1 \tag{66}$$

and therefore

$$q \;=\; nk \qquad k \;=\; 0,\,\pm1,\,\pm2,\,\pm3,\,\ldots \tag{67}$$

This leads to the following consequences:

- A 1-fold symmetry axis ($n = 1$)

  Due to 67 with $k = 0$, ±1 and ±2 all 5 components of the electric-field gradient tensor can be obtained.

- A 2-fold symmetry axis ($n = 2$)

  Now only $k = 0$ and ±1 lead to the allowed q-values 0 and ±2. The ±1 components are missing. According to equations 13 or 15, the 2-fold rotation axis might be chosen as the z-axis of a PAS.

- A '3 or more'-fold rotation axis ($n = 3$, 4 or 6)

  Here only $k = 0$ leads to an allowed $q = 0$, the other components are missing. According to equation 15 the n-fold rotation axis can be chosen as the z-axis of a PAS in which the electric-field gradient is axially symmetric ($\eta = 0$).

We can summarize our first symmetry criterion as follows: *if an electric-field gradient can exist at a given position of which the point group contains at least a 3-fold rotation axis, it will be axially symmetric about that axis.* Note that the proof does not use any properties of the lattice symmetry (space group), only of the point group. This theorem is therefore valid also for atoms and molecules (in the latter case also 5-fold and ($n \geq 6$)-fold rotation axes are possible).

With this theorem we can finally understand the gravitational examples from section 3 from hyperfinecourse A: framework. The axis system chosen for the double ring was found in equation 57 (hyperfinecourse A: framework) to be a PAS. Indeed, the z-axis is an n-fold rotation axis with $n = \infty$, and must therefore according to our theorem be the z-axis of a PAS.

3.6 Theorem 2: a cubic environment

A second theorem is this one: *whenever the point group contains more than 2 distinct ($n \geq 3$)-fold rotation axes, the electric-field gradient at the center of the point group is zero.* A proof valid for molecules and solids goes as follows: according to the first theorem, both rotation axes specify a PAS in which the field gradient is axially symmetric. Only the V_0^2-component can be different from zero in both axis systems, and according to equations 64 and 66 the value of V_0^2 is the same in both systems[10]. As there is freedom to choose the X- and Y-axes in both systems, the relation between both non-zero components is according to 63:

$$V_0^2(S1) \;=\; D_{00}^{(2)}\,(0,\,\beta,\,0)\,V_0^2(S2) \qquad V_0^2(S1) \;=\; V_0^2(S2) \tag{68}$$

with the following explicit expression for the Wigner rotation matrix element ($P_2(x)$ is the second order Legendre polynomial):

$$D_{00}^{(2)}\,(0,\,\beta,\,0) \;=\; P_2(\cos\beta) \;=\; \frac{3\cos^2\beta - 1}{2} \tag{69}$$

Equation 68 must hold for any value of V_0^2 and any value of β. This is possible only if $V_0^2(S1) = V_0^2(S2) = 0$, which makes the electric-field gradient zero.

When we restrict ourselves to crystalline solids, only the cubic point group contains the 2 required high-symmetry axes. Five different cubic point groups exist:

[10] The same conclusion can be obtained by the cartesian form: because of the PAS, both 3×3-matrices are diagonal. They must have the same eigenvalues and $|V_{zz}|$ must be the largest. Therefore both matrices must be equal.

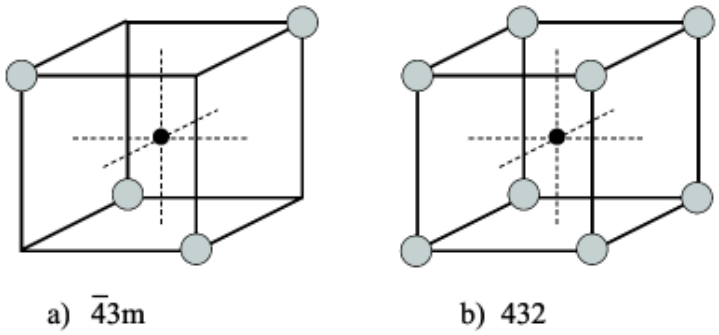

Figure 3: *a) One of the three tetrahedral point groups. b) One of the two octahedral point groups.*

- *Tetrahedral point groups:* These contain four 3-fold axes (and three 2-fold axes). There are three tetrahedral point groups: 23, $\bar{4}$3m and m$\bar{3}$ (T, T_d and T_h respectively in Schönfließnotation). An example of $\bar{4}$3m is drawn in fig. 3-a.
- *Octahedral point groups:* These contain four 3-fold axes and three 4-fold axes. There are two species: 432 and m$\bar{3}$m (O and O_h). An example of 432 is drawn in fig. 3-b.

In molecules also other point groups with the required symmetries can exist.

The inverse of the second theorem is not valid: if the field gradient appears to be zero, this does not necessarily imply the existence of two ($n \geq 3$)-fold axes. An example of this situation is the the double ring of section 3 from hyperfinecourse A: framework with $\sqrt{2}R = h$: an ∞-fold axis and lots of 2-fold axes are present, but no others. However, such situations will occur only in molecules, not in solids.

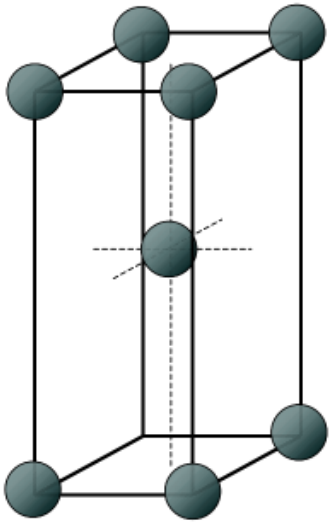

Figure 4: *Body centered tetragonal (bct) crystal structure ($a = b \neq c$).*

3.7 Examples of electric-field gradients in solids

3.7.1 The EFG in bct-In

At room temperature, pure In is a silver-grey, soft metal. It has a body-centered tetragonal lattice structure (space group I4/mmm, Fig. 4), with lattice constants a=b=3.2523 Å and c=4.9461 Å. All atoms in this structure are equivalent, and their point group is 4/mmm. This point group is lower than cubic, hence we expect an EFG at the In-site. There is a 4-fold rotation axis, hence the PAS of the EFG will have its Z-axis parallel to the 4-fold rotation axis, and there will be axial symmetry: the choice of X- and Y-axes does not matter.

3.7.2 The EFG of Fe in Fe_4N

Considering crystallographic symmetry only, one Fe-site (Fe-I) in this compound has a tetragonal point group, the other Fe-site (Fe-II) has a cubic point group. An EFG at the Fe nucleus is possible at the Fe-I site only. The point group of the Fe-I site is the same 4/mmm as in the bct-In example, hence we know immediately that the PAS of the EFG will have its Z-axis along the 4-fold rotation axis, and that there will be axial symmetry. In contrast to the case of bct-In, however, the orientation of this PAS is not the same for all Fe-I atoms (even though they are equivalent!). Indeed, for two Fe-I atoms the 4-fold rotation axis is parallel to the c-axis of the crystal, for two others it is parallel to the b-axis and for the remaining two parallel to the a-axis.

4 Miscellaneous topics

4.1 Ab initio calculations of the EFG tensor

The magnetic field at a nucleus could be separated into local contributions (Fermi, orbital and spin-dipolar contributions) and more distant contributions (Lorentz, demagnetizing and atomic-dipolar contributions). Each of the local contributions could stem from s-, p-, d- or f-electrons. For the electric-field gradient, the number of contributions is much smaller. In a mathematical description that is tailored to the so-called LAPW-method, the EFG can be divided into a contribution from electrons that 'belong'[11] to the atom that contains the nucleus under consideration, and a contribution from more distant electrons[12]. Numerical calculations show the latter contribution to be extremely small. If we want to get more physical insight in the origin of an EFG, the only thing left to do is to see how local s-, p-, d- and f-electrons contribute to this EFG of local origin. For this purpose, let us write the principal component V_{zz} of the EFG in terms of the electron charge density $\rho_e(\vec{r})$:

$$V_{zz} = <\psi_e^{(0)}|\,\hat{V}_{zz}\,|\psi_e^{(0)}> \tag{70}$$

$$= \frac{1}{4\pi\,\epsilon_0}\int \rho_e(\vec{r})\,\frac{3\cos^2\theta-1}{r^3}\,d\vec{r} \tag{71}$$

It is understood that the origin of the axis system (r=0) is at the nucleus of interest. Very close to the nucleus, where r is small, we can expect a large contribution to V_{zz} provided $\rho(\vec{r})$ is sufficiently large. However, near the nucleus the electron density is small. We could also expect the region further away from the nucleus where the highest electron density is, to be contributing most. There however $1/r^3$ is small. For a long time, it has been unclear which of both regions yield the dominant contribution. Only after sufficiently accurate *ab initio* methods became available, it could be shown that the region of small r is absolutely dominant, so dominant that contributions from charges at other atoms are irrelevant (see the discussion about the formulation in the LAPW framework given above, and the reference to P. Blaha given there). To illustrate this, first define the following function:

$$V_{zz}(r) = \frac{1}{4\pi\,\epsilon_0}\int_{|\,\vec{r}|=0}^{|\,\vec{r}|=r} \rho_e(\vec{r})\,\frac{3\cos^2\theta-1}{r^3}\,d\vec{r} \tag{72}$$

Obviously, in the limit of large r we find back the definition of V_{zz}:

$$\lim_{r\to\infty} V_{zz}(r) = V_{zz} \tag{73}$$

[11] Where one can put the boundary between this atom and neighbouring atoms is not obvious. In the LAPW-method an exact definition is used for this boundary. One should not attribute physical meaning to this boundary, however.

[12] P. Blaha, K. Schwarz, and P.H. Dederichs, *Physical Review B* **37** (1988) 2792

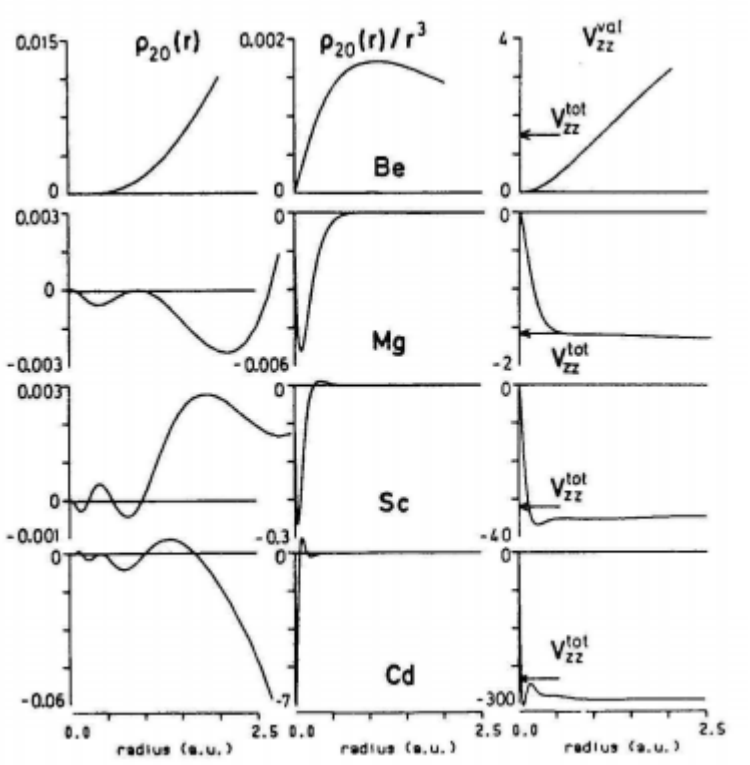

Figure 5: *Illustrating which regions in space contribute to V_{zz}. First column: the function $\rho_e(r)$ from the integrand in equation 72 (without $1/r^3$). Second column: similarly, but with the factor $1/r^3$. Third column: this function integrated up to r, which is equation 72. The arrows indicate the full calculated V_{zz}, including the "lattice contribution" from distant atoms.*

If one plots $V_{zz}(r)$ as a function of r, then in many cases the full value of V_{zz} is obtained already for $r \approx 0.2$ Å, a distance that is 10 times smaller than the radius of a typical atom. This function is plot for several pure hcp materials in Fig. 5, and except for the very light Be atom the EFG is indeed of very local nature.

Some warning words are appropriate here. We just concluded that the EFG is of very local nature. In the literature, one can find at many places statements like "the EFG is a very local property that is determined only by the first few neighbour shells of atoms". This is a statement that is not entirely true[13], and

[13]It is a statement grown under the influence of the obsolete point charge model that will be discussed in the next section.

certainly completely different from the conclusion we just arrived at. It is *true* that the EFG is a very *local* property: only the charge density in region inside the atom and very close to the nucleus determines the EFG. The properties of this part of the charge density, however, are determined by wider environment of the atom under consideration. Chemical bonds with its first nearest neighbours will have an influence on this local charge density. Chemical bonds of these neighbours with their respective neighbours will have an influence as well, through their effect on the properties of the nearest neighbours which will influence the bonds with the original atom, and so on. In this way, the local charge density near the nucleus contains information on what is chemically happening in a region of several Ångstroms around the central atom, typically 5 shells of neighbours. That is still 'local' compared to a macroscopic scale, but a different kind of locality than the 0.2 Å (=deeply within an atom) involved in the relation between charge density and V_{zz}. These two concepts are often confused.

Which are now the electrons that most contribute to V_{zz}? *Ab initio* calculations have shown[14] that the integral 71 can be separated[15] in an integral over ρ_e^p, ρ_e^d and ρ_e^f. For spd-materials, the contribution due to the valence p-electrons is often dominant, even for transition metals that do not have native valence p-electrons. For lanthanides and actinides, the f-contribution becomes dominant if the f-electrons are localized.

Interestingly, these calculations show how a very old, intuitive model to understand the EFG – the Townes-Dailey approximation[16] – has a sound, physical basis. In the Townes-Dailey model, one makes a so-called 'asymmetry count' of the orbitals of a state, taking care of the symmetry of that state. For instance, the p-orbitals consist of 3 mutually perpendicular lobes (p_x, p_y and p_z, see Fig. 6). In a crystal with axial symmetry along the z-axis, the occupation of p_x and p_y will be identical, and different from the occupation of p_z. If the occupation of p_z – call this n_z – is smaller than the occupation of p_x or p_y) – call this $n_x = n_y$ – then the overall p charge density will be oblate (Fig. 6). Intuitively, this corresponds to a negative V_{zz}. The 'asymmetry count' for p-states is defined as

$$\Delta_p \quad = \quad \frac{n_x}{2} + \frac{n_y}{2} - n_z \tag{74}$$

and is also negative. *Ab initio* calculations have shown that there is a fairly good proportionality between this asymmetry count (where the n_i come from calculations) and an accurately calculated p-contribution to V_{zz}. If there is charge accumulation along the Z-axis (prolate charge density), then n_z is larger

[14] See the earlier reference to P. Blaha (1988), and also S. Cottenier, V. Bellini, M. Çakmak, F. Manghi and M. Rots, *Physical Review B* **70** (2004) 155418, and references therein.

[15] Here we simplify a bit. In a correct mathematical treatment, the density can be split according to so-called Gaunt numbers, of which the densities with the p-p, d-d and f-f Gaunt numbers have the dominant contributions. These p-p density can be related to the density due to p-electrons, and therefore we note it here immediately as ρ_e^p.

[16] C.H. Townes and B.P. Dailey, *Journal of Chemical Physics* **17** (1949) 782

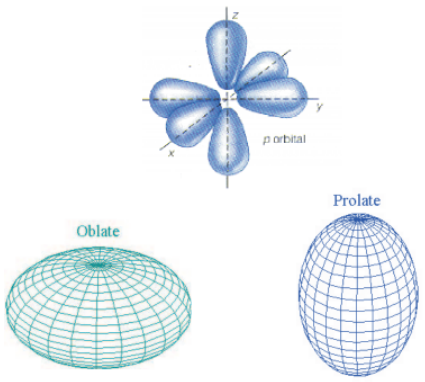

Figure 6: *Schematic picture of p-orbitals. When the occupation in the xy-plane is dominant, the overall p-charge distribution is oblate. If p-charge accumulates along the z-axis, the overall p-distribution is prolate.*

than $n_x = n_y$, and Δ_p is positive. This is in agreement with the positive V_{zz} that is expected. For a cubic environment, $n_x = n_y = n_z$, such that $\Delta_p = 0$, which is consistent with $V_{zz} = 0$ (by symmetry).

For d-electrons as well an asymmetry exists, and it is defined as:

$$\Delta_d \quad = \quad n_{xy} + n_{x^2-y^2} - \frac{1}{2}n_{xz} - \frac{1}{2}n_{yz} - n_{z^2} \tag{75}$$

For many years, *ab initio* calculations that could sufficiently accurately solve for V_{zz} were not available. How to extract physical meaning from the measured EFG's then? An attempt to classify experimental data was the *point charge model*. The underlying assumptions of this model are:

- The key feature of the EFG is the contribution from localized charges at (neighbouring) atomic sites ('lattice EFG'). [*We know meanwhile that such a contribution is negligible.*] If an assumption for the value of these localized charges (point charges) are made, the EFG due to them can be obtained by a simple summation (see further).
- This lattice EFG gets amplified by the electron orbital of the atom under consideration, who get deformed under the influence of the lattice EFG. For every element, the effect of this deformation can be expressed by a single scaling parameter (Sternheimer factor). [*We know meanwhile that the hope for the existence of such a single parameter is unjustified: Nature is much more complicated*]

Although the point charge model is incorrect and obsolete, it has been used a lot in the past and you should know how what it is about in order to understand the older literature. Below, the point charge model is explained in more detail. A critical analysis of one the failures of this model – together with the better *ab initio* interpretation – is given in S. Jalali Asadabadi, S. Cottenier, H. Akbarzadeh, R. Saki and M. Rots, *Physical Review B* **66** (2002) 195010.

Consider the nucleus of an ion, the latter having initially a spherically symmetric electron cloud (as a free ion). Put this ion at a site with lower-than-cubic symmetry in a solid. Due to this low symmetry, the positions of the neighbouring ions are such that they must generate an EFG at the nucleus of interest. Because these neighbours are outside the electron cloud of the ion, we call the principal component of this field gradient V_{zz}^{ext}. The electron cloud of the considered atom makes bonds with the neighbours. It gets therefore deformed, looses its spherical symmetry and takes the same symmetry as the neighbourhood has. This causes an extra field gradient at the nucleus *with the same PAS as the external contribution*. We can hence write the total field gradient as the external contribution times a factor:

$$V_{zz} \;=\; (1-\gamma_\infty)\, V_{zz}^{ext} \tag{76}$$

If γ_∞ is zero, the own electron cloud is not deformed. In many cases γ_∞ is considerably larger then 1 and negative, which means a strong net amplification of V_{zz}^{ext}. For this reason, γ_∞ is called the Sternheimer *antishielding* factor. It is a property which depends only on the considered atom of ion, and reflects the latter's reaction to an external field gradient. A table with calculated values (Hartree-Fock calculations) for a lot of ions can be found in F.D. Feiock and W.R. Johnson, *Physical Review* **187** (1969) pp. 39. Some examples for important atoms are: Fe: -5.244, Sn: -22.34, Cd: -29.27.

Often situations occur where a nonspherical charge distribution is present *within* the electron cloud of the considered atom. In an ionic solid, insulator or semiconductor, this can happen for instance due to a not completely filled 4f-shell. In metals it can be due to conduction electrons penetrating into the atomic volume. In both cases this will yield an *internal* (to the atom) or *local* field gradient with principal component V_{zz}^{loc}. It will again take over the symmetry of the existing $(1-\gamma_\infty)\, V_{zz}^{ext}$ and have therefore the same PAS. The other electrons inside the atomic volume will be deformed by this internal charge distribution, and change the original V_{zz}^{loc}. Now the change is described by a parameter R, which appears to be rather small ($-0.2 \leq R \leq +0.2$), and the total principal component becomes:

$$V_{zz} \;=\; (1-\gamma_\infty)\, V_{zz}^{ext} + (1-R)\, V_{zz}^{loc} \tag{77}$$

It is quite straightforward to get a meaningful number for V_{zz}^{ext}. The neighboring nuclei screened by their electron cloud will appear from a certain distance as point charge Δe, where Δ is the extra number of electrons being at the ion. In ionic solids, Δ is an integer (positive or negative), in metals it is a fractional number. From the result for the gravitational example, we obtain the electric-field gradient tensor for a single point charge Δe at a position $\vec{r}$ from the nucleus ($-Gm_2 \rightarrow \Delta e/4\pi\epsilon_0$, $\rho_2(\vec{r}_2) \rightarrow \delta(\vec{r}_2 - \vec{r})$) in cartesian coordinates[17]. Summing over all ions in the crystal gives:

$$V^{ext} = \frac{e}{4\pi\,\epsilon_0} \sum_i \frac{\Delta_i}{r_i^3} \begin{bmatrix} \frac{3x_i^2}{r_i^2} - 1 & \frac{3x_i y_i}{r_i^2} & \frac{3x_i z_i}{r_i^2} \\ \frac{3x_i y_i}{r_i^2} & \frac{3y_i^2}{r_i^2} - 1 & \frac{3y_i z_i}{r_i^2} \\ \frac{3x_i z_i}{r_i^2} & \frac{3y_i z_i}{r_i^2} & \frac{3z_i^2}{r_i^2} - 1 \end{bmatrix} \tag{78}$$

It is of course not possible to extend the summation really to all ions in the crystal. Usually one calculates first all the matrices due to the first nearest neigbors, then of the second neighbor shell, and so on. As r_i becomes larger, the contributions become smaller and smaller, and the sum will converge. Convergence is very slow however, because shells far away will usually contain many atoms. Short-cuts exist to obtain with less effort (= faster convergence) the same final matrix[18], and for some types of lattices even analytical expressions exist[19].

Anyway, after having found the matrix for V^{ext} – in this context called also often V^{latt}, *latt* from lattice – one can find its PAS by doing a matrix diagonalization. After suitably renaming the axes, one obtains finally a value for V_{zz}^{ext}. If one is interested only in the PAS and not in the magnitude of V_{zz}, then it is sufficient to carry out the summation in 78 only over as many neighbors as is needed to obtain the symmetry of the point group, and do the diagonalization of this matrix.

Because γ_∞ is known from tabulations, we have now a procedure to obtain the external (or lattice) contribution to the electric-field gradient. Such a transparent method does not exist for the local contribution however. Based upon the then available experimental data, Raghavan *et al.*[20] concluded in 1975 that

[17] Point charges cannot occur at the same position of the nucleus, the correction term with $\rho_e(\vec{0})$ is therefore zero.

[18] F. W. De Wette, *The Physical Review* 123 (1961) p. 103, F. W. De Wette and G. E. Schacher, *The Physical Review* 137 (1965) p. A78 and p. A92, and D. B. Dickmann and G. E. Schacher, *Journal of Computational Physics* 2 (1967) p. 87.

[19] For instance, for the Cu-position in a $AuCu_3$-type of structure, one can prove that

$$V^{ext} = V^{latt} = \frac{e\,8.67}{4\pi\epsilon_0\,a_0^3}\,(\Delta_{Au} - \Delta_{Cu}) \tag{79}$$

with a_0 being the lattice constant. (G.P. Schwartz and D.A. Shirley, *Hyperfine Interactions* **3** (1977) 67)

[20] R. S. Raghavan, E. N. Kaufmann and P. Raghavan, *Physical Review Letters* 34(20) (1975) p. 1280

the local contribution in metals (here the local contribution is due to conduction electrons) is proportional to the antishielded lattice contribution and has the other sign, the universal proportionality constant $-K$ being about -3:

$$(1-R)V_{zz}^{loc} \;=\; V_{zz} - (1-\gamma_\infty)\,V_{zz}^{latt} \;=\; -K\,(1-\gamma_\infty)\,V_{zz}^{latt} \tag{80}$$

and hence

$$V_{zz} \;=\; (1-K)\,(1-\gamma_\infty)\,V_{zz}^{latt} \tag{81}$$

This 'universal correlation' with the data set of Raghavan *et al.* is shown in fig. 7-a. In later experiments[21] many exceptions to this plot have been found (for instance by Enrst *et al.*[22], fig. 7-b), making the proportional behaviour far less universal as was once thought. Fig. 7-c shows the available data set in 1983 (R. Vianden).

[21] See R. Vianden, *Hyperfine Interactions* **15/16** (1983) 189-201 for a discussion, and R. Vianden, *Hyperfine Interactions* **35** (1987) 1079-1118 for a tabulation of many more electric-field gradient measurements.

[22] H. Ernst, E. Hagn, and E. Zech, *Physical Review B* **19** (1979) 4460-4469

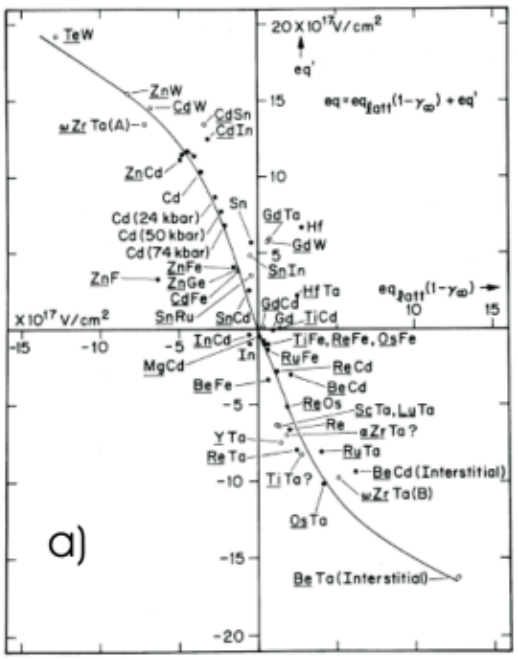

FIG. 1. Correlation of ionic and extraionic field-gradients in metals. Most values refer to room temperature. A typical temperature dependence is shown in the case of *Zn*Cd by an arc of data points. Underlined symbols refer to the host metal. *A* and *B* refer to two inequivalent substitutional sites in ω-Zr. Filled circles indicate data from e^2qQ values of known signs. For open circles, e^2qQ signs are unknown. Locations of these points are predicted.

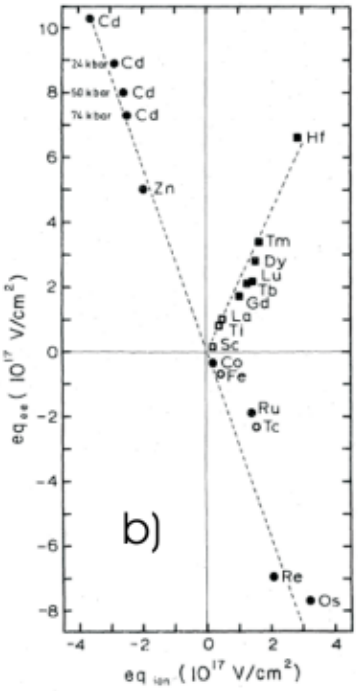

FIG. 7. Correlation of ionic and electronic contributions to the total electric field gradient in pure hexagonal metals. Circles indicate data from group-II*b*, -VIII*b*, and -VIII*b* metals, squares indicate data from group III*b* and IV*b* metals. Open symbols refer to data with unknown signs, their locations are predicted.

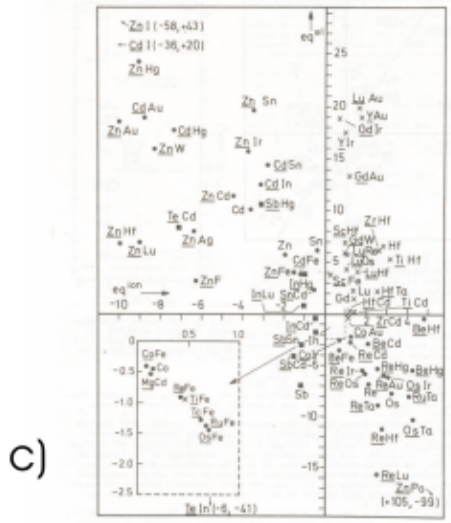

Fig. 4 Plot of eq^{el} versus eq^{ion} for all systems known today. Open 4f shell rare earth and some systems far outside the range of the figure (Tm2, ReTe, Re3) have been omitted. Different symbols are used for different atomic groups of host metals: ● group II, IIIb, VIIb and VIIIb, ✖ group IIIb and IVb, ■ group III, V and VI.

Figure 7: *Pictures of pretended correlations between the total electric-field gradient and the point-charge lattice contribution (with their original captions), with data sets available in 1979 [a): Raghavan, b): Ernst] and 1983 [c): Vianden]. See text for detailed references.*

4.2 Temperature dependence of the electric-field gradient

Up to now we did not mention temperature. In almost all cases, the electric-field gradient lowers when the temperature raises. Fig. 8 shows V_{zz} as a function of temperature for Cd(Cd), Sn(Cd), and Ru(Cd). The kind of temperature dependence is not the same in all classes of materials however. Regular spd-compounds follow a $T^{1.5}$-law:

$$V_{zz}(T) = V_{zz}(0)\left(1 - BT^{1.5}\right) \tag{82}$$

There is no formal justification for the exponent 1.5 and actual values may differ from 1.5 slightly. The factor B has the order of magnitude of $10^{-4} - 10^{-5}K^{-1.5}$. It is highly surprising that so many cases – equation 82 holds equally well for pure compounds as for the field gradient on impurities – can be described by such a simple formula, which contains only a single free parameter ($V_{zz}(0)$ is trivial).

In materials with f-electrons, the temperature dependence is linear:

$$V_{zz}(T) = V_{zz}(0)\left(1 - BT^{1}\right) \tag{83}$$

Broad studies do not exist, but it seems this linear behaviour remains even if the electric-field gradient is measured at a position where no f-atom sits, as the field gradient on ^{111}Cd on the Sn-position in USn_3.

The final picture to understand these temperature dependences at a fundamental level has not yet been worked out. Of course, the field gradient must become smaller if the lattice expands. This effect is too small however to explain the observed temperature variation. Next, one could think about an electronic effect. The higher the temperature is, the more electrons are thermally excited. The bonds which were sharply defined at 0K become hence more and more blurred. 'Blurred' means that spherical symmetry of the electron cloud is more and more restored, and the electric-field gradient will therefore become smaller. But the temperatures needed for this to be an observable effect are orders of magnitude higher than the temperature range of fig. 6-7***. The only remaining possibility is the influence of lattice vibrations (phonons), which indeed are important in the range of 0 - 1000 K. The fact that for impurities in a host-lattice the observed B correlates with the Debye-temperature of the host is an experimental support for this. The final theory to describe $V_{zz}(T)$ will therefore have to deal with phonons in an accurate way (An early and rather successful model for the electron-phonon coupling can be found in P. Jena, *Physical Review Letters* **36** (1976) 418-421 and in D. R. Torgeson and F. Borsa, *Physical Review Letters* **37** (1976) 956-959. Other references can be found in E. N. Kaufmann and R. J. Vianden, *Review of Modern Physics* 51(1) (1979) p. 161, in W. Witthuhn and W. Engel in *Hyperfine Interactions of Radioactive Nuclei*, ed. J. Christiansen, pp. 205-280, 1983, Springer-Verlag, ISBN 3-540-12110-2, in R. Vianden, *Hyperfine Interactions* **15/16** (1983) 189-201, and H. C. Verma and G. N. Rao, *Hyperfine Interactions* **15/16** (1983) 207-210.).

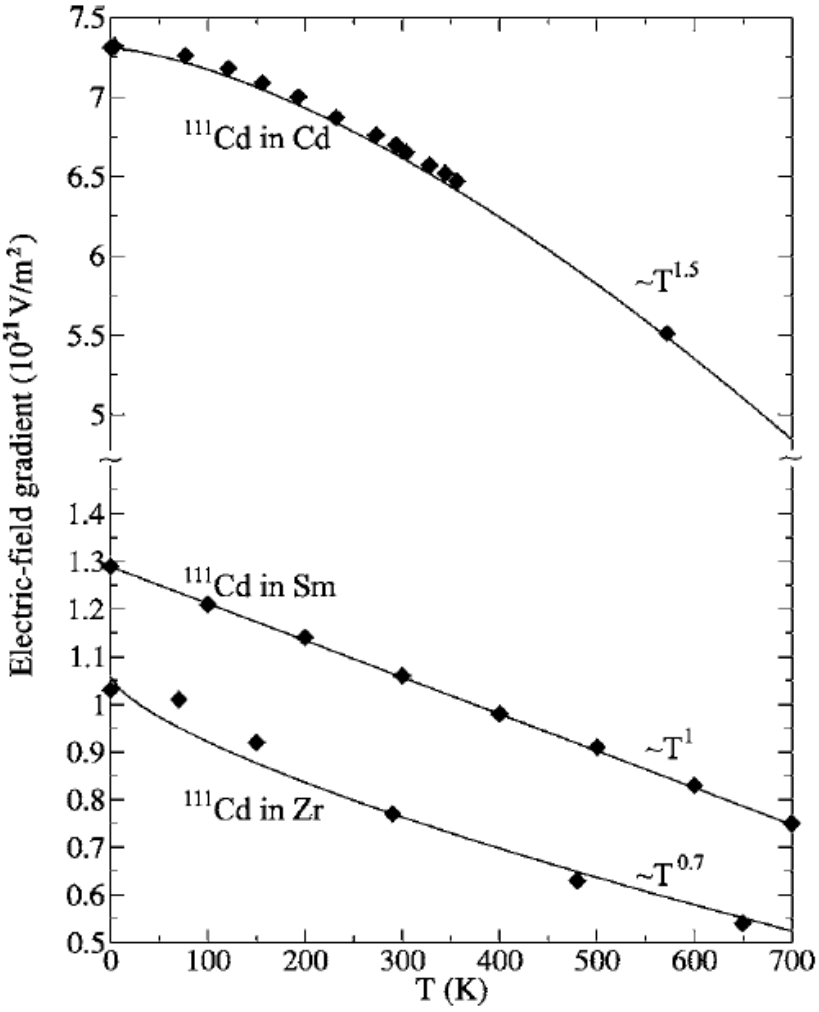

Figure 8: *T-dependence of $V_{zz}(T)$=$V_{zz}(0)$(1-BT^{α}) (solid lines are fits through the experimental values) for Cd(Cd), Sm(Cd), and Zr(Cd). Phys. Rev. B (2006) 144304*

5 Combined interaction

We are ready now to combine the results of this document and the previous one and study the interaction between a nucleus and a magnetic field and electric-field gradient that are present simultaneously. We will discuss the case of solids only. The general solution of this problem is complex, and we will restrict ourselves to a few manageable cases. Cases which are not treated are explicitly mentioned, in order to indicate clearly what is missing here. An important note to make is that a lot of steps use formulas not previously discussed[23]. As the online course only goes briefly over this subject (and not in a strong mathematical way whatsoever), it is more important to understand the different cases than to follow the mathematics behind them.

5.1 General formulation

Consider a nucleus with angular momentum $I \geq 1$, observable magnetic dipole moment μ (or alternatively, g-factor g), and observable electric quadrupole moment Q. Both μ (or g) and Q can be either positive or negative. This nucleus is inside a solid, and feels a magnetic field $\vec{B}(\vec{0})$ and an electric-field gradient $\vec{V}(\vec{0})$ that are fixed with respect to the crystal lattice. The crystal is described in an axis system that is fixed with respect to e.g. the experimental apparatus that is used to study the nucleus, and is therefore sometimes called the LAB-system. Our static $\vec{B}(\vec{0})$ can be described in this LAB-system by 3 components B_x, B_y and B_z. There will be a PAS in which $\vec{B}(\vec{0})$ has only one non-zero component. In order to specify $\vec{V}(\vec{0})$ with respect to the LAB-system, 5 components are needed. Equation 11 shows that also here a PAS can be chosen such that only 3 non-zero components remain (with only 2 degrees of freedom). The description of $\vec{B}(\vec{0})$ and $\vec{V}(\vec{0})$ is simplest in their PAS, but these two PAS in general do not coincide. We will have to choose one of them, and accept the complications for the other interaction which we cannot describe in its PAS.

As we assume $\vec{B}(\vec{0})$ and $\vec{V}(\vec{0})$ to be known quantities, we can again formulate a nuclear Hamiltonian. Diagonalization of the matrix of its matrix elements will lead to the eigenvalues and eigenstates. The general nuclear magnetic Hamiltonian in an axis system not necessarily being the PAS associated with $\vec{B}(\vec{0})$:

$$\hat{H}_{jj}^{nuc} = -\frac{g_I \mu_N}{\hbar} \vec{B}(\vec{0}) \cdot \hat{\vec{I}} \tag{84}$$

The corresponding quadrupole hamiltonian we calculated up to now only in the PAS of the field gradient, in equation 41. By equations 3, 37 and 25 to 27 we can obtain the spherical form in a general axis system:

$$\hat{H}_{qq}^{nuc} = \frac{eQ}{2I(2I-1)\hbar^2} \left[\left(3\hat{I}_z^2 - \hat{I}^2 \right) < V_0^2 >$$

[23] We are not talking about derivations but about e.g. certain transformation formulas.

$$\mp \sqrt{\frac{3}{2}} \left(\hat{I}_z \hat{I}_{\pm 1} + \hat{I}_{\pm 1} \hat{I}_z \right) < V^2_{\pm 1} > \; + \sqrt{\frac{3}{2}} \hat{I}^2_{\pm} < V^2_{\pm 2} > \Bigg] \tag{85}$$

with $\left\langle V_q^2 \right\rangle = \left\langle \Psi_e^{(0)} \right| \hat{V}_q^2 \left| \Psi_e^{(0)} \right\rangle$.

The general problem is now to find the nuclear eigen states and eigen values of $\hat{H}^{nuc}_{jq} = \hat{H}^{nuc}_{jj} + \hat{H}^{nuc}_{qq}$. We will solve this problem in a few special cases.

6 Dominant quadrupole interaction

We first focus on the case where the quadrupole interaction is dominant. 'Dominant' means that if both interactions would act alone, ΔE^{nuc}_{qq} is much larger than ΔE^{nuc}_{jj} (equivalently: $\omega_0 \gg \omega_L$). It is a natural choice then to take the PAS of the electric-field gradient as reference system. If exact calculations would appear to be impossible, the magnetic interaction can be considered to be a perturbation to the quadrupole interaction.

6.1 The collinear case

6.1.1 Axial symmetry

This is the most simple case, and can be solved exactly: $\vec{B}(\vec{0})$ is parallel to the z-axis of the PAS of the electric-field gradient, the latter being axially symmetric. This z-axes of both PAS coincide, and for none of them the choice of x- and y-axes matters, such that both PAS can be chosen to be identical. Under these circumstances, 84 reduces to eq. 31 from hyperfinecourse A: magnetic hyperfine interaction, and 85 to 41 with $\eta = 0$:

$$\hat{H}^{nuc}_{jq} = \frac{e\,Q\,V_{zz}}{4\,I(2I-1)\,\hbar^2} \left(3\hat{I}_z^2 - \hat{I}^2\right) \; - \; \frac{g_I \mu_N}{\hbar} B(\vec{0})\, \hat{I}_z \tag{86}$$

This hamiltonian is already diagonal in the $|\, I,\, m_I >$-basis, with eigenvalues:

$$\begin{aligned} E^{nuc}_{jq}(m_I) &= \frac{e\,Q\,V_{zz}}{4\,I(2I-1)} \left(3m_I^2 - I(I+1)\right) \; - \; g_I \mu_N B\, m_I & (87) \\ &= \hbar\omega_Q \left(3m_I^2 - I(I+1)\right) \; + \; \hbar\omega_L m_I & (88) \end{aligned}$$

The energy level scheme for $I = 5/2$ is given in fig. 7-1*** for $QV_{zz} > 0$ and $g_I B < 0$. This scheme inverts whenever QV_{zz} or $g_I B$ changes sign. The $\pm m_I$ degeneracy from the quadrupole-only case is lifted.

Equation 87 is an exact solution, and does not depend on E_M being small with respect to E_Q. It even holds equally well for the case with dominating magnetic interaction.

Let us examine what happens if one increases B. For particular field strengths,

some energy levels will coincide. From 87 you can derive that $E_{QM}(m_I) = E_{QM}(m'_I)$ if:

$$\frac{\omega_L}{\omega_Q} = -3\,(m_I + m'_I) \tag{89}$$

Apparently, for a given ω_Q several ω_L exist for which this condition holds (fig. 7-2***). For instance, for the situation given in fig. 7-1***, the first coincidence will obviously happen for the levels $m_I = -3/2$ and $m_I = +1/2$. This will be if $\omega_L/\omega_Q = 3$. Such crossings of two levels are crucial for the *Level Mixing Resonance* method, a method which is especially useful to measure hyperfine interaction energies when combined interactions are present.

6.1.2 No axial symmetry

If $\vec{B}(\vec{0})$ and $\vec{V}(\vec{0})$ are collinear, but without axial symmetry for $\vec{V}(\vec{0})$, we are in a situation much similar to section 3.3 from hyperfinecourse A: magnetic hyperfine interaction. We will have the complexity of the non-zero non-diagonal elements, which are exactly the same however as in said section. Only the diagonal elements are changed, due to an additional term from the magnetic interaction. Finding the eigen values will proceed along the same scheme as presented in said section. For half-integer I, if B is sufficiently small a Zeeman-splitting of the degenerate $\pm m_I$ levels will show up. For integer I, almost degenerate levels will Zeeman-split too, and non-degenerate levels will change their mutual distance a little (increase or decrease).

6.2 The non-collinear case

6.2.1 Axial symmetry

Now consider an axially symmetric quadrupole interaction, being much stronger than a magnetic interaction and *not collinear* with it. The PAS of the magnetic hyperfine field can be specified with respect to the PAS of the electric-field gradient by the Euler angles (α, β, γ). α is an orientation about the direction of axial symmetry of the electric-field gradient. Due to this axial symmetry, α should not matter and we can choose the X- and Y-axis of the electric-field gradient PAS such that $\alpha = 0$. Similarly, γ is a rotation about the direction of the magnetic hyperfine field, which is always a direction of axial symmetry because the hyperfine field is a vector. We can choose the X'- and Y'-axis of the magnetic PAS such that $\gamma = 0$. Hence, a simplified set of Euler angles that specifies the magnetic PAS with respect to the electric PAS is (0, β, 0).

We will work in the electric PAS, and therefore we should express the magnetic hyperfine field in the electric PAS. The latter plays the role of the 'new' axis system in the transformation, such that in order to transform, we should know the Euler angles that specify the electric PAS with respect to the magnetic PAS. These are (0, $-\beta$, 0). In the 'old' (magnetic) axis system, the cartesian components of the magnetic hyperfine field are (0, 0, B). The corresponding

spherical tensor that describes the hyperfine field in the magnetic PAS has only one non-zero component: $B_0^1 = B$. Three components in the electric PAS are:

$$B_q^1(\beta) = \mathcal{D}_{0q}^1(0, -\beta, 0)\, B_0^1 \tag{90}$$

$$= (-1)^q \sqrt{\frac{4\pi}{3}}\, B\, Y_q^1(-\beta,\, 0) \tag{91}$$

Explicit expressions are:

$$B_0^1(\beta) = B\cos\beta \tag{92}$$

$$B_{\pm 1}^1 = \mp\frac{B}{\sqrt{2}}\,\sin\beta \tag{93}$$

The spherical form of the nuclear angular momentum operator $\hat{\vec{I}} = \left(\hat{I}_x,\, \hat{I}_y,\, \hat{I}_z\right)$, is :

$$\hat{I}_0^1 = \hat{I}_z \tag{94}$$

$$\hat{I}_{\pm 1}^1 = \mp\frac{1}{\sqrt{2}}\,\hat{I}_\pm \tag{95}$$

Working out the dot product in equation 84 but using spherical components, we find the desired expression:

$$H_{jj}^{nuc}(\beta) = -\frac{g_I \mu_N B}{\hbar}\left(\frac{1}{2}\sin\beta\left(\hat{I}_+ + \hat{I}_-\right) + \cos\beta\,\hat{I}_z\right) \tag{96}$$

The combined hamiltonian H_{jq}^{nuc} is not diagonal any more in the $|\, I,\, m_I >$ basis. The non-zero matrix elements depend on β and are:

$$\langle I,\, m_I|\, H_{jq}^{nuc}(\beta)\,|I,\, m_I\rangle = \hbar\omega_Q\left(3m_I^2 - I(I+1)\right) + \hbar\omega_L m_I\cos\beta \tag{97}$$

$$\langle I,\, m_I|\, H_{jq}^{nuc}(\beta)\,|I,\, m_I \pm 1\rangle = \frac{\hbar\omega_L}{2}\sin\beta\,\sqrt{I(I+1) - m_I(m_I \pm 1)} \tag{98}$$

Due to the off-diagonal matrix elements, the $|\, I,\, m_I >$-states are no eigen states any more. In our first order perturbation procedure where H_{jq}^{nuc} is the perturbing Hamiltonian (with V_{zz} and B the small parameters) with respect to the dominant monopole Hamiltonian, the following matrix must be diagonalized in order to find the new eigen states ($I = \frac{5}{2}$ as an example):

$$\begin{array}{c} +\frac{5}{2}\;\; +\frac{3}{2}\;\; +\frac{1}{2}\;\; -\frac{1}{2}\;\; -\frac{3}{2}\;\; -\frac{5}{2} \\ \left[\begin{array}{cccccc} qj & j & 0 & 0 & 0 & 0 \\ j & qj & j & 0 & 0 & 0 \\ 0 & j & qj & j & 0 & 0 \\ 0 & 0 & j & qj & j & 0 \\ 0 & 0 & 0 & j & qj & j \\ 0 & 0 & 0 & 0 & j & qj \end{array}\right] \end{array} \tag{99}$$

The symbol 'qj' indicates a contribution due to H_{qq}^{nuc} and H_{jj}^{nuc} simultaneously, the symbol 'j' a contribution due to H_{jj}^{nuc} only.

If the quadrupole interaction is dominant, we can apply first order perturbation theory a second time. We can take the monopole Hamiltonian plus H_{qq}^{nuc} as the unperturbed Hamiltonian, and H_{jj}^{nuc} as the perturbation with B as the small parameter ($B \ll V_{zz}$). Under the unperturbed Hamiltonian, the $\pm m_I$ states are degerate:

$$\begin{bmatrix} \langle m_I | H_{jj}^{nuc} | m_I \rangle & \langle m_I | H_{jj}^{nuc} | -m_I \rangle \\ \langle -m_I | H_{jj}^{nuc} | m_I \rangle & \langle -m_I | H_{jj}^{nuc} | -m_I \rangle \end{bmatrix} \tag{100}$$

For $m_I = \frac{5}{2}$ and $m_I = \frac{3}{2}$, this is a diagonal matrix: the eigenstates are unchanged, and the degenerate eigenvalues split (their separation is $2\hbar\omega_L m_I \cos\beta$). For $m_I = \frac{1}{2}$, the matrix is not diagonal:

$$\frac{\hbar\omega_L}{2} \begin{bmatrix} \cos\beta & k \sin\beta \\ k \sin\beta & -\cos\beta \end{bmatrix} \tag{101}$$

with $k = \sqrt{I(I+1) + \frac{1}{4}}$. It is left as an exercise to diagonalize this and find the separation between the two levels.

Note finally that when $\vec{B}(\vec{0})$ is perpendicular to the Z-axis of the PAS of the quadrupole interaction and small, the energies in first order are unaffected, except for $m_I = \pm\frac{1}{2}$.

6.2.2 No axial symmetry

We do not deal with the case of a dominant non-axially symmetric quadrupole interaction combined with a non-collinear magnetic interaction. Note only that now matrix elements with $\Delta m_I = \pm 1$ and $\Delta m_I = \pm 2$ are present in the $|\, I, m_I >$-basis.

7 Dominant magnetic interaction

7.1 The collinear case

7.1.1 Axial symmetry

We already dealt with this case, as the axially symmetric quadrupole interaction with collinear magnetic interaction was solved exactly, irrespective of the relative strength of both interactions.

7.1.2 No axial symmetry

This will not be discussed.

7.2 The non-collinear case

7.2.1 Axial symmetry

If the Z-axis of the PAS of a small electric quadrupole interaction is not parallel to the Z-axis of the PAS of a large magnetic interaction, we better take the latter PAS as our reference frame, and express the quadrupole interaction in this axis system. The magnetic hamiltonian of equation 84 simplifies to:

$$\hat{H}_{jj}^{nuc} = -\frac{g_I \mu_N}{\hbar} B \hat{I}_z \tag{102}$$

while the quadrupole hamiltonian is given in 85. The magnetic PAS is our final reference system here, and the orientation of the electric PAS with respect to the magnetic PAS is specified by the Euler angles (α, β, γ). For the same reasons as in section 6.2.1, the axes can be taken such that α and γ are zero, without loosing generality[24]. We will not make this choice, however. We will start out with general values for all three Euler angles, in order to demonstrate that – with somewhat more work – the α- and γ-dependence will disappear spontaneously from the equations.

First we transform the single non-zero component of the electric-field gradient tensor from its PAS to the magnetic PAS. In order to do so, we need the Euler angles that specify the magnetic PAS with respect to the electric PAS: $(-\gamma, -\beta, -\alpha)$. The transformed components are:

$$\begin{aligned} \left\langle V_q^2 \right\rangle_M &= D_{0q}^{(2)}(-\gamma, -\beta, -\alpha) \left\langle V_0^2 \right\rangle_E & (103) \\ &= d_{0q}^2(-\beta)\, e^{iq\alpha} \left\langle V_0^2 \right\rangle_E & (104) \\ &= \frac{(-1)^q}{2} \sqrt{\frac{4\pi}{5}}\, e^{iq\alpha}\, Y_q^2(-\beta, 0)\, V_{zz} & (105) \end{aligned}$$

(the subscripts M and E indicate components in the magnetic and electric PAS, respectively). The γ-dependence has already disappeared. Now, fill this out in

[24] Note that α and γ are not the same angles as in section 6.2.1: α is now a rotation about the magnetic hyperfine field.

equation 85 in order to find the quadrupole hamiltonian in the magnetic PAS as a function of V_{zz}, α, and β:

$$H_{qq}^{nuc} = \frac{eQ\,V_{zz}}{4I(2I-1)\hbar^2}\left[\underbrace{\frac{3\cos^2\beta-1}{2}\left(3\hat{I}_z^2-\hat{I}^2\right)}_{\hat{a}\,'}\right.$$
$$\left.\underbrace{+\sqrt{\frac{3}{2}}\sin\beta\,\cos\beta\left(\hat{I}_z\hat{I}_{\pm1}+\hat{I}_{\pm1}\hat{I}_z\right)}_{\hat{b}_\pm}\;e^{\pm i\,\alpha}\;+\;\underbrace{\sqrt{\frac{3}{8}}\sin^2\beta\,\hat{I}_\pm^2}_{\hat{c}_\pm}\;e^{\pm 2i\,\alpha}\right] \quad (106)$$

The matrix elements of the total hamiltonian $H_{jj}^{nuc}+H_{qq}^{nuc}$ in the $|\,I,\,m_I>$-basis, now depend on β and α (to simplify notation, assume we are dealing with $I=2$):

$$H(\alpha,\,\beta) = \frac{eQ\,V_{zz}}{4I(2I-1)\hbar^2}\begin{bmatrix} a & b_+\,e^{i\alpha} & c_+\,e^{2i\alpha} & 0 & 0 \\ b_-\,e^{-i\alpha} & a & b_+\,e^{i\alpha} & c_+\,e^{2i\alpha} & 0 \\ c_-\,e^{-2i\alpha} & b_-\,e^{-i\alpha} & a & b_+\,e^{i\alpha} & c_+\,e^{2i\alpha} \\ 0 & c_-\,e^{-2i\alpha} & b_-\,e^{-i\alpha} & a & b_+\,e^{i\alpha} \\ 0 & 0 & c_-\,e^{-2i\alpha} & b_-\,e^{-i\alpha} & a \end{bmatrix} \quad (107)$$

with a the appropriate matrix element of $\hat{a}$, etc. The symbol a is chosen such that the magnetic interaction is correctly incorporated:

$$\hat{a} = \hat{a}\,' - \frac{g_I\,\mu_N\,B\,4I(2I-1)\,\hbar}{eQV_{zz}}\,\hat{I}_z \quad (108)$$

This matrix contains both the magnetic and electric interaction in the diagonal, only the electric interaction in the two side diagonals, and zeros elsewhere. Furthermore, the symbols a, $b_\pm$ and $c_\pm$ depend on β, but not on α. Diagonalization yields the eigenvalues and eigenvectors. This diagonalization can be achieved by a suitable unitary transformation[25]:

$$H^d(\beta,\,\alpha) = U(\beta,\,\alpha)\,H(\beta,\,\alpha)\,U^{-1}(\beta,\,\alpha) \quad (110)$$

where H^d is diagonal in the new basis, and U is a unitary matrix. Next we prove that $U(\beta,\,\alpha)$ can be factorized into a β- and a α-dependent matrix: $U(\beta,\,\alpha) = U\,'(\beta)\,A(\alpha)$. Indeed, one can apply the following unitary transformation which leaves a matrix $H\,'(\beta)$ depending not on α any more:

$$H\,'(\beta) = A(\alpha)\,H(\beta,\,\alpha)\,A^{-1}(\alpha) \quad (111)$$

[25] A unitary transformation of the square matrix B is defined as the operation needed to obtain another square matrix A by

$$A = U\,B\,U^{-1} \quad (109)$$

with U being a unitary matrix, i.e. $U^\dagger = U^{-1}$. ($U^\dagger$ is the conjugate transpose of U).

$$\begin{bmatrix} a & b_+ & c_+ & 0 & 0 \\ b_- & a & b_+ & c_+ & 0 \\ c_- & b_- & a & b_+ & c_+ \\ 0 & c_- & b_- & a & b_+ \\ 0 & 0 & c_- & b_- & a \end{bmatrix} = A(\alpha) \begin{bmatrix} a & b_+\, e^{i\alpha} & c_+\, e^{2i\alpha} & 0 & 0 \\ b_-\, e^{-i\alpha} & a & b_+\, e^{i\alpha} & c_+\, e^{2i\alpha} & 0 \\ c_-\, e^{-2i\alpha} & b_-\, e^{-i\alpha} & a & b_+\, e^{i\alpha} & c_+\, e^{2i\alpha} \\ 0 & c_-\, e^{-2i\alpha} & b_-\, e^{-i\alpha} & a & b_+\, e^{i\alpha} \\ 0 & 0 & c_-\, e^{-2i\alpha} & b_-\, e^{-i\alpha} & a \end{bmatrix} A^{-1}(\alpha)$$

$$A(\alpha) = \begin{bmatrix} e^{2i\alpha} & 0 & 0 & 0 & 0 \\ 0 & e^{i\alpha} & 0 & 0 & 0 \\ 0 & 0 & 1 & 0 & 0 \\ 0 & 0 & 0 & e^{-i\alpha} & 0 \\ 0 & 0 & 0 & 0 & e^{-2i\alpha} \end{bmatrix} \tag{112}$$

In general, $A(\alpha)$ is constructed such that its diagonal runs from $e^{Ii\alpha}$ till $e^{-Ii\alpha}$. As $H'(\beta)$ does not depend on α, the unitary matrix $U'(\beta)$ needed to transform it into H^d will also be β-dependent only. And as an immediate consequence, $H^d(\beta)$ and its eigenvalues will not depend on α too. The complete unitary transformation looks like:

$$H^d(\beta) = \underbrace{U'(\beta)A(\alpha)}_{U(\beta,\,\alpha)}\, H(\beta,\,\alpha)\, \underbrace{A^{-1}(\alpha)U'^{-1}(\beta)}_{U^{-1}(\beta,\,\alpha)} \tag{113}$$

In this way we formally proved that for an axially symmetric electric-field gradient, the eigenvalues of the combined interaction do not depend on α, a property which we said in the beginning was intuitively obvious.

Up to now, we did not require the electric interaction to be small. If we do so, we can use first order perturbation theory, and examine how the magnetic energy levels will change under the influence of the electric interaction. The eigenstates of the unperturbed (=magnetic) hamiltonian are the $|\, I,\, m_I >$-states, the energy corrections E_c are:

$$E_c = < I,\, m_I |\, H_Q |\, I,\, m_I > \tag{114}$$

$$= \hbar\omega_Q\, \frac{3\,\cos^2\beta - 1}{2}\, \left(3m_I^2 - I(I+1)\right) \tag{115}$$

If $\beta = 0°$, we retrieve the exact expression for the collinear case we found previously. The distance between $\pm m_I$-levels remains always constant, unregardless the perturbation. There is also a so-called 'magic angle' $\beta_m \approx 54.74°$ for which $3\cos^2\beta_m - 1 = 0$: for this angle, the original magnetic levels are not changed in first order.

7.2.2 No axial symmetry

And this one we skip again.

8 None of both interactions dominant

Let us finally sketch how to treat the most general case, where none of both interactions is dominant, where the orientation of the Z-axes of both principle axis systems is arbitrary and where the electric-field gradient may have no axial symmetry. Most of the procedure we can copy from previous reasoning.

It does not matter which of both axis systems we take, assume we work in the PAS of the magnetic interaction and specify the electric PAS with respect to this magnetic PAS by Euler angles (α, β, γ). We can transform the electric-field gradient from its PAS to the magnetic PAS (for which you have to use the Euler angles ($-\gamma$, $-\beta$, $-\alpha$)). Contrary to equation 103, the electric-field gradient has V_0^2 and $V_{\pm 2}^2$ as non-zero components in its PAS (below indexed by P). The 5 components in the general axis system (below indexed by G) will therefore *all* depend on both V_{zz} and η:

$$< V_q^2 >_G = D_{0q}^2 < V_0^2 >_P + D_{2q}^2 < V_2^2 >_P + D_{-2q}^2 < V_{-2}^2 >_P \quad (116)$$

$$= d_{0q}^2(-\beta) e^{iq\alpha} < V_0^2 >_P + e^{i2\gamma} d_{2q}^2(-\beta) e^{iq\alpha} < V_2^2 >_P + e^{-i2\gamma} d_{-2q}^2(-\beta) e^{iq\alpha} < V_{-2}^2 >_P \quad (117)$$

Note that the angle γ (rotation about the electric-field gradient principal axis) does not disappear now. The 5 explicit expressions are (V_{zz} and η are with respect to the PAS of the electric-field gradient):

$$< V_0^2 >_G = \frac{1}{4}\sqrt{\frac{5}{\pi}} V_{zz} \left(\frac{3\cos^2\beta - 1}{2} + \frac{\eta}{2} \cos 2\gamma \, \sin^2\beta \right) \quad (118)$$

$$< V_{\pm 1}^2 >_G = \frac{1}{8}\sqrt{\frac{5}{3\pi}} V_{zz} \sin\beta \, e^{\pm i\alpha} \left(\pm 3\cos\beta + \sqrt{\frac{1}{2}}\,\eta \, \left[e^{-i2\gamma}(1 \mp \cos\beta) - e^{+i2\gamma}(1 \pm \cos\beta) \right] \right) \quad (119)$$

$$< V_{\pm 2}^2 >_G = \frac{1}{16} V_{zz} \sqrt{\frac{30}{\pi}} \, e^{\pm i2\alpha} \left(\sin^2\beta + \frac{\eta}{6} \left[e^{i2\gamma}(1 \pm \cos\beta)^2 + e^{-i2\gamma}(1 \mp \cos\beta)^2 \right] \right) \quad (120)$$

The matrix formed by the matrix elements will have the same structure as we encountered in the case with dominant magnetic interaction and axial symmetry, and in exactly the same way the α-dependence can be removed. The eigenvalues will hence depend on γ and β, contrary to the case with axial symmetry. No perturbation theory can be applied now, and therefore the full diagonalization by searching the suitable unitary transformation has to be performed. With some writing effort, you can write down explicitly the matrix elements for instance for $I = 3/2$. You will see that they are complex if $\eta \neq 0$.

It can be proven also that some mutual orientations of magnetic and electric interactions yield the same eigenvalues.

9 Examples

9.1 Fe_4N

The ferromagnetic compound Fe_4N was discussed already in sections hyperfinecourse A: magnetic hyperfine interaction 5.1 and 3.7.2, where we have seen that at the Fe-I sites both a hyperfine field and an electric-field gradient are present. Experimental values are about 25 T for the hyperfine field, and $2.9{\cdot}10^{21}$ V/m^2 for V_{zz}. If we would measure[26] this interaction with the first excited nuclear level of the ^{57}Fe isotope (I=3/2, g_I=-0.1553 μ_N, Q=0.16 b), then the ratio $\omega_0/\omega_L = 0.09$: we are in the situation with dominant magnetic interaction. If the magnetic moments are along the (001) direction, then the angle between the Z-axes of the magnetic and electric PAS is 0° for 2 out of 6 Fe-I atoms (Fe-Ia), while it is 90° for the other 4 (Fe-Ib). Fe-Ia can be treated with the exact equations from section 7.1, while for Fe-Ib the perturbation approach from section 7.2 can be used (it would be a good illustration to compare the energies of the 4 m-levels in both cases).

With the moments along the (111) direction, the angle between both Z-axes is the magic angle of 54.74° for all 6 Fe-I atoms, and we should use the formulae from section 7.2. Verify that the levels are identical to the Zeeman splitting from a pure magnetic interaction.

10 Epilogue

Congratulations, you have reached the end of part A. I hope you had as much fun as I did making these documents. I would like to thank S. Cottenier and M. Rots for the initial syllabus on which these documents are based. S. Cottenier deserves extra thanks for correcting and steering these documents where needed. N. Steyaert gets my appreciations for his emotional support.

That will be all. Have fun in the next section where we learn the practical applications of these tiny energy differences. And good luck in your physics/engineering/... futures.

PS I didn't make the same kind of documents for part B as I am more interested in the theory (part A) than the applications. This does not mean that they aren't as important, certainly in our daily lives. I hope these documents inspire and give some other students the courage to do the same for part B.

[26] This is *almost* what happens in a Mössbauer experiment, although there also the ground state I=1/2 level plays a role.